The *Skyscraper Revolution*: Global Economic Development and Land Savings*

Gabriel M. Ahlfeldt † Nathaniel Baum-Snow ‡ Remi Jedwab §

November 13, 2023

Abstract

Tall buildings are central to facilitating sustainable urbanization and growth in cities worldwide. We estimate average elasticities of city population and built area to aggregate city building heights of 0.12 and -0.17, respectively, indicating that the largest global cities in developing economies would be at least one-third smaller on average without their tall buildings. Land saved from urban development by post-1975 tall building construction is over 80% covered in vegetation. To isolate the effects of technology-induced reductions in the cost of height from correlated demand shocks, we use interactions between static demand factors and the geography of bedrock as instruments for observed 1975-2015 tall building construction in 12,877 cities worldwide, a triple difference identification strategy. Quantification using a canonical urban model suggests that the technology to build tall generates a potential global welfare gain of 4.8%, of which only about one-quarter has been realized. Estimated welfare gains from relaxing existing height constraints are 5.9% in the developed world and 3.1% in developing economies.

Key words: Urban Density; International Buildings Heights; Skyscrapers; Tall Buildings; Sustainable Urbanization; City Growth; Commercial Real Estate; Housing Supply; Urban Sprawl; Land Savings; Housing Affordability; Geographical Constraints; Environment

JEL: R11, R12, R14, R31, R33, O18, O13

*We thank Paolo Avner, Jason Barr, Adrien Bilal, Jan Brueckner, Federico Curci, Donald Davis, Klaus Desmet, Rebecca Diamond, Jonathan Dingel, Gilles Duranton, Edward Glaeser, Gabriel Kreindler, Jessie Handbury, Mariaflavia Harari, Christian Hilber, Matthew Kahn, Jeffrey Lin, Megha Mukim, Guy Michaels, Raven Molloy, John Morrow, David Nagy, Joseph Nichols, Victor Ortego Marti, Lindsay Relihan, Tanner Regan, Frederic Robert-Nicoud, Esteban Rossi-Hansberg, Mark Roberts, Michael Storper, Nick Tsivanidis, Matthew Turner, Tony Venables, C. Luke Watson, David Weinstein, Michael Wong, and numerous seminar audiences for helpful comments.

†London School of Economics. Email: g.ahlfeldt@lse.ac.uk

‡University of Toronto. Email: nate.baum.snow@rotman.utoronto.ca

§George Washington University and NYU Marron Institute of Urban Management. Email: jedwab@gwu.edu

1 Introduction

Chicago's ten-storey 42-meter tall Home Insurance Building, built in 1884-85 and often called the world's first "skyscraper" (Schleier, 1986), was among the first uses of technologies that would prove to transform cities around the world. Since then, technological improvements that have lowered the marginal cost of building high have facilitated the construction of the more than 16,000 km of buildings over 55 meters tall in cities worldwide. Most of this construction has occurred since 1975 for residential use in developing economies. With the equivalent of almost 43,000 Empire State Buildings, the stock of tall buildings worldwide holds an aggregate asset value of more than 15 trillion dollars.[1] Indeed, a look at many global cities today leaves no doubt that the *Skyscraper Revolution* has been transformative (Glaeser, 2012). On average, cities of over 5 million inhabitants now host over 100 km of heights in tall buildings. In cities of over 1 million people, tall buildings account for about 10% of the stock and 18% of aggregate construction costs for existing structures.[2] Like currently developed countries during the 19$^{\text{th}}$ and 20$^{\text{th}}$ centuries, many developing economies are now in a process of rapid urbanization, growth, and structural transformation. With these great pressures, the technology of building tall has allowed cities to accommodate greatly increased populations while saving land for non-urban uses. Hsieh and Moretti (2019) and Duranton and Puga (2019) quantify the extent to which associated expansion in housing supply drives broader economic growth.

In this paper, we empirically and theoretically investigate the extent to which the skyscraper revolution has facilitated sustainable urbanization and urban growth, with a particular focus on cities in developing economies. Our empirical analysis recovers causal effects of the component of 1975-2015 tall building construction driven by technical progress and declines in the marginal cost of height on urban population growth, urban form, and land use. Using data from 12,877 urban agglomerations worldwide, we estimate average elasticities of city population and built-up land area to total city building heights of 0.12 and -0.17, respectively. These estimates are driven by cities in the developing world. For 1975-2015, we find no effects of heights in the developed world outside of North America. Instead, we find population elasticities with respect to heights of 0.14-0.21 in Europe for 1850-1975 and 1900-1975 and in the US for 1920-1975, during these regions' periods of economic development. Tall buildings have facilitated substantial growth in the developing world's largest 100 cities since 1975. Had the current stock of tall building in these cities not been constructed, these cities would be up to 50 percent smaller in population and be up to one-third larger in land area. The skyscraper revolution has been critical to the growth and success of the world's largest cities and the preservation of surrounding rural land, over 80% of which is covered in tree canopy or short vegetation.

[1] This calculation assumes that the construction cost net of depreciation to 2020 is a lower bound on the asset value for most tall buildings. We assume 2% annual depreciation and an average construction cost per meter of height matching the 572 million 2020 dollars for the Empire State Building.

[2] Using data on building volumes, we calculate that the fraction of the building stock in buildings over 55 meters tall are 80% in Hong Kong, 58% Seoul, 39% in Singapore, 35% in Mumbai, 32% in Taipei, 30% in Moscow, 29% in Dubai, 27% in Kuala Lumpur, 26% in Sao Paulo, 23% in Tel Aviv, 22% in Hanoi, 17% in Manila, 16% in Bogota, and 12% in New York. Construction cost per floor area for tall buildings is about twice that for shorter buildings in our data.

For identification, we use an instrumental variables strategy that leverages both cross-sectional and time series variation in the marginal cost of building high. In the cross-section, we use variation in city mean bedrock depth as a key source of identifying variation. Descriptive analysis and building cost function estimates indicate marginal cost of height per building floor area that is U-shaped in bedrock depth, consistent with engineering standards for foundation depth and the narrative in Barr et al. (2011). Bedrock that is too close to the surface must be blasted away at high cost to make room for building foundations. Foundations built above bedrock that is beyond the optimal depth must either be reached with the costly installation of deep wide piles, placed on a more costly raft, or engineered to be underpinned by many very long deeply bored piles. Favorable bedrock depth thus acts as a cost shifter, promoting more construction of tall buildings for a given level of demand. As a result, the elasticity of tall building construction with respect to historical city population, a proxy for the level of demand, is greater at more favorable bedrock depths. Finally, differencing over the 1975-2015 period leverages secular reductions in the marginal cost of height for identification. Particularly in the developing world, costs were sufficiently prohibitive in 1975 to preclude the existence of many tall buildings. Put together, our identification strategy leverages triple difference comparisons of historically large versus small cities on more versus less favorable bedrock depths over time.

To implement the empirical strategy, we compile a unique data set of all 12,877 cities with populations over 50,000 worldwide (in 182 countries), covering about 90% of the world's total urban population. For these cities, we organize census-based population and satellite-based area estimates going back to 1975, allowing us to measure population and land use in and around these cities over time. To capture the vertical size of cities, we use a data set of 270 thousand tall buildings from *Emporis*. This data set has comprehensive information on the location, use, and construction year of all buildings over 55 meters tall worldwide.

To conceptually ground the empirical work and evaluate the welfare consequences of policies that influence building heights, we incorporate building height into a neoclassical urban general equilibrium "representative city" model with frictional rural-urban migration. Potential floorspace rents for the commercial and residential sectors capitalize differences in production and residential amenities, respectively, across space within the city. Developers respond to greater floorspace demand by building taller, facing construction costs that are convex in height (Ahlfeldt and McMillen, 2018), consistent with our empirical evidence. In a competitive market, the land rent is the residual in the profit function that determines whether land is developed for commercial or residential use (Duranton and Puga, 2015). This setup draws from Ahlfeldt and Barr (2022), though it adds migration frictions through heterogeneity in tastes for urban life (McFadden, 1974), incorporating ideas from Harris and Todaro (1970), Bryan and Morten (2018) and Desmet et al. (2018) to accommodate domestic migration. Imperfect mobility of workers means that population *and* the utility of residents are endogenous objects.[3]

In the model, as in the data, reductions in the cost of height cause cities to grow vertically and become more productive and compact, with the vertical expansion partially offset by horizontal

[3]Our setup nests the closed-city and open-city models as special cases under extreme and negligible taste heterogeneity. See Brueckner (1987) for a discussion of these cases in the standard urban model.

contraction. Due to the positive net effect on housing supply, the average floorspace rent falls. Lower rents, in conjunction with higher wages that arise from agglomeration economies, result in greater urban utility. Rural-urban migration is a central element in the model, as it is the way that cities grow in population in response to reductions in the cost of height. Matching estimated population and land area elasticities with respect to height for a sub-sample of cities inferred to have the least burdensome land-use regulations to their model simulated counterparts yields an associated estimated long-run elasticity of migration with respect to the urban real wage of 1.6, which is in line with other evidence in the literature.

Using the model, we undertake counterfactual exercises which indicate that tall buildings have the potential to facilitate 4.2% and 4.8% greater average worker welfare in developing and developed economies, respectively. However, only about one-quarter of these potential welfare gains from heights have been realized because of existing land use and height regulations. Moreover, relaxing existing height constraints would reduce aggregate urban land values by an estimated 4.7% and 9.5% in developing and developed economies, respectively. To come to these conclusions, we compare the simulated height unconstrained model equilibrium for each city in our data to two alternative equilibria. First is the constrained equilibrium given observed city-specific "height gaps", which quantify the fraction of unconstrained equilibrium city heights justified by fundamental cost and demand factors that have not been realized. Second is the alternative constrained equilibrium allocation under a height limit that prohibits all tall buildings, which is typically a more binding constraint for larger cities. Impacts of height constraints are increasing in city size and declining in the cost of height, which is governed by bedrock depth. Aggregate land rents decline most in the largest cities due to the horizontal contraction facilitated by the greater allowed heights. Hence, reducing height regulation redistributes welfare from land to labor. Landlords lose with the lower rents associated with the supply expansion that comes with new heights but workers gain more due to slightly higher wages, enhanced access to preferred locations, and lower rents.

Looking across regions in the developing world, the relaxation of existing height restrictions has the potential to increase the average resident's welfare by 4.8% in Africa, 3.9% in Latin America, and 2.6% in Asia, with associated declines in aggregate land rents that are at least one-third larger in percentage point terms. In developed economies, the greatest potential welfare gains from relaxing height constraints are 7.3% in Asia, 6.6% in Oceania and 6.3% in North America. Variation across regions in welfare and land capitalization effects of relaxing height regulations are determined by differences in the fraction of the population in large cities, the costs of heights (due to variation in bedrock depths), and the amount of existing tall building construction (bite of existing regulations).

A large literature assesses the extent to which various types of capital accumulation, and in particular infrastructure construction, drive urban change. However, this is the first paper to comprehensively study how declines in the costs of building tall have contributed to urban development in cities around the world. Our analysis has many parallels with the large empirical literature exploring the impacts of various types of infrastructure on cities. Like highways (Duranton and Turner, 2012; Faber, 2014), railroads/subways (Gonzalez-Navarro and Turner,

2018a; Heblich et al., 2020), ports (Brooks et al., 2021; Ducruet et al., 2020), airports (Campante and Yanagizawa-Drott, 2018), and sewers (Alsan and Goldin, 2019; Coury et al., 2022), tall buildings form a central component of capital stocks in the world's largest cities, with myriad evidence in the literature of their causal impacts on urban growth and change. Similar to the research on infrastructure, we face the identification challenge of isolating variation in infrastructure supply across cities and over time that is unrelated to local demand conditions. Indeed, our identification challenge is perhaps more demanding than that in many transport studies, as there are few systematic institutional reasons for building heights to vary across cities. Somewhat analogous to Faber (2014)'s use of least cost paths driven by topography as instruments for highway routes in China, we use natural bedrock depth as a source of exogenous variation in changes in the cost of building taller. Our estimates are of similar or greater magnitudes to those in the literature for impacts of other components of urban capital stocks. Duranton and Turner (2012) estimate an elasticity of urban population growth with respect to the level of urban highway infrastructure of 0.15 for the US, which is quite similar to our estimate of 0.12 for the world. Our estimated population density elasticity for tall buildings of 0.29 is about 3 times as large as those found for urban radial highways in the US and China (Baum-Snow, 2007; Baum-Snow et al., 2017) and much larger than for other types of infrastructure. These investigations of how infrastructure drives urban growth are grounded in the classic empirical literature going back to Glaeser et al. (1992), Henderson et al. (1995), and Ades and Glaeser (1995) that study the determinants of urban TFP growth and variation across locations in equilibrium city sizes.[4]

Understanding how the skyscraper revolution fits into the process of urban development is all the more important as cities that do not develop vertically tend to sprawl (Burchfield et al., 2006) and/or become inefficiently spatially configured. Odd urban spatial structures impede growth (Harari, 2020), and associated sprawl typically occupies land that is particularly valuable in non-urban uses. According to World Bank (2022a), urban areas occupied 3.6 million sq km in 2011, whereas 48.0 million sq km of land was in agriculture. As cities are more likely to be sited on agriculturally productive land (Henderson et al., 2018), land savings through increased urban compactness frees up more space for agriculture and tree canopy. Taller cities make us "greener" (Glaeser, 2012) by accommodating more people on less land. In that, the skyscraper revolution has parallels with the Green Revolution, whose goal was to use rural land more intensively in order to use less land globally (Gollin et al., 2021).

Conceptually, our study perhaps most closely relates to the large literature studying land use, housing supply, and regulation. Our modeling framework incorporates insights from the land use and housing production literatures to accommodate height restrictions and general equilibrium linkages across labor and housing markets within and between residential and commercial sectors. Following in the tradition of Muth (1969), we incorporate residential and commercial real estate

[4]Additional papers studying impacts of highways and railroads on cities include Storeygard (2016); Gonzalez-Navarro and Turner (2018b); Gibbons et al. (2019); Baum-Snow (2020); Baum-Snow et al. (2020), and Jedwab and Storeygard (2021). Redding and Turner (2015) provides a comprehensive overview of much of this extensive literature.

production into the neoclassical monocentric land use theory of Alonso (1964) and Mills (1967), with some elements of the more recent quantitative spatial models summarized in Redding and Rossi-Hansberg (2017). Qualitative conclusions thus mirror those from the more targeted modeling frameworks in Bertaud and Brueckner (2005) and Henderson et al. (2021), though we put more emphasis on accommodating variation across cities in the marginal cost of height. The use of the simple monocentric city structure allows our model to reasonably characterize cities of many different sizes and shapes, in part as captured by differences in fundamental productivities and amenities. Our model parameterization uses as important inputs results from the more focused empirical studies of the cost of height (Ahlfeldt and McMillen, 2018) and returns to height (Koster et al., 2013; Danton and Himbert, 2018; Liu et al., 2018). These central parameters shape the verticality of cities in our model (Barr, 2010, 2012), with the dominant idea that tall buildings are a reflection of economic activity at the time they were built (Ahlfeldt and Barr, 2020). Curci (2020) provides evidence that skyscrapers catalyze nearby densification and productivity gains, with complementary evidence of within structure productivity advantages for tall buildings in Liu et al. (2020).

Much research on the existence and implications of housing market regulation has been carried out for developed economies, including Glaeser et al. (2005), Hilber and Vermeulen (2016), Baum-Snow and Han (2019), and Brueckner and Singh (2020), as summarized in Gyourko and Molloy (2015) and Duranton and Puga (2020). The more limited work for cities in the developing world has mostly come to the same conclusion, that height regulations are broadly binding and have negative welfare consequences. There is evidence in Brueckner and Sridhar (2012) for Indian cities, Brueckner et al. (2017) and Tan et al. (2020) for Chinese cities, Henderson et al. (2021) for Nairobi, along with Jedwab et al. (2020)'s meta-analysis for cities around the world. We provide a comprehensive quantitative evaluation of the extent to which reductions in the cost of building high have influenced affordability, rural-urban migration, productivity, and welfare for all cities worldwide. Moreover, we quantify the prospects for further gains through relaxation of existing height regulations.

The use of geological conditions as instruments has been common in the literature concerned with the economic (productivity and amenity) effects of urban density, as summarized by Ahlfeldt and Pietrostefani (2019). Similar to our empirical approach, a few studies in this literature use soil and subsoil geological conditions to instrument for density in the identification of agglomeration spillovers (Rosenthal and Strange, 2008; Combes et al., 2011). Like us, these papers argue that solid bedrock, or favorable geological conditions more generally, reduce the cost of building tall structures, leading to greater employment and population densities for reasons unrelated to features that may have a direct impact on productivity or amenities such as access to coastlines and navigable rivers. This paper builds on these ideas and the more direct evidence in Barr et al. (2011) and Barr (2016) to directly document the causal connections from bedrock depths to building heights, a required intermediate step to density that has heretofore not been comprehensively explored. The large applied agglomeration and urban growth literature, as summarized in Combes and Gobillon (2015), does not closely consider the requirements of the built environment for generating density. This lack of inquiry is likely due to the challenges

associated with putting together data appropriate for the analysis. Our estimates indicate that the lower costs of tall building construction have facilitated cities' vertical expansions as a central vehicle to densification and associated enhanced productivities and amenities. In recent decades, bedrock depth has become an important location fundamental predicting urban size, much like historic city locations and historically relevant topographical features predict the persistence of city locations to today (Davis and Weinstein, 2002; Bleakley and Lin, 2012).

2 Data and Descriptive Evidence

2.1 The Growth in Tall Buildings

Until the 1960s, the vast majority of the world's tall buildings (over 55 meters) were office buildings found in the largest cities of the highest income countries. Starting in the 1970s, the construction of tall buildings spread through many middle income countries and into medium sized and smaller cities worldwide. Moreover, most such construction was for residential rather than commercial use. Figure 1 depicts these patterns. As seen in the left panel, the world's total stock of tall building heights increased slowly from the 1890s, when the first tall buildings were built, until the 1970s. During our primary study period of 1975-2015, the total stock of heights in buildings for which we observe construction years increased from 868 km to 12,387 km. This growth corresponds to more than 90% of the total stock today and is about three times the distance between New York and Los Angeles. The total heights of residential buildings constructed 1975-2015 is seven times that of office buildings (right panel of Figure 1). While most buildings over 100 meters host offices, most buildings between 55 and 100 meters are residential.

Figure 1: Global Evolution of Aggregate Tall Building Heights, 1890-2021

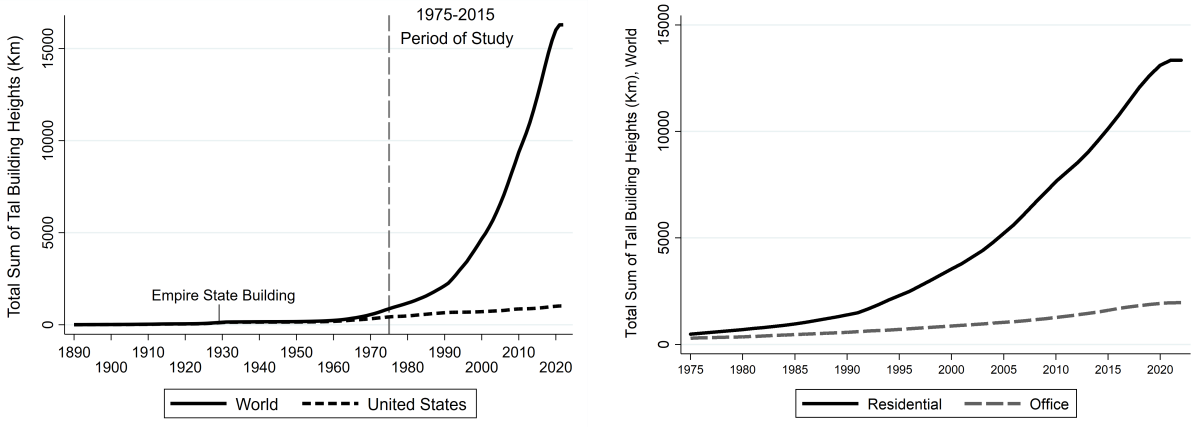

(a) All Tall Buildings

(b) Residential vs. Office Towers

Notes: The left panel shows the evolution of the total stock of tall building heights (km) for the world and the United States 1890-2021. The right panel shows the evolution of the total stock of tall building heights (km) separately for residential buildings and office buildings 1975-2021. Only buildings above 55 meters are included.

Figure 2 shows how widespread tall buildings have become around the world. For an exhaustive data set of 12,877 cities worldwide, it shows the aggregate heights of tall building in 1975 and 2015. While the highest stock cities included New York, Chicago, Hong Kong, Moscow, London, Sao Paulo and Philadelphia in 1975, in 2015 the list is dominated by Seoul, Hong Kong, Moscow, Sao Paolo, Singapore, New York, Guangzhou and Tokyo. In terms of absolute changes per capita 1975-2015, some of the most dynamic cities include Seoul, Hong Kong, Panama City, Singapore, Moscow, Kuala Lumpur, Dubai, and Tel Aviv, reflecting the spread of tall building construction to lower income economies.

The remarkable 1975-2015 tall building construction boom can be explained by both supply and demand factors. On the demand side, the 1975-2015 period saw both rapid urbanization and income growth in many countries. This has manifested as particularly strong demand growth in larger cities. On the supply side, there was technical progress in tall building construction, bringing costs down. Until the 1960s, most tall buildings were steel construction. In the 1970s, there was a shift toward concrete construction. Concrete buildings use lower cost materials but cannot be easily built as tall as steel construction buildings. In the 1975-2015 period, concrete accounts for 80 percent of height in new construction buildings over 55 meters, with the remainder about evenly split between steel and composite. As concrete is heavier than steel, more recently built tall buildings have required more robust foundations to accommodate the extra weight.

Figure 3 provides evidence on reductions in the cost of height over time. For this figure, we use building level data from Emporis on construction cost and floor area for the United States, described in more detail in the following sub-section. This figure is created in two steps. First, a construction cost index is created by residualizing city and decade of construction fixed effects from log cost per building floor area (excluding land acquisition costs). This residualization partials out local input cost differences across cities and over time. Second, this index is smoothed over construction year and building height using a bivariate Gaussian kernel (see Appendix A.1 for details). Because time effects are removed, construction cost per floor area is (approximately) mean 0 in each year. Therefore, this figure speaks only to the changes in construction costs in taller relative to shorter buildings.[5]

Evident in Figure 3 are steep declines in the cost of height over the past century that continued throughout our study period of 1975-2015. In 1975, buildings of 200 meters were on average 3.7% higher cost to build per square meter than 125 meter tall buildings. By 2015, that gap had fallen to just 1.3% greater. Appendix A.3 documents further evidence of secular declines in construction costs that were more rapid for tall buildings than shorter buildings, including in developing economies. Our supply model in Section 2.4 below specifies how a combination of such secular cost declines and variation in levels of demand for real estate across cities of different sizes can have precipitated the post-1975 boom in tall building construction documented in Figure 1 that has been particularly oriented toward the world's largest cities.

[5]We focus on buildings in the United States, as the increasing prevalence of tall buildings in lower income countries over time may introduce composition biases. Figure A1 shows similar patterns of secular decline in the cost of height for buildings in developing economies.

Figure 2: Sum of Tall Building Heights, World Cities, 1975-2015

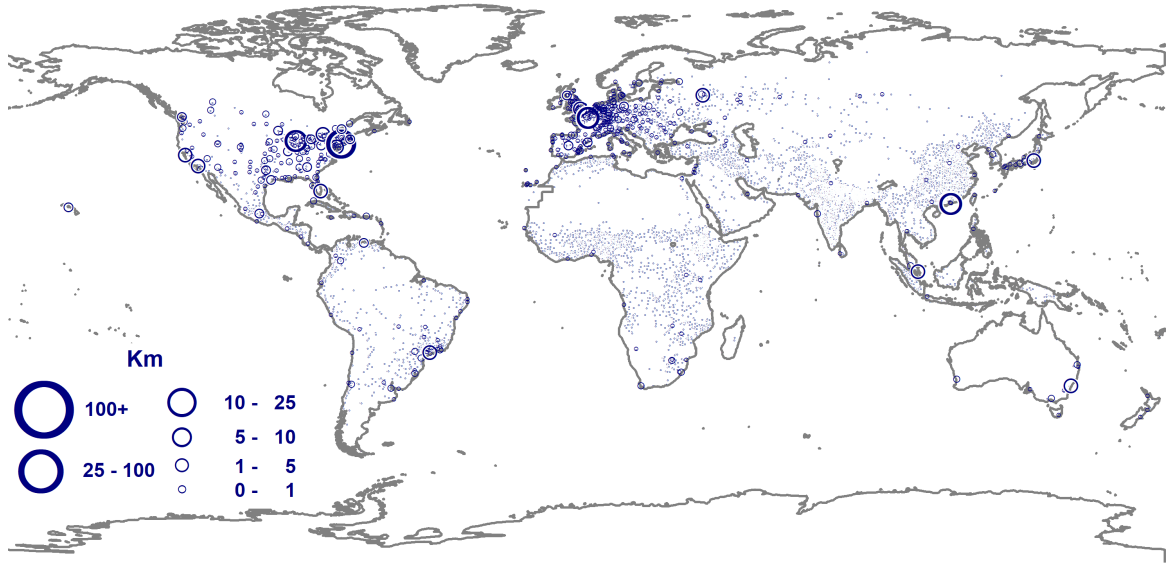

(a) 1975

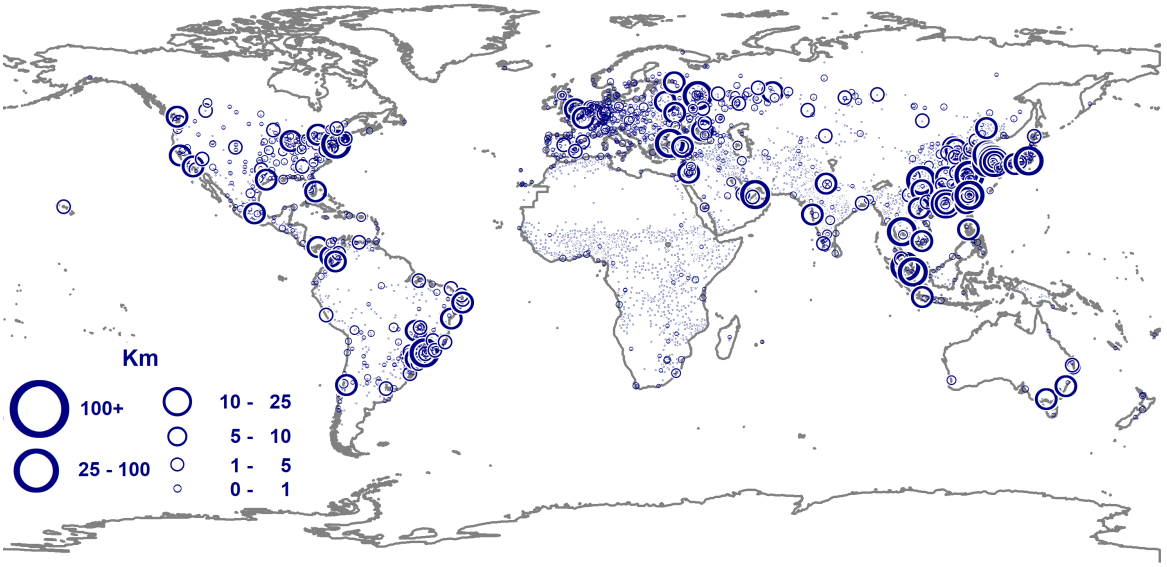

(b) 2015

Notes: This figure shows the total stock of tall building heights (km) for 12,877 world cities of at least 50,000 residents in 2015. Only buildings above 55 meters are included.

Figure 3: Trends in Construction Costs by Height: US

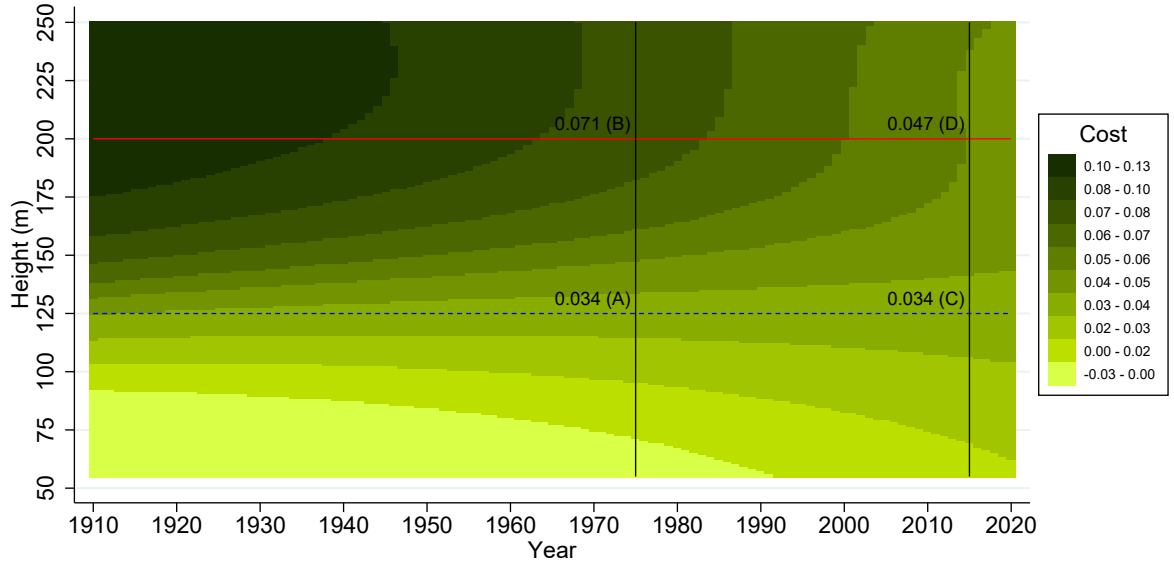

Notes: The sample includes 591 tall buildings in 93 US cities. Appendix Table A1 Panel A has summary statistics. "Cost" is the log cost per floor area, residualized for city fixed effects and decade of construction fixed effects. We use locally weighted regressions with a bivariate Gaussian kernel to estimate local means of the residualized cost measure within the height-bedrock plane with a bandwidth parameter for both covariates of $\kappa = 50$. Appendix Section A.1 provides details and results from locally weighted regressions with univariate kernels that deliver confidence bands for height categories that roughly correspond to the dotted blue line (125 meter building) and the solid red line (200 meter building).

2.2 Data Sources

The empirical analysis uses historical information about urban agglomerations and building heights for 12,877 cities worldwide, 11,273 of which are in developing economies. Also incorporated into the data set are information on city bedrock depth and lights at night. Below we briefly describe each data source.

City Boundaries and Population: Using the *Global Human Settlements-Urban Centre Database* (GHS-UCDB) (Florczyk et al., 2019, version 1.2 from 18/04/2020), we obtain the GIS boundaries of all 12,877 current agglomerations of at least 50,000 inhabitants worldwide, which they call "urban centres" (UCs). These UCs correspond to commuting zones, as in US metropolitan statistical areas.[6] The GHS-UCDB reports the (satellite-based) total *land area* and *built-up area* of each city circa 1975, 1990, 2000 and 2015. Using the built-up area and population census data, the GHS-UCDB also reports population estimates for each city in these same years. As built-up area is more consistently measured over time, this is our main measure of urbanized land. The 12,877 cities account for about 90% of the world's total urban population in 2015 (United Nations, 2018).

Building Heights and Construction Costs: Emporis (2022) (last accessed 02-07-2022) was a global provider of international skyscraper and high-rise building data.[7] Emporis collected information about the full life-cycle of each building, from conception to demolition, covering

[6] We refer to "UCs", "agglomerations" and "cities" interchangeably. For example, the New York UC includes "New York; Islip; Newark; Jersey City; Yonkers; Huntington; Paterson; Stamford; Elizabeth; New Brunswick."

[7] Since September, 2022, information in the Emporis data has been integrated into CoStar Group data products.

thousands of cities worldwide. The database contains data for 693,855 "existing [completed]" buildings.[8] For almost all buildings, we know the exact geographic coordinates, or at least the city in which it is located. This allows us to assign each building to a city in the GHS-UCDB data set. Since we know the year of construction (and demolition if demolished), we obtain the total *sum of heights* for each city-year from the 1890s, when the first tall buildings were constructed, to date. For a select set of 1,053 buildings, the Emporis data set also reports the building's construction cost, though 20 of these do not have floorspace information.

Inspection of the kernel density of 2015 building heights in the Emporis data set (Figure A2) reveals a mode and large spike at 55 meters. Since cities are likely to have more buildings below than above 55 meters, and since the distribution of buildings is relatively smooth after 55 meters, we infer that the data set likely only captures the universe of buildings above 55 meters. As such, our *sum of heights* measure for each city and year only includes buildings of at least 55 meters.

To account for the fact that many cities have no buildings above 55 meters in some years, we primarily use $\ln(\text{Heights}+1)$ to measure the sum of heights in each city. However, all results are robust to using scaling factors other than 1, the inverse hyperbolic sine transformation, or an indicator for whether the city had any tall buildings as alternative measures of city heights. Our empirical approach thus essentially treats heights in the base year in many cities as 0, especially for the sub-sample analysis that uses cities in developing economies only.

Bedrock Depth: Shangguan et al. (2017) reports bedrock depth in meters at a 30 second ($\approx$ 1 km) resolution for the entire world. (For example, there are 8,118 such pixels in the New York UC). We use calculate *mean bedrock depth* in meters (MBD) for each city within its 2015 boundary. Shangguan et al. (2017) indicates "this data set is based on observations extracted from a global compilation of soil profile data (about 1,300,000 locations) and borehole data (about 1.6 million locations)." Looking across all pixels within our city boundaries, 80% of the variance in bedrock depth is between rather than within cities in our data. For pixels within cities of at least 300,000 people in 2015, a Theil decomposition indicates that about three-quarters is from between city variation. Our results are not sensitive to the use of mean bedrock depth across all pixels in each city or the bedrock depth at each city's central business district inferred from the brightest cluster of lights at night pixels.

Lights at Night: While our main analysis considers city population and built area 1975-2015, we also study the effects of tall building construction on lights at night, for which only more recent data are available. Night lights data corresponding to the DMSP satellites are provided by NGDC (2015). We use the radiance calibrated version of this data, which is available for select years 1996-2011, to avoid issues related to top-coding.[9] The data are available at a fine spatial resolution and we use GIS to calculate *total sum of lights at night* across pixels for each city.

[8] We only consider buildings of the following types: "building with towers", "high-rise building", "low-rise building", "multi-story building", and "skyscraper".

[9] This data set records levels of luminosity beyond the normal digital number upper bound of 63.

2.3 Patterns of Vertical Growth in the Data

In 1975, 5% of cities in our full sample had any tall buildings, including only 1% of cities in the developing world. The cities that did have tall buildings were mostly large and in the developed world. Of the 515 cities over 500,000 people in 1975 in our full sample, 41% had at least one tall building. But among the 347 large cities in the developing world, only 23% had any tall buildings. Between 1975 and 2015, cities of all sizes built some tall buildings, but this growth was disproportionately oriented toward larger cities. Only 2% of cities under 100,000 built their first tall buildings in the 1975-2015 period. This number rises to 13% for cities of 100,000-500,000 and 32% for cities over 500,000, despite both of these groups having larger 1975 fractions with tall buildings.

These patterns also hold conditional on bedrock depth and for heights measured in meters, growth rates, or at the extensive margin. For example, among cities of fewer than 100 thousand people in 1975, the average city with medium depth bedrock built 63 meters of heights in buildings over 55 meters, whereas in the largest cities (over 500 thousand people in 1975) the average city built 26.5 km of heights between 1975 and 2015. In the following sub-section, we formally interpret this pattern, which is monotonic in 1975 city population, as reflecting the fact that technical progress, which reduced the marginal cost of height, allowed the greater levels of real estate demand in larger cities to be accommodated by building taller.

Conditional on 1975 city population, we see more tall building construction in cities on intermediate bedrock depths. Between 1975 and 2015, the average large city on mean bedrock depths below 10 meters built 5.2 km of tall buildings, relative to the 26.5 km built in cities on intermediate bedrock depths cited above. Among small cities on shallow bedrock depths, only 9 meters of heights were built, relative to the 63 meters on intermediate bedrock depths cited above. We note that the costs of installing foundations to support tall buildings depend more on soil conditions in areas where bedrock is very deep. As a result, there is more dispersion in height growth among cities on deep bedrock, meaning that they provide less identifying power than do cities on bedrock depths below 30 meters. Nonetheless, mean 1975-2015 height growth is lower in these deep bedrock cities than those on intermediate bedrock conditional on 1975 population.

Rapid 1975-2015 urbanization rates around the world manifested as population growth of 46% and built area growth of 55% in the average city. Our empirical results will indicate that this decline in average population density would have been even greater absent the contemporaneous boom in tall building construction, especially in the largest cities. On average across our sample, the typical city added 895 meters of heights on a base of 67 meters in 1975, with almost all of this growth among cities in the top tercile of the city size distribution. Table A2 presents means of our key outcome variables and three measures of city aggregate height of buildings over 55 meters tall by categories of 1975 city population and city mean bedrock depth (MBD).[10]

[10]The final column in Table A2 shows that height growth was greater in cities of over 500 thousand residents in 1975 than in those cities with between 100 and 500 thousand residents at all three indicated bedrock depths. Differencing relative height growth between intermediate and shallow bedrock depths, we see that larger cities on intermediate depth bedrock experienced more rapid 1975-2015 height growth than did those cities on shallow

2.4 The Data Generating Process for Heights

Here we demonstrate conceptually how greater levels of real estate demand, more favorable bedrock depths, and secular declines in the marginal cost of height have interacted to generate more tall building construction in certain cities. In 1975, only a few very high demand cities had tall buildings. With technical progress and declines in the marginal costs of height, it became viable for more cities to host tall buildings. This increased viability was particularly true for high population cities, where demand was high, with favorable intermediate bedrock depths, where costs of height were lower. As a result, we see more robust height growth in large relative to small cities with intermediate relative to low or high bedrock depths. This triple difference idea, which compares cities of different 1975 populations and bedrock depths over time, leads into our instrumental variables strategy of using 1975 log city population interacted with a flexible function of bedrock depth as a source of exogenous variation in the 1975-2015 growth in building heights across cities.

Having established above that the marginal cost of height secularly declined after 1975, the next step is to provide evidence on how the cost of height is related to bedrock depth in cross-sectional comparisons. Structural engineers have a simple rule of thumb known as Rankine's Theory which indicates the depth of a building's foundation required for stability. Rankine's Theory lays out a proportional relationship between building weight (which is roughly proportional to height) and foundation depth, with the constant of proportionality differing as a function of soil conditions around the foundation. According to Rankine's Theory, the optimal foundation depth is around 10% of the building's height. In order for a building to be stable, the bottom of the foundation must either be anchored to bedrock, have a sufficiently wide base ("raft"), or incorporate many very deeply bored piles. As rafts and numerous deeply bored piles are more costly to construct and install, builders prefer to anchor to bedrock if it is not too deep. However, if bedrock is within only a few meters of the surface, expensive blasting is required to install the foundation. Figure A3 provides a visualization.

Central to our empirical approach is the observation that construction cost per square foot varies with both building height and bedrock depth. Figure 4 provides descriptive evidence on how construction cost varies with bedrock depth. It is constructed using the same methods as Figure 3, with the bivariate smoothing of residualized log construction cost per building floor area performed over bedrock depth and building height. It uses all buildings worldwide for which we have construction cost data.

Figure 4 depicts both the non-monotonicity of construction costs in bedrock depth conditional on height and the rate at which construction costs increase in height. The descriptive evidence is that the cost-minimizing bedrock depth for 125 meter tall buildings is 18 meters (blue lines), while that for 200 meter tall buildings is 25 meters (red lines). Constructing a 125 meter tall building at the optimal bedrock depth saves more than 5% in cost per square meter relative to building on surface level or very deep bedrock. The associated cost savings are much larger for

bedrock. We note that secondary Chinese cities are heavily over-represented in the deep bedrock category for large cities at the bottom of Column (3). In many of these locations, the post-1990 construction boom did not respond to market forces.

200 meter tall buildings. Moreover, Figure 4 shows that unit costs increase in building height much more rapidly where bedrock is deep. (Appendix A.2 has further discussion).

Figure 4: Construction Cost as a Function of Height and Bedrock Depth

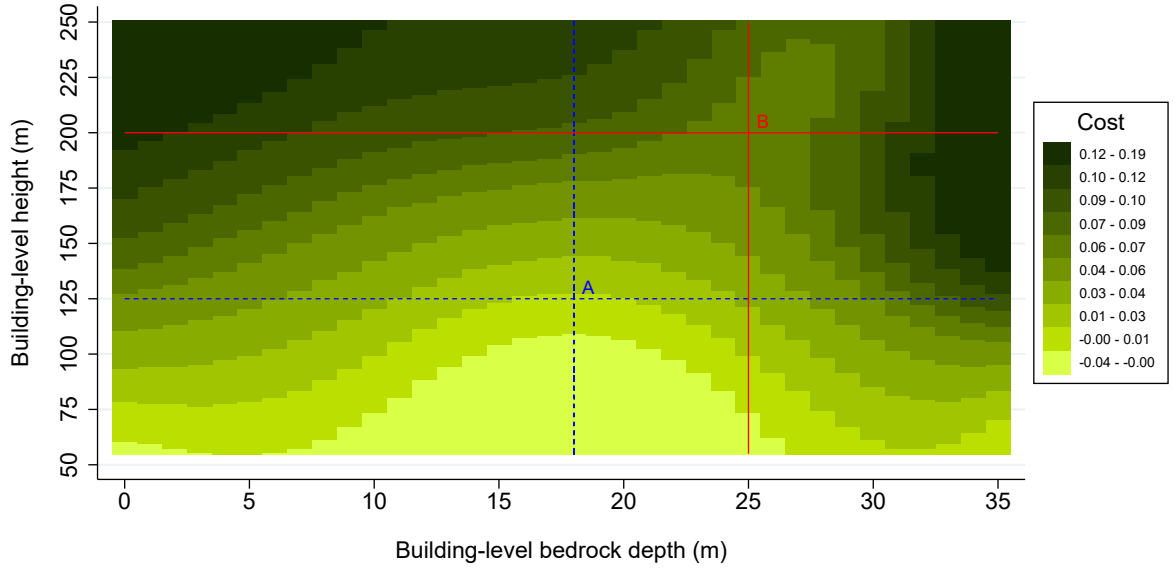

Notes: The sample includes 1,033 tall buildings in 206 world cities and 55 countries. Table A1 Panel B has summary statistics. "Cost" is the log cost per floor area residualized for city fixed effects and country-by-decade of construction fixed effects. Locally weighted regressions with a bivariate Gaussian kernel are used to estimate local means of the residualized cost measure within the height-bedrock plane. We set the bandwidth parameter for bedrock, b, to $\kappa^b = 6$ and for building height, h, to $\kappa^h = 40$, which corresponds to about one third of the standard deviation of each respective covariate. We topcode height at the upper limit on the graph, so 250 m includes all buildings of at least 250 m. Appendix Section A.1 provides details and results from locally weighted regressions with univariate kernels, delivering confidence bands for height categories that roughly correspond to the blue dotted line (for a 125 meter tall building) and the red solid line (200 meters).

The engineering evidence thus suggests that a reasonable approximation of the cost function for developing a building of height S on bedrock depth B_{ac} in city a of country c at time t is

$$C_{act}(S) = c_{act} S^{1+\theta(B_{ac},\psi_t)}. \tag{1}$$

To be consistent with patterns seen in Figure 3, we allow the elasticity of unit cost with respect to height, $\theta(B_{ac}, \psi_t)$, to change over time, as governed by the ψ_t parameters. To be consistent with patterns seen in Figure 4, we allow both the elasticity of unit cost with respect to height and the cost shifter c_{act} to depend on bedrock depth. It is evident from Figure 4 that, commensurate with the engineering discussion, the marginal cost of height per square meter is greater at low and high bedrock depths, meaning that θ is U-shaped in B_{ac} and $\theta_{BB} > 0$. As c is non-parameterically indexed by city and time, it incorporates differences in bedrock depth in addition to labor and materials costs that may change over time. To maintain tractability and simplicity, we maintain separability of time effects from bedrock depth effects in the elasticity of unit cost with respect to height.

To corroborate the descriptive evidence in Figure 4 that θ is U-shaped in B, we recover rough non-parametric estimates of the $\theta(B, \psi)$ function with our limited construction cost data. We regress log construction cost per floor area on building height for each bedrock depth using an instrumental variables locally weighted regression (IV-LWR) approach. Distance to the central

business district (CBD) instruments for building height with controls for city and country-decade fixed effects. As in Ahlfeldt and McMillen (2018) and Ahlfeldt and Barr (2022), identifying variation comes from comparing construction costs of different buildings in the same city exposed to approximately the same bedrock depth but at different CBD distances. The result, depicted in Figure A5, supports the engineering-based hypothesis that bedrock at intermediate depths is associated with lower marginal costs of height. Estimates of θ range from 0.1 at intermediate bedrock depths to 0.9 at very low and moderate depths, and more than 1.0 at high depths. These results support the idea that cities with bedrock in an intermediate range will have a greater ease of accommodating high real estate demand, resulting in lower barriers to growth. Details of this estimation procedure and results are in Appendix A.2.

As construction cost differs by bedrock depth, the profit maximizing level of height also differs by bedrock depth conditional on demand conditions. Competitive building developers have the following profit function associated with building to height $S(x)$ at location x in city ac at time t.

$$\pi_{act}(S,x) = \int_0^S p_{act}(x,s)ds - C_{act}(S) - r_{act}(x). \tag{2}$$

$p_{act}(x,s)$ is the sales price per unit of real estate at location x and height s and $r_{act}(x)$ denotes the fixed cost component of development, which includes both the land price and any regulatory development costs at location x. In Section 4, we lay out a demand structure that justifies the separable form $p_{act}(x,s) = p_{act}(x)s^{\omega}$, where ω is positive and close to 0. (In particular, for the model to be well-behaved we need that $\theta > \omega$.) A positive ω reflects the amenity value associated with improved views and reduced noise.[11] Profit maximization yields the log of the optimal height S^* that depends on the price per unit of real estate services and cost factors.

$$\ln S^*(p_{act}(x), c_{act}, B_{ac}, \psi_t) = \frac{1}{\theta(B_{ac},\psi_t) - \omega}\left(\ln \frac{p_{act}(x)}{c_{act}} - \ln\left[1 + \theta(B_{ac},\psi_t)\right]\right) \tag{3}$$

This expression highlights the fact that the developer's choice of log height depends on the interaction between bedrock depth, as included in $\theta(B_{ac},\psi_t)$, and the level of demand, as included in $p_{act}(x)$.

To understand how optimal heights differ across space within cities, it is convenient to impose some restrictions on the $p_{act}(x)$ function. Following the model developed further in Section 4, we impose that the price per floor area of real estate declines in CBD distance x.

$$p_{act}(x) = p^0_{act} f(x;\rho_{ac}) \tag{4}$$

Each city a in country c at time t faces its own real estate demand conditions, leading us to index CBD rents by this triplet. Each city also has its own transport network driving accessibility to the center, leading us to index the advantages of being near the center by city, where $f'(x;\rho_{ac}) < 0$ and ρ_{ac} governs the city-specific accessibility advantages to the center.

[11] Evidence for both commercial and residential buildings indicate that real estate prices and rents are typically greater on higher floors of tall buildings, reflecting the amenity value of height (Liu et al., 2018; Ben-Shahar et al., 2022; Nase and Barr, 2023).

Equation (3) lays out the logic behind our triple difference empirical strategy as implemented with IV. First, compare locations in two cities in 2015 at a given CBD distance x that are identical in all ways, including the same favorable bedrock depth of 20 meters, except for their CBD rents p^0_{act}. The difference in $\ln p^0_{act}$ between these two cities captures their difference in real estate or height demand. That is the first difference. Second, consider an analogous pair of cities with the same gap in $\ln p^0_{act}$ but with a less favorable bedrock depth of 0 meters. The form of the θ function documented above indicates that these second two cities have a smaller gap in heights, as the elasticity of height with respect to price has an inverse-U shape in bedrock depth. This is the second difference, which can be derived by calculating $\frac{\partial^2 \ln S^*}{(\partial \ln p^0)(\partial B)}$. Finally, the secular decline in the cost of height over time manifests as a reduction in ψ_t. This reduction has facilitated taller construction in high demand locations, *and particularly so in cities with favorable bedrock*. This is the third difference. Differentiating (3) with respect to $\ln p^0_{act}$ then B_{ac} then ψ_t derives this result, given that $d\psi_t < 0$. In 1975, building tall was very costly everywhere. As the marginal cost of height declined for all cities, it is the locations with strong demand conditions *and* favorable bedrock depths that are predicted to increase their heights the most.

We are now in a position to characterize aggregate city building heights as observed in the Emporis data. As real estate prices decline in CBD distance, each city has a unique endogenous distance cutoff within which buildings of over 55 meters exist in each year. (In some cities, this cutoff is 0.) Call this distance cutoff x^{55}_{act}. Then the total stock of heights in city a at time t is

$$H^{55}_{act} = \left(\frac{p^0_{act}}{c_{act}(1+\theta(B_{ac},\psi_t))} \right)^{\frac{1}{\theta(B_{ac},\psi_t)-\omega}} \int_0^{x^{55}_{act}} f(x;\rho_{ac})^{\frac{1}{\theta(B_{ac},\psi_t)-\omega}} \mathcal{L}_{ac}(x)dx \tag{5}$$

In this expression, $\mathcal{L}_{ac}(x)$ is a city-specific function that captures the amount of land that can be developed at each distance. For example, it is $2\pi x$ for a circular city. The integral covers the land in use for tall buildings. This equation shows that the aggregate height in a city depends on the same factors as the profit-maximizing level of height at each specific location.

Following the comparative statics on $\ln S^*$ in Equation (3) for each location within x^{55}_{act} delivers an aggregate of the location-specific gaps, which must follow the same pattern. Cities with greater heights at all locations x must also have a greater aggregate stock of heights when adding up over the same range of x. In addition, any city with a greater height at any location x must also have a greater CBD distance cutoff x^{55}_{act} beyond which heights are below 55 meters, representing an additional force increasing the gap in aggregate heights.

2.5 Predicting City Level Height Growth

Evidence in the prior sub-section indicates that more height should be constructed in larger cities, and even more so in those with favorable bedrock depth. Moreover, this phenomenon should have strengthened over time. We demonstrate these patterns empirically by graphing

estimated coefficients γ_b in the descriptive regression

$$Const_{ac} = \sum_b \gamma_b \left[\ln Pop_{ac75} \mathbb{1}(b \leq MBD_{ac} < b+5)\right] + \delta \ln Pop_{ac75} + \kappa_c + \phi_{b(ac)} + \epsilon_{ac},$$

where b = {0,5,10,...}. The dependent variable is 1975-2015 construction in city a of country c with mean bedrock depth MBD_{ac} binned into 5 meter ranges. Construction is measured either as whether the city had any tall buildings in 2015 but not 1975 or as the change in the log sum of heights in the city. A separate construction elasticity is estimated for each bedrock bin b, and we include bin and country fixed effects. As the regression controls for ln city population, all γ_b coefficients are of the bin-specific impact of 1975 ln population on 1975-2015 construction relative to the population impact in the 0-4 meter bedrock depth bin.

Coefficient estimates γ_b are graphed in Figure 5. Bubble sizes are proportional to the number of observations. Statistical significance (relative to 0) is indicated with stars. Quadratic and more flexible fractional polynomial lines of fit are also indicated.

Figure 5: Relationships Between Tall Buildings and ln 1975 Population by Bedrock Depth

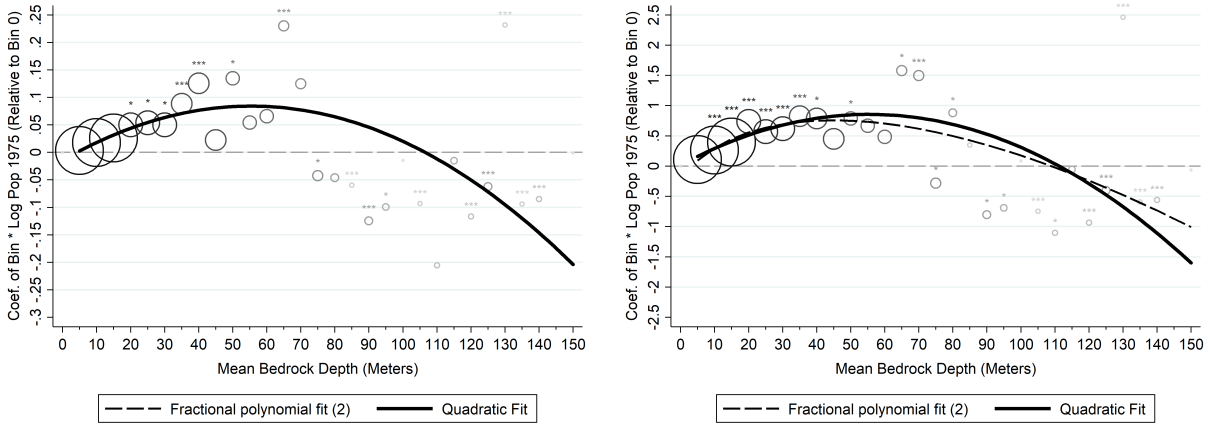

(a) Any Tall Building Construction

(b) Δln(Heights+1)

Notes: Panel A graphs coefficients on ln 1975 city population for each 5 meter bin of city-level mean bedrock depth in which the dependent variable is an indicator for whether the city had any height growth 1975-2015. Panel B graphs analogous coefficients in which the dependent variable is the 1975-2015 change in the log sum of heights plus one. The size of the bubbles indicates the relative number of city observations in each bedrock depth bin. The stars indicate how significantly different from 0 each bin-specific coefficient is. The quadratic fit and the fractional polynomial fit (degree = 2) are weighted using the number of city observations in each bin. Similar graphs with dependent variables measured as levels in 1975 are much flatter in bedrock depth than counterparts using 2015 levels (Figure A6).

Figure 5 shows the inverse U shaped impact of city mean bedrock depth on construction in strong relative to weak demand cities. In particular, the probability of having new tall building construction in response to a doubling of population is about 0.1 higher at a bedrock depth of 30-34 than at 0-4. Similarly, the elasticity of height growth with respect to 1975 population is about 0.65 greater for cities in the intermediate range of bedrock than the low or high ranges. As the quadratic fit (solid line) is similar to the more flexible fractional polynomial fit (dashed line), most of the empirical work uses a quadratic parameterization. We note that as 90% of

cities are in the range of bedrock between 0 and 30, the upward-sloping portion of the population elasticities in bedrock depth seen in Figure 5 provides most of the identifying variation. The supply model predicts that the pattern seen in Figure 5 should be strongest in 2015 and muted in 1975. This is exactly what we see, as shown in Figure A6.

Put together, the first stage estimation equation takes the following form.

$$\begin{aligned} Const_{ac} = k_1 MBD_{ac} + k_2 MBD_{ac}^2 + \delta \ln Pop_{ac75} \\ +\gamma_1 MBD_{ac} \times \ln Pop_{ac75} + \gamma_2 MBD_{ac}^2 \times \ln Pop_{ac75} + \\ +X_{ac75}\xi + \kappa_c + \epsilon_{ac} \end{aligned} \tag{6}$$

The key components of this equation are the interactions with coefficients γ_1 and γ_2. These indicate how the elasticity of construction with respect to population differs by bedrock depth. In (6), the dependent variable can be measured in levels or as 1975-2015 growth.

Table 1 presents the first stage coefficients on city mean bedrock depth interacted with log 1975 city population. Panel A is for cities in all countries and Panel B is for cities in developing economies only. The first two columns show results for an indicator of whether any tall buildings were constructed by the indicated year. The third column shows the difference. The next two columns are analogous except the log of tall building heights plus one in each year is the dependent variable. The final column shows results for the 1975-2015 change. Table A3 reports remaining first stage coefficients.

Table 1: First-Stage Estimates: Main Coefficients

	Tall Building Indicator			ln (Heights + 1)		
	1975	2015	Δ 1975-2015	1975	2015	Δ 1975-2015
	(1)	(2)	(3)	(4)	(5)	(6)
	Panel A: All Countries (Observations = 12,849)					
Bedrock Depth (m)	0.0018***	0.0046***	0.0028***	0.0126***	0.0402***	0.0276***
× ln Pop 1975	[0.0005]	[0.0007]	[0.0007]	[0.0032]	[0.0062]	[0.0054]
(Bedrock Depth)^2	-0.0000***	-0.0000***	-0.0000**	-0.0002***	-0.0003***	-0.0002**
× ln Pop 1975	[0.0000]	[0.0000]	[0.0000]	[0.0000]	[0.0001]	[0.0001]
Adj. R-Squared	0.12	0.23	0.07	0.17	0.33	0.17
	Panel B: Developing Economies (Observations = 11,257)					
Bedrock Depth (m)	0.0004	0.0036***	0.0032***	0.0030	0.0292***	0.0262***
× ln Pop 1975	[0.0005]	[0.0007]	[0.0007]	[0.0028]	[0.0060]	[0.0056]
(Bedrock Depth)^2	-0.0000	-0.0000***	-0.0000**	-0.0000*	-0.0002**	-0.0002**
× ln Pop 1975	[0.0000]	[0.0000]	[0.0000]	[0.0000]	[0.0001]	[0.0001]
Adj. R-Squared	0.13	0.24	0.13	0.14	0.29	0.22

Notes: Each column is a separate regression of the variable indicated at top on the variables indicated on the left, a quadratic in mean city bedrock depth, log 1975 city population, and 179 country fixed effects. Developing economies are economies that were not "high-income economies" according to the World Bank's classification of countries as of 2015. The remaining coefficients are reported in Table A3. Robust standard errors in brackets.

Evident in Table 1 is that coefficients on the interaction between mean bedrock depth and population (γ_1 and γ_2) grow in magnitude over time for both outcomes. Analogous results for

1990 and 2000 reveal that this growth is monotonic in year (not reported). Also of note is that γ_1 and γ_2 are estimated to be approximately 0 in 1975 in developing economies. These locations had very little height in 1975 regardless of bedrock conditions or population. Therefore, for developing country cities, to a first approximation one can view our analysis as using the 2015 level of tall building height as the key measure of the 1975-2015 change in heights.

Before discussing the main results, we consider the implications of these first stage results for identification of causal impacts of heights on urban structure. The main idea for identification is that bedrock depth is a supply factor that is uncorrelated with factors driving demand for height at the city level. However, in order to operationalize this idea, it turns out to be important to interact bedrock depth with a measure of static demand strength, for which we use ln 1975 city population. Bedrock depth by itself is not a strong enough source of identifying variation to generate first stage predictions of height or height growth that are sufficiently powered to be useful in determining causal effects of heights.

Given the need to use interactions as the source of identifying variation, the key identification assumption is more subtle than simply that bedrock is exogenous to city demand shocks. Instead, the identifying assumption is that historically larger cities on more favorable bedrock did not change in different ways from historically larger cities on less favorable bedrock relative to historically smaller cities on favorable relative to unfavorable bedrock. This double difference over time (making a triple difference) is the key argument needed for identification.

As such, any threats to identification would come from correlations between bedrock and latent city demand growth that was different for large and small cities. This would occur if bedrock depths more favorable for tall building construction also somehow allowed large cities to have greater post-1975 growth potential. Our empirical analysis in the following section examines the potential for such omitted variable bias to exist.

3 Empirical analysis

For 12,877 agglomerations a in 182 countries c, long difference regressions of the form in (7) make up the heart of our empirical analysis. Our primary dependent variables of interest y_{ac} are the 1975-2015 growth rates of population or built-up area in agglomeration a of country c.[12] Controls for a quadratic in mean city bedrock depth, log 1975 city population, and country fixed effects are included.

$$y_{ac} = \beta \Delta \ln \left(Heights_{ac} + 1 \right) + \alpha_1 MBD_{ac} + \alpha_2 MBD_{ac}^2 + \alpha_3 \ln Pop_{ac75} + \kappa_c + \varepsilon_{ac} \qquad (7)$$

We primarily examine IV versions of this estimation equation, in which log population in 1975 interacted with a quadratic in city mean bedrock depth enters as instruments for $\Delta \ln \left(Heights_{ac} + 1 \right)$.

[12] An alternative option is to specify (7) as a regression of an outcome measured in 2015 on 2015 heights and indicated controls plus the dependent variable in 1975. Because the sum of heights in 1975 is near 0 in the vast majority of cities in our sample, this alternative specification yields very similar results.

As is formalized in the model in the following section, one can view (7) as capturing differences in the quantities of real estate demanded for cities with different amounts of heights that are exogenously assigned due to differing supply (construction cost) conditions. One central parameter that influences these responses is the elasticity of population with respect to urban utility ($\tilde{\zeta}$). In a closed city, in which $\tilde{\zeta}$ is 0, the real estate supply shock from the lower cost of height manifests as lower floorspace rents and shorter commutes, a clear welfare gain for city residents. Empirically, this scenario maps to a large negative built area elasticity and a zero population elasticity, both with respect to city heights. As ζ grows, in-migration responds more, thereby bidding up rents and lengthening commute times. The result is smaller welfare gains for city residents but more opportunities for outsiders to benefit from the city's improved infrastructure. Empirically, this means larger positive population responses and smaller magnitude negative built area responses.

The inclusion of the mean bedrock depth controls in (7) is not necessary for identification but does make identification stronger. Without these controls, we would be relying on their exclusion from the demand equation for heights for identification. While we think it is reasonable that bedrock depth is not a demand factor, bedrock depth on its own does not provide much identifying variation in heights. Instead, we need to interact bedrock depth with a level demand factor, for which we use 1975 ln city population, in order to predict supply shocks to heights with sufficient power. For this reason, we leave in the bedrock depth controls in (7). However, excluding them does not affect any of our results.

We note that OLS estimates of β in (7) are muted relative to IV estimates at 0.05 for the population outcome and -0.09 for the built area outcome. As standard threats to identification would typically bias both OLS coefficients in the same direction, we conclude that these smaller magnitudes primarily reflect measurement error in heights. If demand factors were a central driver of city growth in heights, conditional on controls, the OLS population and built area elasticities would both be biased upwards. IV estimates that correct this endogeneity problem would thus be smaller (or more negative) than corresponding OLS estimates for both outcomes. Instead, measurement error, which seems sensible, would lead to attenuation bias. By only using buildings over 55 meters tall to measure heights, we do not measure all buildings that are relevant to real estate supply. There are also many idiosyncracies across cities in tall building construction that are disconnected from fundamental supply and demand forces. On the taller side, this includes prestige skyscrapers that are not by themselves economically viable. On the shorter side, local zoning regulations may lead to considerable construction up to a cap that is high but below 55 meters in some cities. By isolating common supply factors for identification, we smooth out these idiosyncracies, thereby increasing the magnitudes of estimated coefficients.

3.1 Main IV Results

Table 2 presents our headline empirical results. Panel A shows results for all cities and Panel B shows results for cities in developing economies only. Column 1 shows that a 100 log point increase in heights leads to about a 12 percent increase in city population. This magnitude of

height increase is the average for cities in the top tercile of 1975 population, while the average city had 1975-2015 height growth of 46 log points. The second column of Table 2 shows that a 100 log point increase in heights caused the built-up land area of a city to decline by about 17 percent. This is very similar to the 15 percent response for total city area (Column 3). Putting the results in Columns 1 and 3 together, it is clear that exogenous height growth has substantially increased population density. When population density is explicitly put on the left-hand side of the regression, the estimated heights coefficient is 0.27 (Column 4), matching the population coefficient in Column 1 minus the area coefficient in Column 3. Results for developing economies, representing 87% of the cities in our data, are very similar to those for the full sample. The final column of Table 2 shows results for the growth rate in the total sum of lights at night 1996-2011, a measure of total city economic growth due to heights. This is not significantly different from the population growth result in the first column. Lights per capita is also estimated to positively respond to heights, with an elasticity of 0.04 (or 0.06 for developing economies), but is not statistically significant (unreported).[13]

Table 2: Main IV Results

Period *s-t*:	Δ ln Population 1975-2015	Δ ln Built Area 1975-2015	Δ ln Urban Area 1975-2015	Δ ln Pop Dens. 1975-2015	Δ ln Lights 1996-2011
			Panel A: All Countries (Observations = 12,849)		
Δ ln(Heights+1)	0.12***	-0.17***	-0.15**	0.27***	0.15***
	[0.03]	[0.04]	[0.06]	[0.07]	[0.06]
First Stage F	28.42	28.42	28.42	28.42	16.83
			Panel B: Developing Economies (Observations = 11,257)		
Δ ln(Heights+1)	0.13***	-0.16***	-0.18**	0.31***	0.17***
	[0.03]	[0.04]	[0.08]	[0.08]	[0.06]
First Stage F	22.84	22.84	22.84	22.84	16.32

Notes: Each entry is from a separate regression of the indicated variable at top using the full sample in Panel A and cities in developing economies only in Panel B. Equation (7) shows the regression specification used. The final column uses $\Delta \ln(\text{Heights} + 1)$ for 1990-2015. Table A4 reports coefficients on control variables for Panel A. Population density is defined using total urban area. Robust standard errors in brackets.

Next, we demonstrate that these baseline results are robust to inclusion of additional demand side controls, functional forms, and the measure of bedrock depth used. We then justify our interpretation of these results as treatment effects that apply broadly across cities of different types and provide evidence that they primarily reflect urban growth rather than redistribution.

Robustness to Additional Controls: One potential concern is that trends in the amenity value of cities, or other demand factors, may be differentially correlated with bedrock depth in large versus small cities. However, inclusion of additional controls for infrastructure and regional connectedness, which we similarly interact with log city population size in 1975, does not affect results. These infrastructure controls are the presence of subways and measures of market access

[13] Correcting standard errors for arbitrary spatial autocorrelation using a triangular kernel out to 200 km or 400 km, or clustering at the administrative level, up to doubles standard errors and does not affect inference. The built area equation coefficients are more sensitive to these standard error adjustments (Table A5).

in 1975. Alternatively, we can drop subway cities in 2015. Controls for location and geography, including coastal proximity, lakes, agricultural suitability, and temperature, also do not affect results. Estimates also hold when controlling for distance to mines and/or oil and gas fields, or excluding cities within 50 km of either.[14] More generally, locations with shallow bedrock may find it more costly to develop their agricultural sector or expand their infrastructure. However, results hold excluding cities on bedrock up to 6 meters deep, the 25th percentile of the bedrock depth distribution.[15] Finally, using 100 meters rather than 55 meters as the height cutoff to define tall buildings also has no effect on results. Table A6 presents all of these results for the full sample and cities in developing economies only. Results are similarly robust to dropping cities within 50 km of the coast or a lake, at high altitudes (750 meters, 1000 meters, or 1400 meters), or above the 75^{th} or 90^{th} percentiles of ruggedness.

Functional Forms: Our baseline specification uses mean bedrock depth and its square interacted with log city population in 1975 as instruments. Bedrock depth and its square are then added as controls, though results also hold if we add them as instruments instead (Table A7 Columns 1 and 5). That is, our IV strategy imposes a quadratic form for the height impact of bedrock depth in larger cities. The standard monotonicity requirements for instrument validity are thus somewhat opaque. Moreover, it is not clear whether key identification comparisons are between shallow or deep bedrock cities against intermediate depth bedrock cities, or whether both types of comparisons are needed simultaneously to identify parameters of interest.

Results in Tables A8 and A9 demonstrate that our instrumental variables strategy respects monotonicity conditions and that either or both types of bedrock depth comparisons can be used for identification. To show this, we replace the bedrock depth polynomial with a piece-wise linear spline function, in which one kink captures the "optimal" bedrock depth and a second kink captures the point beyond which bedrock depth no longer affects the cost of height. We find that the first-stage F-statistic is maximized with the first kink at a bedrock depth of 22 meters and the second kink at the maximum depth observed in the data of 158 meters, though results are insensitive to second kink locations of 80-158 meters. Moreover, this specification allows us to demonstrate that variation in bedrock depth on each side of the optimal depth independently contributes to identification, with second-stage results close to the baseline. When including the spline as two separate instruments, first stage coefficients on distance to the kink are a significant 0.04 on the deep bedrock side of 22 meters (25% of cities) and 0.03 on the shallow bedrock side of 22 meters (75% of cities), yielding second stage population and built area elasticities of 0.13 and -0.22, respectively (Table A8). Breaking out these two instruments one by one, it becomes apparent that stronger identification comes from the deep bedrock side of the kink, with a first stage F-statistic of 61.1. The first stage F-statistic using only the shallow side for identification is 23.0 (Table A9). Using identifying variation within shallow bedrock depths and controlling for 1975 ln city population interacted with bedrock depth below 22 meters, estimated population

[14] While access to natural resources may also influence construction costs, we undertake these checks with the idea that cities with natural resource-oriented economies may have different trends in demand than other cities.

[15] The roots of almost all crops (including vine crops and tree crops) never go as deep as 6 m. That is also the case for utility lines.

and built area elasticities are 0.13 and -0.23, respectively. Conversely, using identifying variation within deep bedrock depths and controlling for 1975 ln city population interacted with bedrock depths of less than 22 meters, estimated population and built area elasticities are 0.20 and -0.36, respectively. However, neither of these pairs of estimates are significantly different from each other. Appendix B.1 provides additional details on this spline estimation procedure and results.[16]

In our main city population growth regression, log city population in 1975 appears in the dependent variable, as a component of the instrument, and as a control variable. Table A7 shows results indicating that while we must control for base year urban demand conditions in some way, results are robust to various strategies for doing so. In particular, results hold if we: (i) also include log built area in 1975 as a control, which is especially relevant for the built area regressions; (ii) carry out the analysis for 1990-2015 while continuing to use log city population in 1975 to construct the instruments and as a control; and (iii) use log population 2015 as the outcome and log heights 2015 as the instrumented variable (without changing anything else in the specification).[17]

Measurement of Bedrock Depth: We use mean bedrock depth (MBD) across all 30 seconds ($\approx$ 1 km) square pixels in each 2015-definition urbanized area as our main measure of bedrock depth. However, bedrock depth varies within cities, thereby raising potential concerns about sensitivity to its measurement. For example, it could be reasonable to only use bedrock depth at each city's most central pixel or to aggregate over fewer central pixels.

We demonstrate that bedrock depth does not systematically vary by location within cities by distance to the central business district (CBD) and verify that choices of pixels to include in its measurement do not affect results. We identify the CBD of each city as the brightest mega-cell of 9 night lights cells at 30 seconds ($\approx$ 1 km) resolution. Across cities, the coefficient of correlation between MBD within 2.5 km (5 km) of the CBD and is 0.98 (0.99). Likewise, within cities, bedrock depth does not depend on CBD distance (unreported). Finally, the IV results hold if we use MBD calculated only using pixels within 2.5 km or 5 km of CBDs (Table A10). As most tall buildings are built near city centers, the instruments are stronger using central MBDs than with overall or peripheral MBDs.

LATEs: About one-third of the gaps between OLS and IV estimates can be explained by the fact that they capture different local average treatment effects (LATEs). Variation across cities within countries with more variation in city size interacted with bedrock depth identifies IV coefficients. In contrast, within-country variation in heights for all countries identifies corresponding OLS coefficients. Yet, Table A11 shows gaps between the OLS and IV estimates that are about one-third smaller when restricting the sample to larger countries with greater variations in bedrock depth. In particular, we select the 7,473 cities in countries with at least 5 cities and a Gini index

[16] As the first stage spline coefficient is larger for deep bedrock depths and this region only covers 25% of the data, our parametric quadratic specification fits less well for cities with bedrock depths of greater than 22 meters. As a result, shallow depths provide most of the identifying variation in our baseline quadratic specification.

[17] Estimated population and built area elasticities are 0.09 and -0.23 respectively using 1990 as the base year. Those using 2015 levels rather than 1975-2015 changes are 0.09 and -0.11, respectively. However, none of these differences are statistically different from the headline results in Table 2.

of the distribution of mean bedrock depth across cities above the 75th percentile value in the Gini index across all countries. Measurement error in heights likely accounts for the remaining differences.

Heights versus Volumes: An increase in city heights influences outcomes of interest, and ultimately welfare, because it increases the amount of real estate services provided. As tall buildings typically have less usable floor space on higher stories, differences in the sum of heights across cities may not accurately reflect differences in real estate services provided. We can better measure real estate services using data on building volumes, which we observe worldwide at the 80x80 meter pixel level in 2015 (Esch et al., 2023). While we do not observe building volumes in 1975, we can estimate how volumes respond to heights in 2015 to recover a sense of these causal impacts. To measure tall building volumes in 2015, V^H_{2015}, we aggregate pixels with an average building height of least 40 meters, with this height cut-off set sufficiently low so as to capture 55m+ buildings that share pixels with smaller neighboring buildings and unbuilt land (streets, courtyards, etc.).

To derive the causal effects of tall building volumes on outcomes of interest y, we use the identity

$$\frac{d\ln y}{d\ln V^H_{2015}} = \frac{d\ln y}{d\ln(H_{2015}+1)}\frac{d\ln(H_{2015}+1)}{d\ln V^H_{2015}}.$$

With the same IV strategy as for our main outcomes of interest y, we estimate the causal effect of $\ln(H_{2015}+1)$ on $\ln(V^H_{2015})$ to be 0.93^{***} (first stage F-stat = 19.91). Therefore $\frac{d\ln Pop}{d\ln V^H_{2015}} \approx \frac{d\ln Pop}{d\ln(H_{2015}+1)}$, for which we found 0.13 in Table 2. Use of tall building heights versus volumes thus matters little.[18]

Interpretation: Finally, we believe that our estimated elasticities primarily capture migration of people from rural areas to cities rather than displacement between cities. Borusyak et al. (2022) demonstrates the econometric challenges associated with endogenous migration flows between regions in the empirical setting in which local outcomes are regressed on exogenous region-specific shocks for the universe of regions in a country. As our data does not include rural units, our analysis is not subject to these biases provided that city growth in response to exogenously assigned heights draws only from the rural hinterland rather than from other cities. As we focus on developing economies that were little urbanized and had very few tall buildings in 1975, our empirical context is one of primarily rural-to-urban migration. This setting matches that of developed economies in history and our finding, discussed below, of similar population elasticities in the developed world for periods starting in 1850, 1900 or 1920 as those for developing economies in the 1975-2015 period.

We carry out three types of exercises to evaluate the prevalence of displacement in our data. First, we explore robustness to different levels of regional and sub-national fixed effects. As migration occurs at higher rates more locally, we expect there to be greater displacement between cities for fixed effects covering smaller regions. If coefficient estimates do not grow with the use of more local fixed effects, that is evidence that our estimated elasticities reflect rural-

[18] IV estimates of $\frac{d\Delta\ln Pop}{d\ln V^H_{2015}}$ are also 0.13^{***}.

urban migration. Second, we explore robustness to a sub-sample that only includes countries with urbanization rates below 20% in 1975, in which case the vast majority of migrants to cities must have come from rural areas. Finally, in the spirit of Borusyak et al. (2022), we control for height changes in alternative cities that are likely to be viewed by migrants as substitutes.[19]

Table A12 shows the results of the first two exercises. IV estimates for population grow by at most 0.03 when including finer fixed effects and decline by 0.02-0.03 when using sub-region rather than country fixed effects. None of these differences are statistically different from our headline population elasticity estimate of 0.13 for developing economies. Table A12 also shows results for the sample restricted to countries that were less than 20% urban in 1975. The population elasticity remains stable at 0.13. Built area elasticities are somewhat more sensitive to the inclusion of various levels of fixed effects and sample. These estimates grow in magnitude to as much as -0.25 with alternative fixed effects. However, the elasticity shrinks to -0.08 for rural countries, with a large standard error of 0.05. Once again, none of these estimates are statistically different from our primary built area elasticity of -0.16 for developing economies.

For the third exercise, we calculate market potential (MP) terms that summarize accessibility of each city ac to other population centers and their heights. We calculate the MP for heights for city a in country c and year t as

$$MP^H_{act} = \sum_{a' \in C(a), \neq a} \frac{Heights_{a'ct} Pop_{a'c75}}{Pop_{ac75} dis(a,a')^{\alpha}}. \tag{8}$$

That is, we sum over heights in all other cities in the country of city a, scaling by relative city size and discounting by the distance between city a and a' raised to the power α, which we vary between $\frac{1}{3}$ and 3. From these measures in 1975 and 2015, we build $\Delta \ln MP^H_{act}$ to include as a control variable in the main regressions. With this specification, heights in MP^H_{act} are scaled to be of comparable magnitudes to heights in city ac itself. A given percentage increase in heights on a small base will have the potential to redirect fewer migrants as a share of city ac's 1975 population than on a large base.

As heights in other cities may be endogenous to trends in demand factors in city ac, we build an instrument for $\Delta \ln MP^H_{act}$ that follows the same logic as our instruments used in the main analysis. In particular, we build instruments by replacing $Heights_{a'c75}$ in (8) with $Pop_{a'c75} MBD_{a'c}$ and $Pop_{a'c75} MBD^2_{a'c}$. Then, analogous to our main estimation equation (7), we also control for three additional terms capturing the discounted sums of 1975 city populations and bedrock depths by replacing $Heights_{ac75}$ in (8) with $Pop_{a'c75}$, MBD_{ac}, or MBD^2_{ac} and taking logs. Lastly, since MP^H in (8) also directly includes $\frac{Pop_{a'c75}}{Pop_{ac75}}$, we create an additional MP term based on these relative 1975 city populations only.

Table A13 shows the results with these market potential controls. The big message is that we find no evidence that displacement effects between cities in our sample are driving elasticity estimates. We show OLS results for $\alpha = 0.33, \alpha = 0.5$ and $\alpha = 1$, and both OLS and IV results

[19] Fully carrying out the proposed fix in Borusyak et al. (2022) requires observing migration flows in a base period; unfortunately, this is information we do not have for most countries in our global data.

for $\alpha = 2$ and $\alpha = 3$. As bedrock depth tends to be spatially correlated, we need strong spatial decay in order for instruments to be able to separate out height growth in other cities from that in city *ac*. But whether instrumenting for $\Delta \ln MP^H$ or not, estimated population and built area elasticities remain very stable. We come to the same conclusion when separately considering the largest 10 cities and the other cities in the country in MP terms (and assuming a lower distance decay parameter for larger cities) or when controlling separately for height growth in each of these cities (unreported). The coefficient on the height market potential control is 0 or positive when instrumented, which may reflect a growth effect of improved access to markets. The lack of movement in our main elasticity estimates of interest indicates that MP terms are conditionally uncorrelated with our instruments for height growth in city *ac*.

3.2 Heterogeneity in Estimates

In this sub-section, we examine how height elasticity estimates differ by world region, historical period, building use, and city population.

Regional Estimates: Table 3 Panels A and B show heterogeneity of our main IV estimates by region of the world. The first column presents population and built area growth coefficients for all developing economy cities in Asia except the Middle East of 0.17 and -0.20, respectively. Remaining cities in the developing world generate similar estimates of 0.15 and -0.26, though these are slightly underpowered with a first-stage F-statistic of 7.9. Because most of our data is for the developing world, and the population and land use pressures are greatest in these countries, we focus most of our policy analysis on this sample. No developing economy region other than Asia has enough observations to generate strong first-stage identification. Column 3 presents results for cities in developing economies that we infer to have relatively lax building restrictions. We defer the discussion of these results to Section 3.5.

Estimates in the right block of Table 3 Panels A and B are for cities in developed economies. These are subject to more complicated interpretation, as the majority of large cities in developed economies had significant heights in 1975. Moreover, these countries had largely completed their transitions from rural to urban by 1975. While we find no overall average impact of heights on city structure in developed economies for the 1975-2015 period, estimated coefficients are quite large in magnitude, though under-powered, for cities in the USA and Canada. This pattern fits with the idea that building height restrictions are relatively lax in North America and severe in Europe, which contributes most of the observations to the "Others" developed economies sample. However, the estimates for North America are more likely to in part reflect displacement between cities rather than rural-urban migration. Cities in Eastern Europe are a major driver of the 0 results for developed economies, which is consistent with their mostly centrally planned histories.

Historical Regressions: To further understand why estimates differ for developing and developed economies, we look back in time to the 1850-1975 period for a large sample of developed economy cities and 1920-1975 for cities in the US. These are periods of development that better match the sorts of changes experienced in developing economies during the 1975-2015 period, including structural change out of agriculture and rapid urbanization. Moreover, no tall buildings

Table 3: IV Results by World Region and Time Period

	Developing Economies (1975-2015)			Developed Economies (1975-2015)		
	Asia (no ME)	Others	Unconstrained	Total	USA+Can	Others
			Panel A: Δ ln Population			
Δ ln(Heights+1)	0.17***	0.15**	0.21***	0.00	0.30**	0.01
	[0.03]	[0.07]	[0.04]	[0.03]	[0.12]	[0.02]
			Panel B: Δ ln Built Area			
Δ ln(Heights+1)	-0.20***	-0.26***	-0.39***	-0.04	-0.67*	-0.03
	[0.04]	[0.09]	[0.09]	[0.03]	[0.35]	[0.02]
First Stage F	20.92	7.88	11.36	14.28	5.77	13.68
Observations	6,990	4,267	5,315	1,592	372	1,220
			Panel C: Δ ln Population (Historical Regressions)			
Countries:	55 Developed		39 Euro	USA	USA	USA
Period:	1850-1975	1900-1975	1850-1975	1920-1975	1920-1975	1920-1975
Δ ln(Heights+1)	0.14**	0.22***	0.20**	0.21	0.21	0.21†
	[0.06]	[0.07]	[0.10]	[0.17]	[0.15]	[0.13]
First Stage F	10.94	8.44	5.51	4.05	4.82	7.66
Observations	918	918	1,095	324	324	323
$\ln(\text{Heights}+1)_{1920}$ Ctrl	N	N	N	N	Y	Y
Drop Las Vegas	N	N	N	N	N	Y

Notes: Each entry is from a separate IV regression using data from cities in world regions indicated in column headers over the indicated time period. "Asia (no ME)" refers to countries in Asia except the Middle East. "Unconstrained" refers to countries with no history of communism and with below median regulatory environments. Section 3.5 explains in more detail how this sample is selected. "55 Developed" refers to 918 cities in 55 developed countries (as of 2015) during the period 1850-1975 or 1900-1975 (Buringh and Hub, 2013). "39 Euro" refers to 1,095 cities in 39 European countries from Portugal to Russia (Bairoch, 1988a)). "NHGIS" refers to 324 U.S. metro areas for which we were able to reconstruct historical population data using county-level data from the IPUMS national historical geographic information system (NHGIS) (Manson, 2020)). Robust SEs in brackets. *** p<0.01, ** p<0.05, * p<0.10, † p<0.15.

existed in Europe in 1850 and few existed in the US in 1920. As we do not have city footprints in 1850, 1900 or 1920, we focus on population elasticities. The specifications are the same as above except for the different base years. Results are reported in Table 3 Panel C.[20]

We find population elasticities of 0.14-0.20 for the world, 0.20 for Europe, and 0.21 for the US. However, most of these estimates are underpowered, with first-stage F-statistics below 10. For the US, we can increase the first stage F-statistic to 7.7 by controlling for 1920 city heights and excluding Las Vegas, with no effect on the elasticity estimate. The coefficient is, however, only significant at the 15% level. Overall, the main takeaway is that the 0 estimate for developed economies only applies to the modern era; we find population elasticities that are in line with those for the developing world in the period of European and American development.

Commercial vs. Residential Heights: Next, we examine the distinction between impacts of commercial versus residential heights. While we can observe building use in the Emporis data, we do not have separate instruments for these two types of buildings. Instead, we make use of the fact that country-specific industrial structure and land use planning regimes influence the extent to which tall buildings host residential or commercial tenants. Service-oriented economies tend to have a higher share of tall buildings in commercial use, as do higher-income economies with fewer restrictions on urban sprawl. In the developing world, Egypt and Pakistan have about 50% of their tall buildings dedicated to commercial uses. In contrast, countries with land constraints and fewer office workers tend to have a higher share of tall buildings in residential use. Example countries include Brazil, India, and South Korea. Because the residential share of tall buildings is in part driven by such country-specific factors (and we have country fixed effects), we can learn about impacts of the construction of residential versus commercial heights by restricting the sample to only include cities in countries with at least some baseline share of tall buildings in residential use. We do this recognizing that various sources of unobserved heterogeneity between countries are interacting with height growth to generate these effects.

Figure 6 shows estimates by country residential share of tall buildings. The top portion shows the positive estimated population height elasticities and the bottom portion shows the negative built area height elasticities. Red lines are for subsets of cities in the developing world and blue lines are for subsets of cities worldwide. Moving from left to right, the sample becomes more constrained to only include cities in countries with at least the residential share of tall buildings indicated on the horizontal axis.

The results in Figure 6 are striking. Cities in countries that built more residential heights accommodated more population and saved more land, especially in the developing world. Population elasticities rise from 0.13 to 0.21 when moving from the sample of developing world countries with at least 50% of tall buildings residential to those with at least 90% residential.

[20] Appendix Figure A7 shows the evolution of heights separately for the US and other developed nations. For 918 cities in 55 developed economies for 1850-1975 or 1900-1975, we use data from Buringh and Hub (2013) (Panel C Columns 1-2). While this sample is global, its coverage is less extensive for Europe than Bairoch (1988b), which reports population data for 1,095 cities in 39 countries (Column 3). For the US (Columns 4-6), we reconstruct historical population data (N = 324) using county-level data from the IPUMS-NHGIS (Manson, 2020). We start in 1920, predating the roaring 1920's construction boom, so that variation in initial city size is large enough to generate some first stage identifying power.

Figure 6: Effects of Heights by Country Tall Building Residential Share

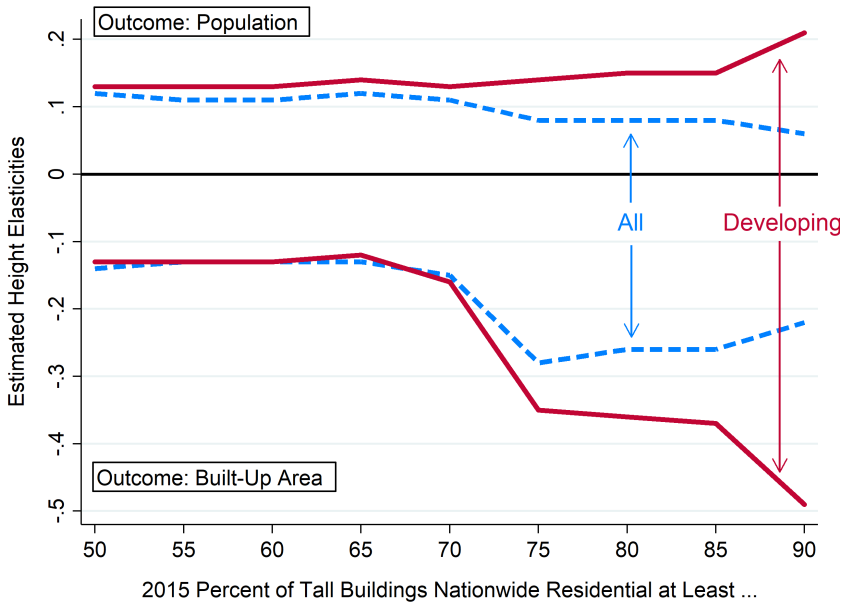

Notes: This figure shows four sets of estimated coefficients on the change in log heights in IV regressions of the form in (7). The top portion of the graph indicates coefficients for which the 1975-2015 change in log population is the outcome. The outcome in the bottom half of the graph is 1975-2015 change in log city built area. Moving from left to right, the sample becomes increasingly constrained to include only countries with at least the fraction of tall buildings nationwide in 2015 residential use indicated on the horizontal axis. Red lines are coefficients for cities in the developing world only ("Developing"). Blue lines ("All') include all cities in the world with at least the indicated 2015 residential share.

The residential impact is even greater for built area. Built area elasticities monotonically decline from -0.13 to -0.50, with more than half of this decline driven by the progressive exclusion of countries with 70-75% tall buildings in residential. The broad implication of evidence in Figure 6 is that the type of tall buildings matters. As residential real estate is much more space intensive than offices per-capita, it is not surprising that residential buildings have bigger effects than commercial buildings. The model developed in the following section is parameterized to respect this observation.

Estimates by City Size: Finally, we look at coefficient heterogeneity by 1975 city population. For separate samples of Asian cities outside the Middle East and other cities in the developing world (including the Middle East), we estimate instrumental variables locally weighted regressions (IV-LWR) by city population. This process is the same as standard IV estimation of (7), but with a separate coefficient on the change in heights estimated for each observation in the data set. These estimates are calculated using a separate weighted IV regression for each observation, with greater weights assigned to observations that are closer in 1975 city log population. See Appendix B.2 for further details.

Figure 7 shows the results for city population growth. Evident in this figure is the non-monotonicity in height effects by city population, with the largest causal effects of heights for the smallest and largest cities. For Asian cities, the population elasticity of height is about 0.3 for cities of about 50,000 residents in 1975 (ln pop $\approx$ 11), falling to 0.11 at a population of 1 million (ln pop $\approx$ 14), and then rising to 0.16 for the very large cities. For other cities in

the developing world, estimates follow the same pattern and are slightly larger but are also less precisely estimated. We calculate analogous estimates for the built area outcome (Fig. A8). For both regions, these hover around -0.20, do not vary much by 1975 city population, and are less precisely estimated than the population responses. First stage F-statistics are shown as dashed lines and are strong for all city sizes in the Asian sample but only for small cities in other areas.[21]

Figure 7: IV-Locally Weight Regression Population Estimates: Developing World

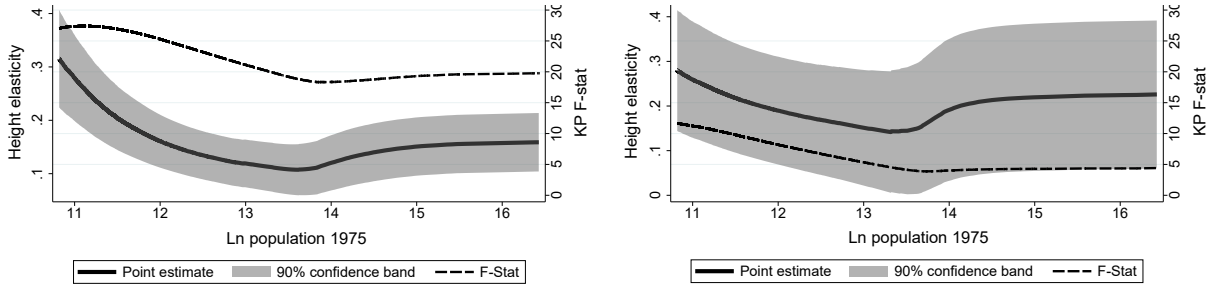

(a) Asian Cities (Excl. the Middle-East) (b) Other Developing Cities

Notes: Figures show non-parametric estimates of height elasticities estimated with an LWR-IV approach. In each LWR, we estimate the height elasticity from a regression of the 1975-2015 long-difference in log city population against the long-difference in log building height using a second-order polynomial of bedrock depth interacted with initial 1975 log population as instrumental variables. Controls are a second-order polynomial of bedrock depth, initial log population, and country fixed effects. We use a Gaussian kernel with a locally varying bandwidth that is inversely related to the density of observations.

3.3 Implied Aggregate Impacts of Height

Using estimates presented above, we provide an accounting of the extent to which post-1975 expansions in building heights have accommodated city population and land savings. With rapid urbanization in many developing economies, cities are facing historic population pressures (Jedwab and Vollrath, 2019). Moreover, due to high trade costs historically, the land surrounding the largest cities in most countries is among the most agriculturally productive (Henderson et al., 2018). We show that lower costs of tall building construction can play a central role in alleviating some of the pressures of urbanization.

Aggregate Population and Land Area Effects: Using the IV-LWR estimates of population, built area, and urban area elasticities with respect to city heights reported in Figures 7, A8, and A10, we obtain the predicted absolute change in population, built area, and total urban area in each city $\widehat{\Delta y_{ac}}$ caused by the actual change in height observed in the data, $\Delta H_{ac75-15}$. We begin with values of each outcome in the initial period y_{ac75} and apply estimated causal height elasticity parameters $\widehat{\beta^{ac}}$ for each city ac. The following expression shows how we calculate the resulting city-specific change in the outcome predicted by our city-specific regression estimates and 1975-2015 growth in heights.

$$\widehat{\Delta y_{ac}} = y_{ac75} \times \left(\exp\left(\widehat{\beta^{ac}} \times \Delta \ln \left(Heights_{ac} + 1 \right) \right) - 1 \right) \tag{9}$$

[21] Corresponding results for the entire sample and developing world cities only are in Figure A9. Figure A10 presents analogous results for total urban area.

This procedure takes the observed height growth as exogenous. Therefore, it reflects the 1975-2015 population growth or area savings that occurred had all of the heights constructed during this time period been assigned in a way that is uncorrelated with covariates or the error term in (7). To the extent that demand growth drove some actual tall building construction conditional on 1975 construction costs, this calculation likely overstates the associated growth in urban populations and declines in urbanized areas that can be causally attributed to reductions in the cost of height. As we focus on cities in the developing world, this analysis reasonably assumes limited inter-city reallocation.

Table 4: Aggregate Effects of 1975-2015 Tall Building Construction

City Pop. 000s (2015)	Number of Cities	1975-2015 ΔHeight km	Share of Height Δ	% of Pop Accomm.	% Area Saved Built	% Area Saved Urban	% Tree Cover	% Other Veg.	% Non Veg.
Panel A: Asian Cities, except Middle East									
0-500	6,514	59	0.02	2	2	1	11	77	12
500-1,000	268	76	0.03	10	9	8	9	75	16
1,000-2,000	114	192	0.07	21	18	15	10	72	18
2,000-5,000	61	527	0.18	47	33	29	9	74	17
5,000+	38	2,001	0.70	58	37	31	10	76	14
All	6,995	2,855	_	23	17	12	10	75	15
Panel B: Cities in Other Developing Regions									
0-500	3,969	68	0.05	4	5	3	16	76	8
500-1,000	164	123	0.09	20	21	18	17	74	10
1,000-2,000	75	205	0.16	28	28	20	17	70	14
2,000-5,000	54	410	0.31	32	32	24	15	71	13
5,000+	16	501	0.38	38	38	29	16	59	26
All	4,278	1,307	_	18	21	13	16	68	16

Notes: Estimates in each panel are based on separate sets of locally weighted regressions of Δ ln population, built area or urban area on the change in log heights. Estimated elasticities for each city are applied to the 1975-2015 height growth in each city to determine the associated predicted % of city-specific population accommodated and built and total urban areas saved. % Tree Cover, % Veg., and % Non-Veg. indicate percentages of the city-specific estimated buffer of land saved in 1975-2015 that corresponded to tree canopy, non-tree vegetation, and bare vegetation / non-vegetated land, respectively, circa 1982.

Table 4 presents the results of this exercise for five 2015 population categories. In Asia, there are 213 cities in the top three size categories of cities over 1 million people, out of 6,995 cities total. These cities constructed 95% of the heights over the 1975-2015 period. Elsewhere in the developing world, cities over 1 million people in 2015 built 85% of the heights during this period. Given that the largest cities built the lion's share of new tall buildings, it is natural that the largest impacts are concentrated in these cities.

For Asian cities above 5 million, an estimated 58 percent of population is accommodated by new tall buildings constructed 1975-2015, saving 37 percent of the built area and 31 percent of the land area. For the smallest Asian cities, only 2 percent of 2015 population is accommodated, saving 2 percent of the built area and 1 percent of the land area. These substantial differences mainly come from the fact that the largest cities built so many tall buildings. Outside of Asia, the patterns of effects are similar though the population responses are somewhat muted,

as the largest non-Asian developing country cities built fewer tall buildings. Overall, our estimates indicate that 23% of Asian urban population and 18% of the urban population in other parts of the developing world is accommodated because of 1975-2015 tall building construction. Moreover, tall buildings have saved about 12% of 2015 urban land area in the developing world from urban uses. A big message from Table 4 is that the technological change that facilitated the construction of tall buildings has fundamentally altered the largest cities in the world. It has allowed them to accommodate a large fraction of their populations while reducing their built-up footprints.

The final three columns of Table 4 provide an accounting of the types of land saved through tall building construction. For each city with 1975-2015 height growth, we calculate the city's land savings. We then generate a buffer around each city boundary to match the area of land saved and aggregate the various land uses circa 1975 within these buffers.[22] This exercise shows that about 10% of land saved around Asian cities is tree canopy and 75% is non-tree vegetation. In other regions, even more tree canopy is saved, at 16%. Both in Asia and elsewhere in the developing world, tall buildings have saved land that is about 85% covered in some sort of vegetation.

Land Use Inside Urbanized Regions: While tall buildings saved peripheral land around cities from urbanization, they also caused urbanized regions to become *less* green. The construction of tall buildings has crowded out tree canopy and green space within 2015 urbanized regions. To quantify these responses, we run regressions similar to those in Table 2 but with changes in various land use measures within urbanized areas as dependent variables. Panel A of Table 5 shows results for all cities and Panel B shows results for developing country cities.

Column (1) shows that heights promoted infill urbanization. An approximate doubling of heights increased urbanization of 2015 UC land by 16% on a base average of 20 percent urbanized (all cities) and 21% on a base average of 21 percent urbanized (developing country cities) between 1982 and 2015. For a 100 log point increase in heights, the average for cities in the top tercile of the 1975 population distribution, an average of 3.2% of 2015 UC land urbanized (full sample) and 4.4% did so in cities in developing economies. Results in columns (2) and (3) show that the urbanization of land was roughly evenly split between reduction in tree cover and short vegetation (yards, parks, and cropland). An approximate doubling of heights reduced tree cover by 22 percent and short vegetation by 2 percent within urbanized areas. When multiplied by the initial fractions of 2015 definition agglomerations that were covered by tree canopy or vegetation, we see that about 1.8% of 2015 UCs were converted from tree cover and 1.4% were converted from short vegetation given an approximate doubling of heights in 1975-2015. Using data from 2000-2015, for which cropland can be broken out from short vegetation, we find that cropland accounts for a small and statistically insignificant fraction of the short vegetation response.

One big message is that tall buildings both save peripheral land and reduce sprawl by promoting infill urbanization. These results are consistent with those in Burchfield et al. (2006),

[22]For this analysis and the other analyses below, we rely on the 1982-2015 *Global Land Change Data* of Hansen and Song (2018). For each ≈5X5 km pixel worldwide, this satellite-based data set records whether there was tree canopy, short vegetation or urbanized/bare vegetation land cover in 1982 (used for 1975) and 2015.

Table 5: Land-Use Changes Inside 2015 Urbanized Boundaries

Dependent Variable:	Δ Log ... Area 1982-2015		
	Bare Vegetation	Tree Cover	Short Vegetation
	Panel A: All Economies (N = 12,849)		
Coeff. on Δ ln Height	0.16***	-0.22**	-0.02**
	[0.03]	[0.03]	[0.01]
Avg Frac of Area, Base Year	0.20	0.08	0.72
First Stage F-Statistic	28.41	28.41	28.41
	Panel B: Developing Economies (N = 11,257)		
Coeff. on Δ ln Height	0.21***	-0.24***	-0.03**
	[0.03]	[0.04]	[0.01]
Avg Frac of Area, Base Year	0.21	0.07	0.72
First Stage F-Statistic	22.83	22.83	22.83

Notes: Each column in each panel is associated with a separate IV regression of the growth rate in land with the use indicated at top on the change in log heights using the same specification as in Table 2. Total urban area is decomposed into bare vegetation area (which includes urbanized area), tree cover area, and short vegetation area. Height growth is measured between 1975 and 2015. See the text for data sources. Robust standard errors in brackets.

which finds that US cities with more centralized sector employment and less hilly terrain (among other factors) had less sprawling new development over the 1976-1992 period. Centralized sector employment is made up primarily of office workers, which can be accommodated in tall buildings. Rugged terrain, which is correlated with low bedrock depth, increases the costs of building tall, thereby also leading to more sprawl.

Aggregate Land Savings: To calculate how tall buildings influence land use inside and outside of 2015 definition urban areas in aggregate, we add the "outside UC" results reported in the final 3 columns of Table 4 to "inside UC" results constructed as follows. As in Figures 7, A8, and A10, we estimate separate IV locally weighted regression impacts of 1975-2015 heights on 1982-2015 changes in tree cover and non-tree vegetation land use within 2015 urban boundaries as functions of 1975 city population by region of the developing world. The average treatment effects across all cities in our data match those reported in Table 5. Given 1975-2015 heights constructed in each city and adding up over all cities in our data, results indicate that the total amounts of short vegetation and forested land at the edges of cities saved by tall building construction reported in Table 4 is about twice the total amount of vegetated land lost inside urbanized regions (unreported).

While we find that tall buildings have generated net gains of vegetated land, these overall gains are small relative to the total amount of urban land, agricultural land or forested land in the world. According to World Bank (2022b), the cities in developing economies with populations over 50,000 in our sample account for 90% of the developing world's total urban population but only one-third of total urban land area. Moreover, the ratios of agricultural and forested

land to all urban land worldwide are 25 and 17, respectively. Given that tall buildings have saved about 5% of vegetated land in cities over 50K worldwide (half of 85%*12% from Table 4), this amounts to less than 0.1% of agricultural or forested land worldwide. However, the land at the edge of cities is among the most agriculturally productive in the world (Henderson et al., 2018). Urbanized land is twice as suitable for agriculture as remaining land, as calculated using suitability data from Schneider et al. (2022). Across the 12,873 cities in our data, land suitability also increases convexly with city population size within countries (unreported).[23]

3.4 City Height Gaps

One object of the model in the following section is to quantify the implications of allowing unrestricted heights in cities worldwide. This calculation requires measures of the extent to which each city constrains tall building construction. To this end, we develop a "height gap" measure, which is the fraction of potential heights in each city justified by fundamental supply and demand conditions that has not been realized.

We build on the analysis in Barr and Jedwab (2023) to determine each city's potential heights under no height constraints. We adapt their regression model to predict city heights using fundamental demand and supply factors that have some commonalities across cities and do not include land use regulation. Predictors in this regression are measures of regional lights at night, city population category interacted with quadratics in national per-capita GDP, city population category interacted with quadratics in mean bedrock depth, earthquake risk, elevation, ruggedness, and year fixed effects. The model is fit using semi-decadal data on 12,755 GHS cities for the 1995-2020 period, resulting in an R-squared of 0.64. Resulting height predictions for 2015 are measures of the heights justified by each city's fundamental demand and cost factors, absent local regulation.

After ordering cities by their predicted log heights, we calculate the 95$^{\text{th}}$ percentile (3rd ranked city) of actual log height for the moving window of 51 cities centered on each city in the data (except the top and bottom ranked 24 cities). This accommodates the possibility that one or two cities in each group of 51 has built particularly tall for idiosyncratic reasons that do not carry over to other cities. Finally, we smooth this 95$^{\text{th}}$ percentile function using local polynomial regression. The resulting function of predicted log heights $h^{95}(\cdot)$ (depicted in Figure A11) describes our inferred unconstrained heights. Appendix B.3 provides additional details on this procedure.

The height gap measure for city ac follows as

$$Gap_{ac} = \max\left(1 - \frac{Heights_{ac2015}}{H^{95}(\widehat{LHEIGHTS}_{ac2015})}, 0\right), \tag{10}$$

where $H^{95}(\cdot) = \exp\left[h^{95}(\cdot)\right]$ and $\widehat{LHEIGHTS}_{ac2015}$ is predicted log heights for city ac in 2015.

[23] We verify that these land savings estimates are not biased by disproportionate tall building construction in cities with low agricultural suitability. Weighting regressions in Table 2 column (2) by the fraction of city land that is suitable for agriculture (mean=0.57) does not affect estimates.

By construction, Gap_{ac} is between 0% and 100%. We emphasize that while this gap measure is reasonable on average conditional on observables and is plausible for most cities, it will not accurately measure building constraints in every city worldwide.[24] At the regional level, the population weighted height gaps are largest in developed economies in Oceania (90%), Europe (85%), and North America (77%) and smallest in developing economies in Asia (41%), Africa (48%), and Europe (48%) (see Table 7 below). These magnitudes reflect the greater real estate demand in developed economies along with the observation that the largest Asian cities have expanded their stock of heights the most in the developing world (Table 4), despite relatively unfavorable bedrock conditions.

3.5 Model-Relevant Estimates

The main objective of the empirical work has been to recover averages of population and built area elasticities with respect to building heights across all cities in the world and for various sub-samples. It is these averages that are most relevant for developing a retrospective understanding of how tall buildings have influenced the sizes and shapes of cities. However, these averages surely mask many dimensions of underlying heterogeneity, including height limits and land use regulation.

Under its baseline parameterization, the model developed in the following section describes an environment in which fundamental supply and demand forces determine a city's equilibrium heights, population, and area. While height limits can be accommodated by the model, strong assumptions would be needed to use estimated elasticities for constrained cities to fit the model. As such, we will estimate the model under a baseline parameterization without height limits. Credible model quantification thus requires elasticity estimates for a sub-sample of cities that are unregulated. In order to maintain the same specification and identification assumptions as for the empirical analysis on the broader sample, we select this unconstrained city sample to include all cities in the most unregulated countries.

As a basis, we use the same 2015 city-level regression residuals used in the first step of constructing city height gaps explained in Section 3.4. We aggregate these residuals to the country level with city population weights. We select all cities in developing economy countries without a history of communism with this aggregated residual above 0. This yields a sample of 5,315 cities located in 38 developing economies.[25]

As expected, the elasticity estimates for this sample, reported in the third column of Table 3, are larger than our broader average estimates reported in Table 2. In particular, we find an unconstrained population elasticity of 0.21 and an unconstrained built area elasticity of -0.39, both of which are statistically significant.

[24] As examples, gaps are 0% for Chicago, Seoul, Sao Paulo and Shanghai, 11% for Guangzhou, 26% for NYC, 70% for Boston, 80% for Buenos Aires and 93% for Cairo.

[25] Unconstrained countries include: Brazil, Colombia, Costa Rica, and Panama in Latin America; Malaysia, the Philippines, Thailand, and Turkey in Asia; and Kenya, Ivory Coast, Libya, and South Africa in Africa. We drop the 20 countries in Europe and 18 in other regions with a history of communism, as these countries disproportionately built residential public housing towers in sometimes economically undesirable locations, and generally did not build in response to market forces.

4 Theoretical Analysis

This section develops a theory that facilitates conceptual and quantitative analysis of the role of tall buildings in shaping urban economic development. This version of the urban monocentric city model follows in the tradition of Muth (1969), while incorporating and expanding on the real estate development technology in Section 2.4, explicitly including a commercial sector with endogenous land use, and allowing for endogenous migration to the city. This "representative city" model is intended to be flexible enough to capture the key forces that link tall building construction to urban growth and change that are common to cities of many different shapes, sizes, and stages of development. The model is stylized but can also be applied quite generally to cities in our data. In Section 4.2, we quantify the model. This includes matching observed population and area elasticities. In Section 4.3, we use the quantified model to calculate the welfare benefits of the tall buildings technology and the consequences of relaxing height restrictions for all cities in our data.

4.1 Model Setup

We expand on the standard urban model with endogenous heights (Duranton and Puga, 2015; Ahlfeldt and Barr, 2022) by allowing rural residents to have the discrete choice of entering the city, following Ahlfeldt et al. (2022)'s approach to modelling labor market entry. Thus, we obtain an *imperfectly* open city which nests the conventional closed-city and open-city versions of the monocentric model as special cases. The model generates a positive (finite) height elasticity of population and a negative height elasticity of area, as observed in the data, through a floor space supply channel. These responses strike a balance between the 0 population and large negative area elasticities in a closed-city model (Alonso, 1964) and the infinite population and small positive area elasticities in an open-city model (Ahlfeldt and Barr, 2022).

Environment: We consider a circular city of endogenous radius. The city is embedded in a country of $\bar{N}$ workers, which also has a rural hinterland. $\mathcal{L}(x) = 2\ell\pi x$ units of land are available for development at each distance x from an exogenously located historic city center, where $\ell = [0, 1]$ is the fraction of land that is developable. The area beyond the endogenous city margin at $x = x_1$ is the rural hinterland.

Workers: All workers are ex-ante identical and choose to live inside or outside the city. The utility of worker ν is described by:

$$U(\nu) = \max_{o}[U^o \exp(a^o(\nu))], \tag{11}$$

where $o \in \{inside, outside\}$ and $a^o(\nu)$ is an idiosyncratic taste shock for living in location o. Workers living in the agricultural hinterland receive an exogenous subsistence utility $U^{o=outside} = \widetilde{U}^{1/\zeta}$. All workers choosing to live in the city enjoy the same endogenous utility $U^{o=inside} = \bar{U}$. The idiosyncratic shocks $a^o(\nu)$ are drawn from the same Gumbel distribution

with distribution function

$$G(a^o(\nu)) = \exp[-\exp(-\zeta a^o(\nu) - \Gamma)]. \tag{12}$$

$\zeta > 0$ is the taste dispersion parameter and Γ is the Euler-Mascheroni constant, included so that the Gumbel shocks are mean 0.

Utility maximization delivers the urban population N as the share μ of the country population $\bar{N}$.[26]

$$N = \mu\overline{N} = \frac{\overline{U}^{\zeta}}{\overline{U}^{\zeta} + \widetilde{U}}\overline{N} \tag{13}$$

The resulting elasticity of urban population with respect to urban utility (the migration elasticity) is $\zeta(1-\mu)$, with $1-\mu$ reflecting the stock of available rural residents at risk of moving to the city.

City utility depends on a local amenity, tradeable goods consumption g, and residential floor space f^R. Each worker's choice of residential location, on floor s in a building located at distance from the city center x, must deliver the same utility level $U(x,s) = \bar{U}$ in equilibrium. Utility is Cobb-Douglas with a floor space expenditure share of $0 < (1-\alpha^R) < 1$. The amenity value of each location $A^R(x,s)$ depends on horizontal (x) and vertical (s) locations. Put together, we have

$$U(x,s) = A^R(x,s)\Big(\frac{g}{\alpha^R}\Big)^{\alpha^R}\Big(\frac{f^R(x,s)}{1-\alpha^R}\Big)^{1-\alpha^R}. \tag{14}$$

The amenity decays with distance from the center and rises with height, taking the form

$$A^R(x,s) = \bar{a}^R e^{-(\tau^R \max(0, x - \underline{x}^R))} s^{\tilde{\omega}^R}.$$

$\tilde{\omega}^R > 0$ is the height elasticity of the residential amenity, capturing benefits such as better views or less exposure to noise and pollution. $\tau^R > 0$ determines the rate at which utility declines in distance from the edge of a central district located at $x = \underline{x}^R$, with $\bar{a}^R$ the amenity within this district. $\tau^R > 0$ generates the centripetal force of rising residential demand nearer to the city center and can be interpreted as the utility cost of commuting an additional unit distance. Workers face the budget constraint

$$y = p^R(x,s)f^R(x,s) + g,$$

in which the endogenous wage y can be spent on housing, with endogenous unit price $p^R(x,s)$, and the tradeable good.

Utility maximization and imposing $U(x,s) = \bar{U}$ yields the residential floor space bid rent for location (x,s) of

$$p^R(x,s) = A^R(x,s)^{\frac{1}{1-\alpha^R}} y^{\frac{1}{1-\alpha^R}} \bar{U}^{-\frac{1}{1-\alpha^R}}. \tag{15}$$

Averaging across all floors of a building of height $S^R(x)$ at every location delivers the horizontal

[26] See Ahlfeldt et al. (2022) for a formal derivation. This is almost isomorphic to using Frechet random utility draws with dispersion parameter ζ, with the advantage that this formulation justifies cases in which $0 < \zeta < 1$.

residential bid rent

$$\bar{p}^R(x) = \frac{1}{1+\omega^R}\left[\frac{\bar{a}^R y}{\bar{U}} e^{-(\tau^R \max(0, x-\underline{x}^R))}\right]^{\frac{1}{1-\alpha^R}} S^R(x)^{\omega^R}, \tag{16}$$

where $\omega^R = \frac{\tilde{\omega}^R}{1-\alpha^R}$ is the height elasticity of residential rent. This follows the form asserted in Section 2.4. $\bar{p}^R(x)$ is declining in x both because of declining amenities, as captured by $\tau^R > 0$, and declining equilibrium building heights $S^R(x)$.

The mass of residents at each location in the residential zone, in which residential use outbids commercial and agricultural use, is

$$n(x) = \frac{\mathcal{L}(x) S^R(x)}{y^R} \frac{\bar{p}^R(x)}{1-\alpha^R}. \tag{17}$$

In this expression, higher housing costs are associated with higher population densities because of lower individual floor space consumption.

Firms: Atomistic perfectly competitive firms produce the tradeable good using labor l and commercial floor space f^C with the Cobb-Douglas production function

$$g(x,s) = A^C(x,s)\left(\frac{l}{\alpha^C}\right)^{\alpha^C}\left(\frac{f^C(x,s)}{1-\alpha^C}\right)^{1-\alpha^C}. \tag{18}$$

Productivity at each location is shifted by

$$A^C(x,s) = \bar{a}^C N^\beta e^{-(\tau^C \max(0, x-\underline{x}^C))} s^{\tilde{\omega}^C}.$$

$\tilde{\omega}^C > 0$ is the height elasticity of productivity, capturing benefits such as signaling and workplace amenity effects (Liu et al., 2018). The agglomeration elasticity of productivity $\beta > 0$ describes how productivity increases in city employment N (Combes and Gobillon, 2015). $\tau^C > 0$ determines the rate at which productivity declines in distance from the edge of a central urban core at $\underline{x}^C$, with $\bar{a}^C$ the exogenous productivity within this core. One way to rationalize this setting is to assume that all workers have to meet within this center to exchange knowledge.[27]

Profit maximization and zero profits delivers the commercial bid rent

$$p^C(x,s) = A^C(x,s)^{\frac{1}{1-\alpha^C}} y^{\frac{\alpha^C}{\alpha^C-1}}. \tag{19}$$

Averaging across all floors of a building with height $S^C(x)$ at each location x delivers the horizontal commercial bid rent

$$\bar{p}^C(x) = \frac{1}{1+\omega^C}\left[\bar{a}^C N^\beta e^{-(\tau^C \max(0, x-\underline{x}^C))}\right]^{\frac{1}{1-\alpha^C}} y^{\frac{\alpha^C}{\alpha^C-1}} S^C(x)^{\omega^C}, \tag{20}$$

[27] By flattening amenities and productivity at the city center, we avoid the peaking of bid-rents and profit-maximizing heights at unrealistically high levels.

where $\omega^C = \frac{\tilde{\omega}^C}{1-\alpha^C}$ is the height elasticity of commercial rent. This form resembles (16).

Then, labor demand at each location in the commercial zone is

$$L(x) = \frac{\alpha^C}{1-\alpha^C} \frac{\bar{p}^C(x)}{y^C} \mathcal{L}(x) S^C(x). \tag{21}$$

This expression reflects the unitary elasticity of substitution between labor and floor space embodied in the Cobb-Douglas production technology.

Developers: We extend the representative developer's problem laid out in Section 2.4 to index by type of use, commercial (C) or residential (R). Using (16) for residents and (20) for firms, the use-specific profit-maximizing building height matches (3), indexing all parameters by use. We require $\theta^U > \omega^U$ and $p^U(x) > c^U(1+\theta^U)$ for the solution to be well-behaved.

The developer may be subject to a height limit $\bar{S}^U$ imposed by the planning system. Conditional on building type U, the developer's resulting choice of height is thus

$$\tilde{S}^U(x) = \min(S^{*U}(x), \bar{S}^U). \tag{22}$$

Inserting into (2) and imposing zero profits, we obtain the use-specific bid rent for land[28]

$$r^U(x) = a^U(x) \left[\tilde{S}^U(x)\right]^{1+\omega^U} - c^U \left[\tilde{S}^U(x)\right]^{1+\theta^U}. \tag{23}$$

If planning restrictions do not bind, this function is declining in distance from the center x, reflecting greater willingness to pay for better access to the center.

Spatial Equilibrium: For given values of the city-wide endogenous objects $\{y, N, \bar{U}\}$, all location-specific endogenous variables are uniquely determined. We obtain floor space rents from (16) and (20), heights from (22), and use-specific land rents from (23). Land use then goes to the highest bidder at each location x given agricultural bid-rent r^A. Under the restriction that the commercial rent gradient is steeper than the residential rent gradient, which is consistent with plausible parameter values and empirical evidence, there is a distance x_0 at which commercial and residential land rents equate: $r^C(x_0) = r^R(x_0)$. At shorter distances, commercial developers outbid residential developers when competing for land; thus x_0 defines the boundary of the central business district (CBD).[29] Similarly, there is a distance x_1 at which residential and agricultural land rents intersect, $r^R(x_1) = r^A$, and the city ends.

[28] $a^C(x) \equiv \frac{1}{1+\omega^C} [\bar{a}^C N^\beta e^{-(\tau^C \times \max(0, x - \underline{x}^C))}]^{\frac{1}{1-\alpha^C}} y^{\frac{\alpha^C}{\alpha^C - 1}}$ and $a^R(x) \equiv \frac{1}{1+\omega^R} [\frac{\bar{a}^R y}{\bar{U}} e^{-(\tau^R \max(0, x - \underline{x}^R))}]^{\frac{1}{1-\alpha^R}}$.

[29] In our quantification, two parameter restrictions together ensure a commercial center surrounded by a residential area. The housing share in production is smaller than the housing share in consumption and $\tau^C > \tau^R$.

General equilibrium: Aggregating labor supply (17) and labor demand (21) across the city, the labor market must clear at the city population N.

$$N = \int_{x_0}^{x_1} n(x)dx = \int_{0}^{x_0} L(x)dx \tag{24}$$

This implies an equilibrium wage of

$$y = \frac{\alpha^C}{1-\alpha^C} \frac{\int_0^{x_1} \bar{p}^C(x)\mathcal{L}(x)S^C(x)dx}{N}. \tag{25}$$

Aggregate housing market clearing is then

$$(1-\alpha^R)yN = \int_{x_0}^{x_1} \bar{p}^R(x)\mathcal{L}(x)S^R(x)dx. \tag{26}$$

Inserting (16) into (26) delivers equilibrium urban utility

$$\bar{U} = \left[\frac{\frac{1}{1+\omega^R} y^{\frac{1}{1-\alpha^R}} \int_{x_0}^{x_1} \tilde{A}(x)^{\frac{1}{1-\alpha^R}} (S^R(x))^{(1+\omega^R)} \mathcal{L}(x)d(x)}{(1-\alpha^R)yN} \right]^{1-\alpha^R}. \tag{27}$$

Equations (13), (25), and (27) constitute the exactly identified system of equations that solves for the general-equilibrium constants $\{y, \bar{U}, N\}$.

Welfare: Given Gumbel-distributed preference shocks, expected utility across all workers living inside and outside of the city is[30]

$$\mathcal{V} = \left(\widetilde{U} + \overline{U}^{\zeta} \right)^{\frac{1}{\zeta}}. \tag{28}$$

The aggregate land rent is

$$\mathcal{R} = \int_{x_1}^{x_0} r^R(x)\mathcal{L}(x)dx + \int_{x_0}^{0} r^C(x)\mathcal{L}(x)dx + \int_{x_1}^{\bar{x}} r^A\mathcal{L}(x)dx. \tag{29}$$

We do not combine these two components of welfare, as any aggregation scheme would be arbitrary given our lack of information about land ownership.

4.2 Quantification

Given parameters $\{\alpha^U, \beta, \omega^U, \theta^U, \tau^U, \underline{x}^U, \bar{a}^U, c^U, \bar{S}^U, r^A, \zeta, \ell, \tilde{U}\}$ and endowments $\{\bar{N}, \bar{x}\}$, we solve for the city-wide endogenous objects $\{y, N, \bar{U}\}$ and the functions $\{L(x), n(x), \bar{p}^U(x), r^U(x), \tilde{S}^U(x)\}$ using the numerical procedure described in Appendix C.1. Table 6 lists central parameter values; brief rationales are provided in the narrative below. Appendix C.2 provides further details.

[30] See Ahlfeldt et al. (2022) for a formal derivation.

Table 6: Baseline Parameterization

	Parameter	Value	Further Reading
$1-\alpha^C$	Share of floor space in production	0.15	Lucas and Rossi-Hansberg (2002)
$1-\alpha^R$	Share of floor space in consumption	0.33	Combes et al. (2019)
β	Agglomeration elasticity in production	0.03	Combes and Gobillon (2015)
θ^C	Commercial height elasticity of construction cost	0.5	Ahlfeldt and McMillen (2018)
θ^R	Residential height elasticity of construction cost	0.55	Ahlfeldt and McMillen (2018)
ω^C	Commercial height elasticity of rent	0.03	Liu et al. (2018)
ω^R	Residential height elasticity of rent	0.07	Danton and Himbert (2018)
τ^C	Production amenity decay	0.014	Appendix Section C.2
τ^R	Residential amenity decay	0.016	Appendix Section C.2
ζ	Preference heterogeneity	2.3	Appendix Section C.2

Notes: Parameter values for $\{\alpha^U, \beta, \theta^U, \omega^U\}$ are also used in Ahlfeldt and Barr (2022). The last column provides references for further reading. We set the scale parameters to $\bar{a}^C = \bar{a}^R = 2, c^C = c^R = 150, r^A = 50$, $\bar{N} = 10$M, ℓ =0.5, $\bar{x} = 100$km and invert $\widetilde{U}$ so that $\mu = 0.3$. In the baseline parameterization, height limits are not binding ($\bar{S}^C = \bar{S}^R = \infty$).

While values for $\{\alpha^U, \beta, \theta^U, \omega^U\}$ can be taken from the literature, remaining parameters apply more specifically to our inquiry. These involve the spatial organization of the city and the interaction between the city and the rural hinterland. We set the radius of the urban core $\underline{x}^C = \underline{x}^R$ to 1 km, resulting in a central core of the tallest buildings with an area of slightly more than one square mile. We set the share of built-up land ℓ to the observed mean ratio of built-up area over total land area across all cities in our data. Targeting a city of 3 million as a baseline, we set the national population to $\bar{N} = 10$ million and the extent of the hinterland from the city center $\bar{x} = 100$ km. Together, this generates a country population density of about 300 workers per km^2 and the urban fraction μ of 0.3, similar to those for regions surrounding the largest cities in Latin America and Asia, given appropriate choices for the scale parameters $\{\bar{a}^U, c^U, r^A, \tilde{U}\}$.

The structural amenity decay parameters τ^U must rationalize urban height, population, and rent gradients. We set these parameters to reflect commercial and residential log building height CBD distance gradients of -0.20 and -0.10, respectively, estimated using 2022 property assessment data in CoreLogic for Chicago (Table A14). Chicago has an estimated height gap of 0% and is of monocentric structure. Chicago's is in the middle of estimated gradients using remote-sensed building volumes data for the set of large unconstrained world cities.[31]

This leaves us with the preference heterogeneity parameter, ζ. This is a central parameter, as it governs the migration response to any shock that affects the attractiveness of the city. The larger is ζ, the more city population grows and the less city land area shrinks in response to a positive shock to the supply of tall buildings. With ζ sufficiently large, the city expands both vertically and horizontally. That is, city population and area elasticities are monotonic in ζ. These relationships are depicted in Figure 8. At the left of the graph is a closed city, in which ζ is 0. In this environment, new tall buildings associated with a reduction in the cost of height θ do not draw in any population but instead make the city more compact. The associated supply shock to city real estate lowers rents. The greater spatial concentration of production raises the

[31]This building volumes data set does not include building use and is too spatially coarse to allow for accurate measurement of height gradients by use. Appendix Section C.2.1 has further details.

wage through an agglomeration force. Moving to the right in Figure 8, it becomes easier for people to move into the city. This results in higher population, area, and rent elasticities. At $\zeta = 2.3$, the real estate supply shock effect of lowering the cost of height gets balanced by the general equilibrium migration response such that rents do not respond to heights. For greater values of ζ, where population elasticities are very large, rent elasticities are slightly positive.

Figure 8: Height elasticities in model by preference heterogeneity (ζ)

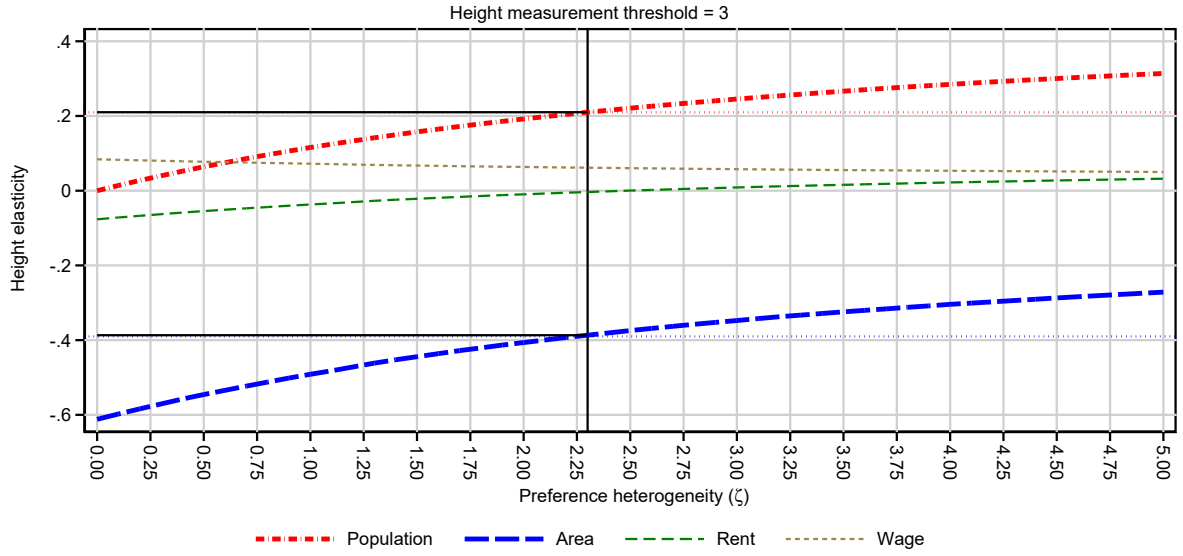

Note: Dotted horizontal lines are our estimates of the height elasticity of population and the height elasticity of area from cities that are unconstrained by height regulation (the empirical moments). Solid horizontal lines are matched moments in the model. To generate these moments in the model, we set one value of ζ and then solve the model under varying values of θ^U. This way, we generate variation in heights and the four outcomes that originates from the building supply side, exclusively.

To identify ζ, we use a simulated method of moments (SMM) approach, treating the height elasticities of population and area as moments to match between the model and the data. We solve the model under varying values of θ^U for each value of ζ, delivering variation in population and area that mimics the bedrock-induced variation in the cost of height in our empirical analysis. In each run, we also compute a measure of tall building height. Log-linear regressions of model-generated population and area against model-generated heights produce our simulated moments.

Differences in land use and building patterns between the data and the model require attention when matching moments. As our building heights data is bottom-coded at 55 meters, model generated heights must also be bottom-coded. However, unlike in the model, the data also exhibit variation in building heights at each CBD distance and buildings that tend to taper towards the top. Moreover, about half of land in the data is not built up near CBDs. For all of these reasons, the threshold above which to measure building heights in the model should be well below 55 meters ($\approx$ 14 stories). As it is unclear which height threshold $\mathcal{T}$ to use in the model, we treat $\mathcal{T}$ as an additional parameter to be estimated through SMM, thereby rendering model parameters just identified. In the counterfactual exercises below, $\mathcal{T}$ also serves as our minimum tall building height. Under $\mathcal{T} = 3$ and $\zeta = 2.3$, we exactly match the estimated population and area elasticities. As long as $\mathcal{T} \geq 3$, we obtain a ζ value around 2.3 (see Figures A12 and

A13).[32] We see $\mathcal{T} = 3$ as a reasonable magnitude. Using CoreLogic data from Chicago, the CBD distance ring of 750 to 1000 meters has total residential and office building floorspace that is 3.7 times the land area and average building heights of 12.8 stories.

The implied labor supply (migration) elasticity to the city $\zeta(1-\mu)$ of about 1.6 should be viewed as a broad-based long-run average that integrates over many different environments. As our estimate applies to a 40 year time horizon, it is sensible that it exceeds the estimates in the literature that are based on similar modeling frameworks but are applied to annual frequencies. Moreover, our look at changes in stocks rather than migration flows, as has been typical in the migration literature, will tend to increase elasticity estimates to additionally account for fertility and death rate responses to real estate supply shocks. Using flow data and a similar conceptualization of location choice to ours, Caliendo et al. (2019) and Caliendo et al. (2021) find annual elasticities of 0.5 for the US and Europe, respectively, and Porcher (2020) estimates heterogeneous annual elasticities of less than 0.4 for Brazil. Tombe and Zhu (2019) finds 1.5-2.5 between provinces in China over worker life-cycles and Bryan and Morten (2018) finds 2.7 for Indonesia. Using more reduced form methods, Beaudry et al. (2014) finds a decadal labor supply elasticity to US metro areas of about 2.0 and Morten and Oliveira (2018) finds 4.5 using Brazilian data, focusing on variation from the linking up of the new capital Brasilia into the highway network. Our ability to reproduce the empirical moments within our model under a canonical parameterization adds to our confidence in the identification strategy employed in Section 3.

4.3 Counterfactuals

In this sub-section, we use the quantified model to explore the implications of changes in the cost of height and of imposing height limits in different types of cities.

4.3.1 Illustrative examples

The starting point is the equilibrium under the baseline parameterization from Table 6, which we illustrate in the first row of Figure 9. Slopes of use-specific floor space bid-rent functions are co-determined with height gradients and bid-rent functions for land. The resulting land use pattern has a commercial district in the center surrounded by a residential district and then rural land. The small discontinuities in floor space rents and heights at the commercial-residential land use boundary x_1 arise endogenously as a result of a net-cost of height $\theta^U - \omega^U$ that is smaller for commercial than residential developments. The flat rent and height functions at the center are artifacts of the imposition of the constant productive amenity value a for locations $x < \underline{x}^C$.

The second row of Figure 9 uses the same parameterization except that the costs of height are increased by 20% to emulate an environment with less favorable bedrock depth. Relative to the first row, this is a negative height supply shock. Changes in aggregate outcomes from the baseline to this counterfactual equilibrium are reported in Table A15. Building heights

[32] Good model fit requires $\mathcal{T}$ to be below the height of the tallest model-generated residential buildings.

fall and the city area expands by 16%. The relocation of firms and residents to more peripheral locations increases commuting costs (or, equivalently, reduces residential amenities) by 2.6% and lowers productivity (commercial amenities) by 0.9%. Due to the reduction in floor space supply, average commercial rents increase by 8%. Lower productivity and higher commuting costs make the city less attractive, thereby reducing housing demand and leading to slightly lower average residential rents, despite the reduction in residential floor space. Lower productivity and higher commercial rents reduce labor demand; reduced accessibility to the center reduces labor supply. The result is a reduction of 2.5% in the equilibrium wage. Due to the lower wage and greater commuting costs, city utility $\bar{U}$ falls by 5.3%. Since living in the city has become less attractive, the population falls by 8.2%. Expected utility across all workers inside and outside the city, $\mathcal{V}$, falls by 1.6%. Aggregate land values fall by 0.2%. Owners of land in the city center are worse off, as this is where the intensity of land use falls. Owners of land near the city periphery are better off, as this land is more urbanized.

Figure 9: Urban spatial structure, cost of height, and regulation

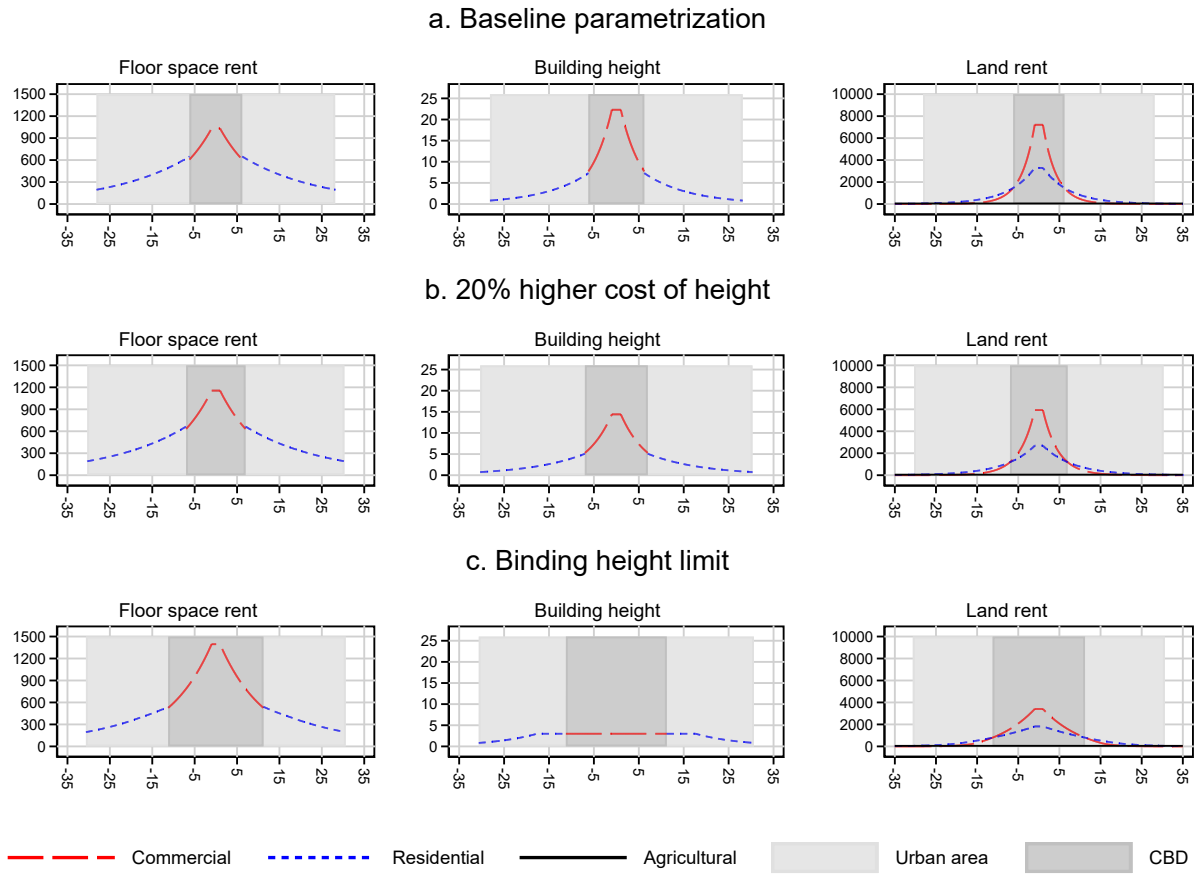

Note: Figure illustrates the solution to the model under the parameter values from Table 6 (upper panels), a counterfactual where we increase the cost of height to $\theta^C = 0.6, \theta^R = 0.65$ (middle panels), and a counterfactual in which we introduce a height limit of $\bar{S}^C = \bar{S}^R = \mathcal{T} = 3$. See Table A15 in the Appendix for the impact of the greater cost of height and a binding height limit on aggregate outcomes.

In the third row, we revert to the same parameters as in the first row but impose the height cap $\bar{S}^C = \bar{S}^R = \mathcal{T} = 3$ such that there are no (model-defined) tall buildings. Relative to an unconstrained city, this height cap results in a substantial horizontal expansion of the

CBD. Although we have imposed a tighter constraint on vertical growth, the horizontal area of the city increases only slightly more (at 18%) than in the cost counterfactual. The more pronounced horizontal expansion of the CBD results in an 8% increased average commuting cost and 5% reduction in average productivity. With a 7% decline, the wage falls more than in the cost counterfactual. The result is a reduction in housing demand that is so large that, despite the negative shock to residential floor space supply, residential rents fall substantially by 14%. The increase in commuting costs and the lower wage, however, dominate the effect of rents on indirect utility in the city, which decreases by 10%, leading to a decline in expected utility $\mathcal{V}$ of 3.0%. Population falls by 17%, about 50% more than in the cost counterfactual. Driven by the conversion of rural into residential and residential into commercial land use, aggregate land values notably increase by 13%. The height limit redistributes income from the mobile labor factor to the immobile land factor. A major welfare cost of height limits arises from the induced spatial misallocation of firms away from locations at which they are most productive. This example includes details that underlie our analysis of welfare consequences of height restrictions calculated for all cities in our data, carried out below. We emphasize that as height caps bind more tightly for larger cities, associated welfare consequences are greater for these cities. Moreover, welfare consequences for urban residents are more than triple those for the average person, as the city hosts about one-third of the imperfectly mobile population.

4.3.2 Heterogeneity in welfare effects

When evaluated relative to an unconstrained market equilibrium, the welfare impact of height regulations depend on the cost of height. Welfare impacts of the same height regulation are larger in cities with lower costs of height. Indeed, introducing the same height limit as in the third row of Figure 9 under a 20% greater cost of height, the impact on population and expected utility falls by about one third and the effect on area about halves (Table A15).

Figure 10 illustrates how the welfare effect associated with a height limits depends on population and the cost of height. To generate this figure, we solve the model varying the height cost (θ^U), height limit ($\bar{S}^U$), and rural utility $\tilde{U}$ values. We exploit that there is a unique mapping from urban and rural utility to population in (13) to find $\{\bar{S}^U, \tilde{U}\}$ values that rationalize any given combination of population and height gap using the procedure described in Algorithm 4. We use this procedure to compute welfare effects for all combinations of cost of height $\{0.2, 0.3, ..., 1\}$ and height gaps $\{0\%, 10\%, ..., 100\%\}$, as defined in (10). We show results for cities of half a million and three million residents. For a given cost of height and height gap, we engineer the model to generate larger population cities by reducing rural utility $\tilde{U}$, thereby also generating greater demand for height in the city.

Figure 10 confirms that losing height results in greater expected utility losses if the cost of height in a city is low (e.g. due to favorable bedrock). Lowering the cost of height from 0.6 to 0.3 approximately triples the relative utility loss at any given height gap in a city with a population of three million (top right panel). Demand conditions also matter. Holding the cost of height constant, we observe greater effects in larger cities. Height limits tend to be more

Figure 10: Heterogeneity in welfare effects

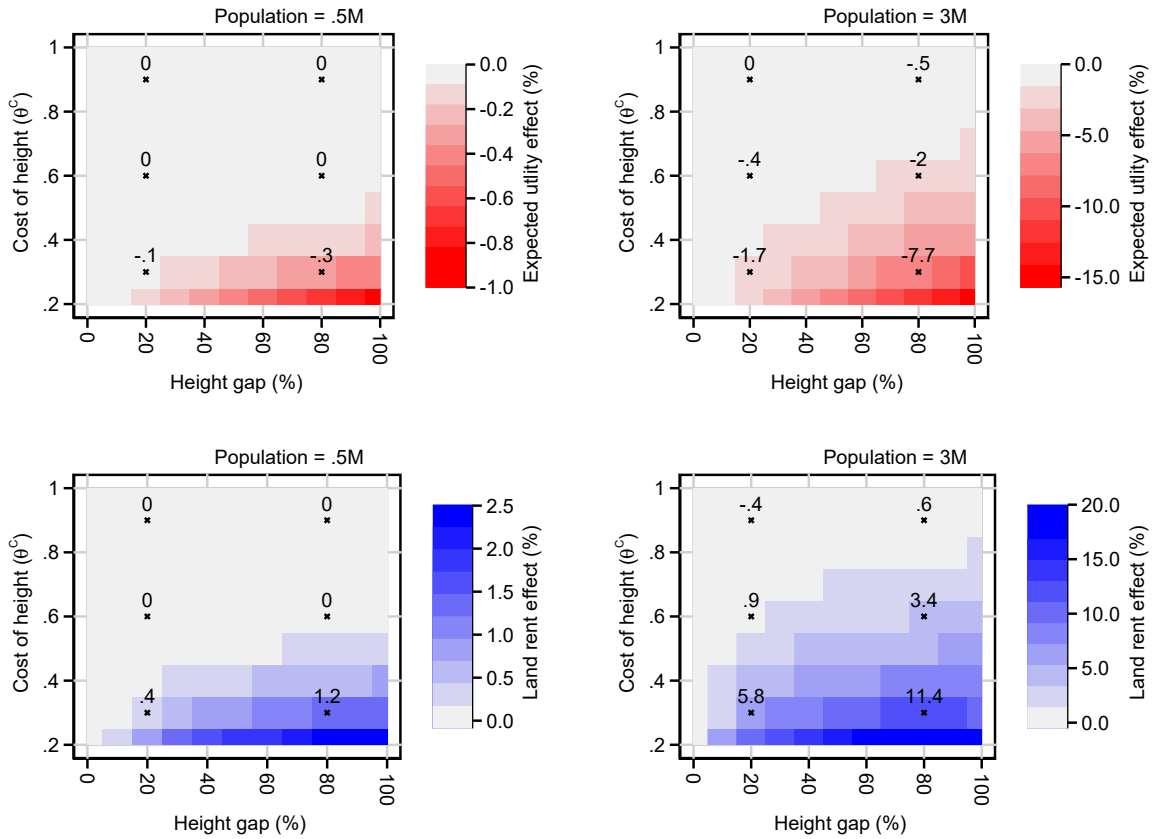

Note: To generate each panel, we solve the model under different values of $\{\theta^C\}$, setting $\theta^R = \theta^C + 0.05$. We find values of $\{\tilde{S}, \tilde{U}\}$ to rationalize a given combination of population and height gap, conditional on given θ^U values. We hold all other parameter values constant at the value described in Table 6. The height gap is the fraction of free-market total tall-building height that is not developed due to a height limit.

costly in cities with fundamentals that increase the demand for and/or the supply of height. As vertical compression leads to horizontal expansion, binding height limits increase average land values. This uplift is generally large enough to more than compensate for the decline in land rent in the more constrained central part of the city, as seen in the bottom two panels of Figure 10. Impacts on aggregate land rent are much greater in cities with lower costs of height, where the loss of heights are particularly large. This primarily reflects redistribution of production and residences to more peripheral locations, with only small responses in aggregate demand for living in the city.

4.4 The Contribution of Tall Buildings to Welfare

We use the model to evaluate the welfare effects of tall buildings for the 12,877 cities used in the empirical analysis. As in Figure 10, we invert the model to rationalize observed populations and height gaps conditional on the observed cost of height for each city in our data (see Algorithm 4 for details). We obtain city-specific estimates of the cost of height using mean bedrock depths and the non-parametric estimated relationship between bedrock depth and the cost of height illustrated in Figure A5.

Table 7: Wefare effects of tall buildings by world region

World region	Urban pop. (BN)	City characteristics: In cities >1 mill.	City characteristics: Cost of height θ	City characteristics: Est. height gap	Expected utility ($\mathcal{V}$): No tall building	Expected utility ($\mathcal{V}$): Actual height limit	Agg. land rent ($\mathcal{R}$): No tall building	Agg. land rent ($\mathcal{R}$): Actual height limit
Africa, G	0.55	34.7%	0.44	48.1%	–5.0%	–4.8%	6.6%	6.6%
Asia, G	1.95	44.5%	0.59	40.8%	–3.8%	–2.6%	4.8%	4.0%
Europe, G	0.04	29.2%	0.49	48.5%	–1.0%	–0.6%	1.6%	1.2%
LAC, G	0.33	52.9%	0.41	62.7%	–5.5%	–3.9%	6.9%	6.4%
Mean, Developing (G)	2.87	43.3%	0.54	44.8%	–4.2%	–3.1%	5.3%	4.7%
Asia, D	0.19	77.2%	0.39	64.0%	–10.3%	–7.3%	12.6%	11.2%
Europe, D	0.25	41.4%	0.32	84.6%	–5.8%	–4.9%	7.4%	8.3%
LAC, D	0.02	48.6%	0.99	59.4%	–0.9%	–0.6%	1.2%	0.9%
North America, D	0.17	67.3%	0.43	76.6%	–8.3%	–6.3%	10.0%	10.4%
Oceania, D	0.01	64.2%	0.34	90.0%	–6.9%	–6.6%	8.1%	8.3%
Mean, Developed (D)	0.64	59.6%	0.39	75.9%	–7.7%	–5.9%	9.5%	9.5%
Mean, All (G & D)	3.51	46.3%	0.51	50.5%	–4.8%	–3.6%	6.1%	5.6%

Notes: Entries are population-weighted averages across cities in each indicated region. City-specific welfare effects are from model-based counterfactuals using parameterizations that match population and the cost of height for each city. Results in "No tall building" and "Actual height limit" columns report average changes in expected utilities and aggregate land rents relative to city unconstrained equilibria. City height gaps are estimated as described in Section 3.4. "No tall building" imposes a height limit of 3 floors. "Actual height limit" imposes estimated city height gaps.

Table 7 reports the city population weighted mean welfare effect by world region. While we weight by city population, we also include rural potential migrants in our welfare calculations. We report the incidence on the mobile (labor) and immobile (land) factors for two scenarios. First, we calculate the welfare loss associated with banning all equilibrium tall buildings, or going from the $\bar{S}^U = \infty$ equilibrium to the $\bar{S}^U = \mathcal{T}$ equilibrium for each city. Second, we calculate the welfare consequences of going from no height restrictions ($\bar{S}^U = \infty$) to actual height gaps (Gap_{ac} from (10)), which delivers the welfare cost associated with each city's inferred current height regulations.

Globally, imposing a height restriction of no tall buildings is predicted to reduce worker welfare by 4.8% relative to unconstrained equilibria (bottom row). As imposing current height constraints on unconstrained equilibria reduces worker welfare by 3.6%, only about one-quarter of this height potential has been realized under current regulations. Commensurate with our discussion above of the final row of Figure 9 and the bottom two panels of Figure 10, aggregate land rents rise when height constraints are imposed. Magnitudes are reported in the final two columns of Table 7. Current height restrictions are estimated to cause city aggregate land rents to be 5.6% greater than in the unrestricted regime.[33]

City population, the cost of height, and the height gap all influence the magnitude of welfare benefits associated with relaxing height limits. With height limits more binding in the developed world, in part because of a greater share of its urban population in large cities and a lower cost

[33]Imposing height restrictions leads to lower wages, lower average property rents and higher commuting costs (or equivalently, lower amenities), with the rent response not sufficient to make up for the other two negative influences on welfare. About 75% of the welfare losses are due to the higher commuting cost (lower amenity) component. Exact magnitudes for different world regions are reported in Table A16.

of height due to better bedrock depths, its welfare cost of height limits are greater than that for the developing world, at 5.9% and 3.1%, respectively. As cities in developed areas of Asia are large, this region's opportunities for welfare gains from eliminating height constraints are greatest across all world regions at 7.3%.

In the developing world, Africa has the most to gain from relaxing height limits, at 4.8%, as its cities' average costs of height are a low 0.44. The Latin America/Caribbean and Asian regions have realized more of their potential gains from heights, such that relaxing inferred height restrictions in these regions would lead to welfare gains of 3.9% and 2.6% respectively. The larger cities, lower costs of height, and larger height gaps in the Latin America/Caribbean region justifies its greater potential welfare gains.

While already large, the welfare costs of height limits are likely to grow over time. The history of tall buildings is one of technological innovations that have lowered the cost of height. Extant estimates suggest that the cost-of-height parameter, θ, has declined by about 2% per year over the past 50 years (see Ahlfeldt and Barr (2022) and Appendix Section A.3). Even if this rate halves, the cost of height will fall by 20% within a generation. Our simulations suggest that even if cities adjust to keep the relative bite of height regulation constant, the welfare cost will increase by about one-third on average, from 3.6% to 4.6% overall (Table A17), with considerable variation across regions.

5 Conclusion

Our comprehensive examination of 12,877 cities worldwide from 1975 to 2015 reveals that the construction of tall buildings driven by reductions in the costs of height has allowed cities to accommodate greater populations on less land. We estimate average elasticities of city population and built land area with respect to aggregate city building heights to be 0.13 and -0.16, respectively, in developing economies. Corresponding treatment effects that are allowed to flexibly differ by 1975 city population imply that one-third of the aggregate population in cities of over 2 million people in the developing world, and 20% for all cities, is now accommodated because of the tall buildings constructed in these cities since 1975. Moreover, the largest cities would cover almost 30% more land without these buildings, and almost 20% across all cities, keeping this peripheral land in use mostly for agriculture instead.

In the context of a quantitative urban model, the enhanced urban compactness facilitated by tall buildings manifests as gains in both productivity and affordability. As a result, we calculate that imposing a height limit that eliminates all tall buildings in cities around the world would reduce worker welfare by about 1.2%, while at the same time increasing aggregate land values by about 0.5% relative to the current equilibrium. Given the gap between actual and potential building heights we calculate for each city in our data, only about one-quarter of the potential welfare gains and land value losses from heights have been realized, with per-capita welfare gains of 5.9% and 3.1% available by eliminating height regulations in developed and developing economies, respectively. As the cost of building tall structures decreases with technical progress, such potential for welfare gains will only increase into the future. The implicit costs of height

restrictions will only grow over time.

With the losses in land values that would come with deregulation, it is perhaps not surprising that so many cities restrict tall building construction. Given our estimated migration elasticity of about 1.6, the population (city demand) response to any tall building supply shock associated with deregulation would not be sufficiently large to overcome a decline in land values. As a result, in most cities it is in landowners' interest to maintain regulatory regimes that limit tall building construction, despite the benefits that would come to workers, especially if they are renters. The political economy of such deregulation is fraught, as benefits may be greatest for those who would move into the city with the new construction to take advantage of the higher real wages and lower commuting costs. Even though aggregate gains associated with allowing more tall building are to be found, in many cities these gains are distributed to only a minority of the local electorate.

Beyond the political economy frictions, there are additional reasons for which tall building construction may be disruptive in many cities. There may be negative amenity and productivity responses from the congestion associated with increased urban density. Moreover, there is likely to be heterogeneous demand for height; we tend to see only middle and high income residents and high productivity firms locating in new tall buildings. And construction is locally disruptive. For all of these reasons, tall building construction may be regressive and costly in the short run, even if it expands real estate supply to the benefit of all renters in the long run. A priority for future research should be to develop a better understanding of the extent to which each of these potential reasons for the opposition to densification hold up empirically, and to devise potential policy remedies.

References

Ades, Alberto F and Edward L Glaeser, "Trade and circuses: explaining urban giants," *The Quarterly Journal of Economics*, 1995, *110* (1), 195–227.

Ahlfeldt, Gabriel M. and Daniel P. McMillen, "Tall buildings and land values: Height and construction cost elasticities in Chicago, 1870-2010," *Review of Economics and Statistics*, 2018, *100* (5), 861–875.

_ and Elisabetta Pietrostefani, "The economic effects of density: A synthesis," *Journal of Urban Economics*, 2019, *111* (February), 93–107.

_ and Jason Barr, "Viewing urban spatial history from tall buildings," *Regional Science and Urban Economics*, 11 2020, p. 103618.

_ and _ , "The economics of skyscrapers: A synthesis," *Journal of Urban Economics*, 5 2022, *129*, 103419.

_ , Duncan Roth, and Tobias Seidel, "Optimal minimum wages," *CEPR Discussion Paper 17026*, 2022.

Alonso, William, *Location and Land Use*, Cambridge, MA: Harvard Univ. Press, 1964.

Alsan, Marcella and Claudia Goldin, "Watersheds in child mortality: The role of effective water and sewerage infrastructure, 1880–1920," *Journal of Political Economy*, 2019, *127* (2), 586–638.

Bairoch, Paul, *Cites and Economic Development, from the dawn of history to the present*, Chicago: University of Chicago Press, 1988. translated by Christopher Braider.

_ , *Cities and economic development: from the dawn of history to the present*, University of Chicago Press, 1988.

Barr, Jason, "Skyscrapers and the Skyline: Manhattan, 1895–2004," *Real Estate Economics*, 2010, *38* (3), 567–597.

_ , "Skyscraper Height," *Journal of Real Estate Finance and Economics*, 2012, *45* (3).

_ , *Building the Skyline: The Birth and Growth of Manhattan's Skyscrapers*, Oxford University Press, 2016.

_ **and Remi Jedwab**, "Exciting, boring, and nonexistent skylines: Vertical building gaps in global perspective," *Real Estate Economics*, 2023.

_ **, Troy Tassier, and Rossen Trendafilov**, "Depth to Bedrock and the Formation of the Manhattan Skyline, 1890–1915," *The Journal of Economic History*, 2011, *71* (4), 1060–1077.

Baum-Snow, Nathaniel, "Did Highways Cause Suburbanization?," *Quarterly Journal of Economics*, 2007, *122* (2), 775–805.

_ , "Urban transport expansions and changes in the spatial structure of us cities: Implications for productivity and welfare," *Review of Economics and Statistics*, 2020, *102* (5), 929–945.

_ **and Lu Han**, "The Microgeography of Housing Supply," *Working paper*, 2019.

_ **, J Vernon Henderson, Matthew A Turner, Qinghua Zhang, and Loren Brandt**, "Does investment in national highways help or hurt hinterland city growth?," *Journal of Urban Economics*, 2020, *115*, 103124.

_ **, Loren Brandt, J Vernon Henderson, Matthew A Turner, and Qinghua Zhang**, "Roads, Railroads, and Decentralization of Chinese Cities," *The Review of Economics and Statistics*, 1 2017, *99* (3), 435–448.

Beaudry, Paul, David A. Green, and Benjamin M. Sand, "Spatial equilibrium with unemployment and wage bargaining: Theory and estimation," *Journal of Urban Economics*, 2014, *79*, 2–19. Spatial Dimensions of Labor Markets.

Ben-Shahar, Danny, Yongheng Deng, Eyal Solganik, Tsur Somerville, and Zhu Hongjia, "The Value of Vertical Status: Evidence from the Real Estate Market," 2022.

Bertaud, Alain and Jan Brueckner, "Analyzing building-height restrictions: predicted impacts and welfare costs," *Regional Science and Urban Economics*, 2005, *35* (2), 109–125.

Bleakley, Hoyt and Jeffrey Lin, "Portage and path dependence," *The quarterly journal of economics*, 2012, *127* (2), 587–644.

Borusyak, Kirill, Rafael Dix-Carneiro, and Brian Kovak, "Understanding migration responses to local shocks," *Available at SSRN 4086847*, 2022.

Brooks, Leah, Nicolas Gendron-Carrier, and Gisela Rua, "The local impact of containerization," *Journal of Urban Economics*, 2021, *126*, 103388.

Brueckner, Jan and Kala Seetharam Sridhar, "Measuring welfare gains from relaxation of land-use restrictions: The case of India's building-height limits," *Regional Science and Urban Economics*, 2012, *42* (6), 1061–1067.

_ **and Ruchi Singh**, "Stringency of land-use regulation: Building heights in US cities," *Journal of Urban Economics*, 2020, *116*.

Brueckner, Jan K., "The structure of urban equilibria: A unified treatment of the muth-mills model," *Handbook of Regional and Urban Economics*, 1987, *2*, 821–845.

Brueckner, Jan, Shihe Fu, Yizhen Gu, and Junfu Zhang, "Measuring the stringency of land use regulation: The case of China's building height limits," *Review of Economics and Statistics*, 2017, *99* (4), 663–677.

Bryan, Gharad and Melanie Morten, "The Aggregate Productivity Effects of Internal Migration: Evidence from Indonesia," *Journal of Political Economy*, 12 2018.

Burchfield, Marcy, Henry G Overman, Diego Puga, and Matthew A Turner, "Causes of sprawl: A portrait from space," *The Quarterly Journal of Economics*, 2006, *121* (2), 587–633.

Buringh, Eltjo and Urbanization Hub, "The Clio-infra database on urban settlement sizes: 1500–2000," 2013.

Caliendo, Lorenzo, Luca David Opromolla, Fernando Parro, and Alessandro Sforza, "Goods and factor market integration: A quantitative assessment of the EU enlargement," *Journal of Political Economy*, 2021, *129* (12), 3491–3545.

_ , Maximiliano Dvorkin, and Fernando Parro, "Trade and Labor Market Dynamics: General Equilibrium Analysis of the China Trade Shock," *Econometrica*, 5 2019, *87* (3), 741–835.

Campante, Filipe and David Yanagizawa-Drott, "Long-range growth: economic development in the global network of air links," *The Quarterly Journal of Economics*, 2018, *133* (3), 1395–1458.

Combes, Pierre-Philippe and Laurent Gobillon, "The Empirics of Agglomeration Economies," in Gilles Duranton, J Vernon Henderson, William C B T Handbook of Regional Strange, and Urban Economics, eds., *Handbook of Regional and Urban Economics*, Vol. 5, Elsevier, 2015, pp. 247–348.

_ , Gilles Duranton, and Laurent Gobillon, "The identification of agglomeration economies," *Journal of Economic Geography*, 2011, *11* (2), 253–266.

_ , _ , and _ , "The Costs of Agglomeration: House and Land Prices in French Cities," *The Review of Economic Studies*, 10 2019, *86* (4), 1556–1589.

Coury, Michael, Toru Kitagawa, Allison Shertzer, and Matthew Turner, "The value of piped water and sewers: Evidence from 19th century chicago," Technical Report, National Bureau of Economic Research 2022.

Curci, Federico, "The taller the better? Agglomeration determinants and urban structure," *Working paper*, 2020.

Danton, Jayson and Alexander Himbert, "Residential vertical rent curves," *Journal of Urban Economics*, 2018, *107*, 89–100.

Davis, Donald R and David E Weinstein, "Bones, bombs, and break points: the geography of economic activity," *American economic review*, 2002, *92* (5), 1269–1289.

Desmet, Klaus, DÃ¡vid KrisztiÃ¡n Nagy, and Esteban Rossi-Hansberg, "The Geography of Development," *Journal of Political Economy*, 1 2018, *126* (3), 903–983.

Ducruet, César, Réka Juhász, Dávid Krisztián Nagy, and Claudia Steinwender, "All aboard: The effects of port development," Technical Report, National Bureau of Economic Research 2020.

Duranton, Gilles and Diego Puga, "Urban Land Use," in Gilles Duranton, J. Vernon Henderson, and William C. Strange, eds., *Handbook of Regional and Urban Economics*, Vol. 5, Elsevier, 2015, chapter 8, pp. 467–560.

_ and _ , "Urban growth and its aggregate implications," Technical Report, National Bureau of Economic Research 2019.

_ and _ , "The Economics of Urban Density," *Journal of Economic Perspectives*, 2020, *34* (3), 3–26.

_ and Matthew A. Turner, "Urban Growth and Transportation," *The Review of Economic Studies*, 2012, *79* (4), 1407–1440.

Emporis, *Emporis* 2022.

Esch, Thomas, Klaus Deininger, Remi Jedwab, and Daniela Palacios-Lopez, "Outward and Upward Construction: A 3D Analysis of the Global Building Stock," Working Papers 2023-09, The George Washington University, Institute for International Economic Policy September 2023.

Faber, Benjamin, "Trade Integration, Market Size, and Industrialization: Evidence from China's National Trunk Highway System," *The Review of Economic Studies*, 7 2014, *81* (3), 1046–1070.

Florczyk, A., M. Melchiorri, C. Corban, M. Schiavina, L. Maffenini, M. Pesaresi, P. Politis, F. Sabo, S. Carneiro Freire, D. Ehrlich, T. Kemper, P. Tommasi, D. Airaghi, and L. Zanchetta, "Description of the GHS Urban Centre Database 2015," *Publications Office of the European Union*, 2019.

Gibbons, Stephen, Teemu Lyytikäinen, Henry G Overman, and Rosa Sanchis-Guarner, "New road infrastructure: the effects on firms," *Journal of Urban Economics*, 2019, *110*, 35–50.

Glaeser, Edward, *Triumph of the City: How Our Greatest Invention Makes Us Richer, Smarter, Greener, Healthier, and Happier* 2012.

Glaeser, Edward L, Hedi D Kallal, Jose A Scheinkman, and Andrei Shleifer, "Growth in Cities," *Journal of Political Economy*, 5 1992, *100* (6), 1126–1152.

_ , Joseph Gyourko, and Raven E Saks, "Why have housing prices gone up?," *American Economic Review*, 2005, *95* (2), 329–333.

Gollin, Douglas, Casper Worm Hansen, and Asger Mose Wingender, "Two Blades of Grass: The Impact of the Green Revolution," *Journal of Political Economy*, 2021, *129* (8), 2344–2384.

Gonzalez-Navarro, Marco and Matthew A. Turner, "Subways and urban growth: Evidence from earth," *Journal of Urban Economics*, 11 2018, *108*, 85–106.

_ and Matthew A Turner, "Subways and urban growth: Evidence from earth," *Journal of Urban Economics*, 2018, *108*, 85–106.

Gyourko, Joseph and Raven Molloy, "Regulation and housing supply," in "Handbook of regional and urban economics," Vol. 5, Elsevier, 2015, pp. 1289–1337.

Hansen, M. and X. Song, *Vegetation Continuous Fields (VCF) Yearly Global 0.05 Deg.* 2018.

Harari, Mariaflavia, "Cities in bad shape: Urban geometry in India," *American Economic Review*, 2020, *110* (8), 2377–2421.

Harris, John R and Michael P Todaro, "Migration, Unemployment and Development: A Two-Sector Analysis," *The American Economic Review*, 2 1970, *60* (1), 126–142.

Heblich, Stephan, Stephen J Redding, and Daniel M Sturm, "The Making of the Modern Metropolis: Evidence from London," *The Quarterly Journal of Economics*, 11 2020, *135* (4), 2059–2133.

Henderson, J Vernon, Tanner Regan, and Anthony Venables, "Building the city: from slums to a modern metropolis," *The Review of Economic Studies*, 2021, *88* (3), 1157–1192.

_ , Tim Squires, Adam Storeygard, and David Weil, "The global distribution of economic activity: nature, history, and the role of trade," *The Quarterly Journal of Economics*, 2018, *133* (1), 357–406.

Henderson, Vernon, Ari Kuncoro, and Matt Turner, "Industrial Development in Cities," *Journal of Political Economy*, 5 1995, *103* (5), 1067–1090.

Hilber, Christian AL and Wouter Vermeulen, "The impact of supply constraints on house prices in England," *The Economic Journal*, 2016, *126* (591), 358–405.

Hsieh, Chang-Tai and Enrico Moretti, "Housing Constraints and Spatial Misallocation," *American Economic Journal: Macroeconomics*, 2019, *11* (2), 1–39.

Jedwab, Remi and Adam Storeygard, "The Average and Heterogeneous Effects of Transportation Investments: Evidence from Sub-Saharan Africa 1960â2010," *Journal of the European Economic Association*, 06 2021, *20* (1), 1–38.

_ and Dietrich Vollrath, "The Urban Mortality Transition and Poor-Country Urbanization," *American Economic Journal: Macroeconomics*, January 2019, *11* (1), 223–75.

_ , Jason Barr, and Jan Brueckner, "Cities without Skylines: Worldwide Building-height Gaps and their Implications," 2020.

Koster, Hans R A, Jos van Ommeren, and Piet Rietveld, "Is the sky the limit? High-rise buildings and office rents," *Journal of Economic Geography*, 5 2013, *14* (1), 125–153.

Liu, Crocker, Stuart S Rosenthal, and William C Strange, "The Vertical City: Rent Gradients and Spatial Structure," *Journal of Urban Economics*, 2018, *106*, 101–122.

_ , _ , and _ , "Employment Density and Agglomeration Economies in Tall Buildings," *Regional Science and Urban Economics*, 2020, *84*.

Lucas, Robert E Jr. and Esteban Rossi-Hansberg, "On the Internal Structure of Cities Author," *Econometrica*, 2002, *70* (4), 1445–1476.

Manson, Steven M, "IPUMS national historical geographic information system: version 15.0," 2020.

McFadden, Daniel, "The measurement of urban travel demand," *Journal of Public Economics*, 1974, *3* (4), 303–328.

Mills, Edwin S, "An Aggregative Model of Resource Allocation in a Metropolitan Area," *The American Economic Review*, 1967, *57* (2), 197–210.

Morten, Melanie and Jaqueline Oliveira, "The effects of roads on trade and migration: Evidence from a planned capital city," *NBER Working Paper*, 2018, *22158*, 1–64.

Muth, R, *Cities and Housing*, Chicago: Chicago University Press, 1969.

Nase, Ilir and Jason Barr, "Game of Floors: The Determinants of Residential Height Premiums," 2023.

NGDC, *Global Radiance Calibrated Nighttime Lights* 2015.

Porcher, Charly, "Migration with costly information," *Unpublished Manuscript*, 2020, *1* (3).

Redding, Stephen J. and Esteban Rossi-Hansberg, "Quantitative Spatial Economics," *Annual Review of Economics*, 2017, *9* (1), 21–58.

_ and Matthew A. Turner, "Transportation Costs and the Spatial Organization of Economic Activity," in "Handbook of Regional and Urban Economics," Vol. 5 2015.

Rosenthal, Stuart S and William C Strange, "The attenuation of human capital spillovers," *Journal of Urban Economics*, 2008, *64* (2), 373–389.

Schleier, Merill, *The Skyscraper in American Art, 1890â1931* 1986.

Schneider, Julia M, Florian Zabel, and Wolfram Mauser, "Global inventory of suitable, cultivable and available cropland under different scenarios and policies," *Scientific Data*, 2022, *9* (1), 527.

Shangguan, Wei, Tomislav Hengl, Jorge Mendes de Jesus, Hua Yuan, and Yongjiu Dai, "Mapping the global depth to bedrock for land surface modeling," *Journal of Advances in Modeling Earth Systems*, 2017, *9* (1), 65–88.

Storeygard, Adam, "Farther on down the Road: Transport Costs, Trade and Urban Growth in Sub-Saharan Africa," *The Review of Economic Studies*, 04 2016, *83* (3), 1263–1295.

Tan, Ya, Zhi Wang, and Qinghua Zhang, "Land-use regulation and the intensive margin of housing supply," *Journal of Urban Economics*, 2020, *115*, 103199.

Tombe, Trevor and Xiaodong Zhu, "Trade, migration, and productivity: A quantitative analysis of china," *American Economic Review*, 2019, *109* (5), 1843–1872.

United Nations, *World Urbanization Prospects: The 2018 Revision* 2018.
World Bank, *World Development Indicators* 2022.
_ , *World Development Indicators* 2022.

WEB APPENDIX NOT FOR PUBLICATION

A Data and stylized facts

A.1 Data on Tall Buildings

The full Emporis data set includes 693,855 buildings worldwide. These include buildings of various types, heights and sizes. While Emporis attempted to collect extensive information about the world's buildings, it could not do so comprehensively. As a result, we are concerned about the selection of buildings recorded in the data set. Our empirical strategy requires measuring the universe of buildings above some height cutoff. To determine this height cutoff, we inspect the nonparameteric density of building heights in the full Emporis data set in Figure A2. Evident in Figure A2 is a spike in the distribution of building heights at just above 55 meters. It is for this reason that we use the 55 meter height threshold above which to measure the sum of heights for each city.

For a subset of our tall buildings data set, we observe not only the height of a tall building, but also the cost of construction (excluding cost of land acquisition) and the floor area. In this section, we describe how we process the data to generate the heat maps in Figure 3 and 4 and provide complementary LWR estimates using bivariate kernels that provide non-parametric point estimates of the cost-bedrock relationship by height groups aongside confidence bands.

Table A1, provides summary statistics about the Emporis construction cost data. Panel A summarizes the sample of US cities used for Figures 3, A14, and A4 and Table A18. We use this sample for most of our longitudinal analysis, to ensure that variation in the cost of height over a long time period is identified within one country that roughly follows a common trend. Panel B summarizes the multinational sample that we use in Figures 4, A5, and A15 for cross-sectional analyses.

A.1.1 Residualized log unit cost

Our analysis of building construction costs begins with a construction cost index. We build this index to net out various factors that contribute to construction costs but are unrelated to height and bedrock depth. These factors include the price of labor and construction materials and exchange rate differences. In particular, we residualize observed construction cost $C_{i,m(i),c(i),t}$ per unit of floor area $F_{i,m(i),c(i),t}$ of each building i, constructed in city m in country c during decade t using the following regression:

$$\ln C_{i,m(i),c(i),t} - \ln F_{i,m(i),c(i),t} = \mu_{m(i)} + \eta_{c(i),t} + \varepsilon^{C}_{i,m(i),c(i),t},$$

where $\mu_{m(i)}$ is a time-invariant fixed effect controlling for arbitrary demand and supply shifters at the city level and $\eta_{c(i),t}$ is a country by decade effect that controls for time-varying effects such as increasing demand due to economic growth or varying costs of construction materials. From this regression, we recover the residual, $\varepsilon^{C}_{i,m(i),c(i),t}$, as a relative cost measure that describes log

deviations from country-trend-adjusted city averages.

A.1.2 LWR using a bivariate kernel

As discussed in Section 2, innovations in construction technology may have affected the construction cost for buildings of different height differently. For example, improvements in mainframe computing and software that allow for refined structural engineering to withstand collateral wind loads may have reduced the cost of building taller. Likewise, the engineering literature suggests that in determining construction cost, building height and bedrock depth interact in a complex fashion. For tall buildings, there is generally a cost-minimizing bedrock depth, but this depth is likely to vary by height—taller buildings require deeper foundations—and so does the importance of bedrock—bedrock is generally more important to anchor taller buildings. To evaluate such complex relationship non-parametrically, we employ a locally weighted regressions approach (Cleveland and Devlin, 1988; McMillen, 1996) using a bivariate kernel.

Assume we have a set of variables $s \in \{s^1, s^2\}$ that determine our construction cost index. For each combination of grid values along those dimensions $\tilde{s}^1 \in \tilde{S}^1, \tilde{s}^2 \in \tilde{S}^2$ we run the locally weighted regression

$$\varepsilon_i^C = \bar{\varepsilon}^{\tilde{s}^1,\tilde{s}^2} + \tilde{\varepsilon}_i^{\tilde{s}^1,\tilde{s}^2}$$

using the Gaussian kernel weight

$$\begin{aligned} W_i^{\tilde{s}^1,\tilde{s}^2} &= \frac{w_i^{\tilde{s}^1,\tilde{s}^2}}{\sum_{j=i}^{J} w_j^{\tilde{s}^1,\tilde{s}^2}}, \text{where} \\ w_i^{\tilde{s}^1,\tilde{s}^2} &= \prod_{s=\in\{s^1,s2\}} \frac{1}{\kappa^s\sqrt{\pi}} \exp\left[-\frac{1}{2}\left(\frac{s_i - \tilde{s}}{\kappa^s}\right)^2\right]. \end{aligned} \tag{30}$$

where κ^s are bandwidth parameters.

Hence, we run $\tilde{S}^1 \times \tilde{S}^2$ locally weighted regressions to recover $\tilde{S}^1 \times \tilde{S}^2$ parameters $\bar{\varepsilon}^{\tilde{s}^1,\tilde{s}^2}$ which are local means that we plot on the height-bedrock plane in Figures 3 and 4. This amounts to 112 (years) $\times$ 195 (height values) = 21,840 regressions in Figure3 and 35 (bedrock depth values) $\times$ 195 (height values) = 6,825 regressions in Figure 4.

A.1.3 LWR using a univariate kernel

The strength of the heatmaps in Figures 3 and 4 is to provide an accessible presentation of a non-parametric function in two dimensions. In doing so, we focus on point estimates and abstract from confidence bands. For an illustration of the latter, we subdivide the data set into groups defined by building height and estimate the the relationships between cost and either the year of construction or bedrock height groups using LWR and univariate kernels that are otherwise identical to Eq. (30). Since we include only one dimension in our kernel, we use smaller bandwidth parameters. The blue and the red lines for 100-150 m and 150-250 m in Figures A14 and A15 roughly correspond to the blue and red lines in Figures 3 and 4, respectively.

The results presented in Figure A14 confirm that the construction cost of very tall buildings exceeding 150 m in the US have fallen significantly more that in other height categories. In particular, costs in this category have fallen throughout our 1975-2015 and 1920-1975 study periods.

The results presented in Figure A15 confirm that the cost-minimizing bedrock depth for buildings of about 125 m is about 18 m, whereas it is 25 m for buildings of about 200 m. In addition, we can reject that the cost is the same at lower or greater depths. Finally, it is notable that this U-shaped relationship between cost and bedrock depth applies more clearly to taller buildings.

A.2 Cost of height and bedrock depth

A convenient way of summarizing the cost of height is the elasticity of per-unit construction cost with respect to height (Ahlfeldt and McMillen, 2018; Ahlfeldt and Barr, 2022). The engineering literature and stylized evidence discussed in Section 2 suggests that this elasticity should non-linearly depend on bedrock depth.

To empirically substantiate this notion, we use a LWR-IV approach to estimate how bedrock depth influences unit cost responses to building heights. For implementation, we require a demand-side instrumental variable to remove the effect of supply-side factors such as ruggedness that could be correlated with sub-soil geology. We use distance from the CBD as an instrument for building heights since it affects building heights via the demand side (Brueckner, 1987; Ahlfeldt and Barr, 2022) and has empirically been shown to be a strong predictor of height (Ahlfeldt and McMillen, 2018; Ahlfeldt and Barr, 2022). The city center is defined as follows. If the city has buildings exceeding 100 meters in heights, it is the median coordinate of these buildings. Otherwise, it is the location of the tallest building in the city.

Concretely, we estimate the first stage

$$\ln h_{i.m(i),c(i),t} = \alpha^{\tilde{b}} \ln DCBD_{i,m(i)} + \tilde{\mu}^{\tilde{b}}_{m(i)} + \tilde{\eta}^{\tilde{b}}_{c(i),t} + \tilde{\varepsilon}^{\tilde{b}}_{i,m(i),c(i),t} \tag{31}$$

and a second stage:

$$\ln C_{i,m(i),c(i),t} - \ln F_{i,m(i),c(i),t} = \theta^{\tilde{b}} \widehat{\ln h}_{i.m(i),c(i),t} + \mu^{\tilde{b}}_{m(i)} + \eta^{\tilde{b}}_{c(i),t} + \varepsilon^{\tilde{b}}_{i,m(i),c(i),t} \tag{32}$$

for each LWR $\tilde{b} \in \tilde{B}$ using a weighted 2SLS estimator. $h_{i,m(i),c(i),t}$ is the height of building i, constructed in city m in country c during decade t, $DCBD_{i,m(i)}$ is building i's distance from the center of city $m(i)$, $\ln C_{i,m(i),c(i),t} - \ln F_{i,m(i),c(i),t}$ is the log of the cost per unit of floor area, $\{\mu^{\tilde{b}}_{m(i)}, \mu^{b}_{m(i)}\}$ are city fixed effects, $\{\eta^{\tilde{b}}_{c(i),t}, \eta^{b}_{c(i),t}\}$ are country by decade fixed effects, and $\{\tilde{\varepsilon}^{\tilde{b}}_{i,m(i),c(i),t}, \varepsilon^{\tilde{b}}_{i,m(i),c(i),t}\}$ are error terms.

In each LWR $\tilde{b} \in \tilde{B}$ we weight observations by the Gaussian kernel weight

$$\begin{aligned} W_i^{\tilde{b}} &= \frac{w_i^{\tilde{b}}}{\sum_{j=i}^{J} w_j^{\tilde{b}}}, \text{where} \\ w_i^{\tilde{b}} &= \frac{1}{\kappa^{\tilde{b}}\sqrt{\pi}} \exp\left[-\frac{1}{2}\left(\frac{b_i - \tilde{b}}{\kappa^{\tilde{b}}}\right)^2\right]. \end{aligned} \tag{33}$$

Notice that Eq. (33) uses a univariate version of the same kernel as in Eq. (30), except that we employ a LWR-specific bandwidth. This is because we wish to allow for a more flexible fit via a smaller bandwidth in the in the more populated part of the bedrock distribution where we also expect more variation in θ, whereas we wish to reduce standard errors in the right tail of the bedrock distribution that is more sparsely populated and where we expect less variation in θ. To this end, we use a variant of Scott's rule of thumb for bandwidth selection and define

$$\kappa^{\tilde{b}} = \mathcal{M}\frac{3.49\hat{\sigma}^{\tilde{b}}}{\left(N^{\tilde{b}}\right)^{\frac{1}{3}}},$$

where the standard deviation $\hat{\sigma}^{\tilde{b}}$ and the number of observations $N^{\tilde{b}}$ are computed for rolling subsamples that satisfy $|b_i - \tilde{b}| \leq \mathcal{B} = 10$. We scale the rule-of-thumb bandwidth by a factor of $\mathcal{M} = 2$ since the non-parametric estimation of derivatives generally requires larger bandwidths than the estimation of levels (Henderson and Parmeter, 2015, Section 5.9).

The results in Figure A5 support the engineering-based hypothesis that bedrock at intermediate depths reduces the construction cost of tall buildings. Within the sample of buildings for which we observe height, construction cost, and floor area, the marginal cost of increasing height is minimized at a bedrock depth of about 15 meters. At depths below about 5 meters or greater than 25 meters, the cost of height is significantly larger. This range is roughly consistent with the descriptive evidence from Figures 4 and A15, given an average building height of 109 meters in our sample. The results in Figure A5 support the idea that as demand for height increases over time, cities with bedrock within an intermediate range will have a greater ease of accommodating that demand, resulting in lower barriers to growth.

A.3 Cost of height over time

As discussed in more detail by Ahlfeldt and Barr (2022), several technological innovations have contributed to the emergence of tall buildings as an increasingly widespread urban phenomenon. Around the turn of the 20$^{\text{th}}$ century, the elevator and and steel frame made tall commercial and residential structures economically viable. Starting in the 1960s, mainframe computers allowed for more sophisticated structural engineering, facilitating lighter and taller buildings that could withstand stronger collateral wind loads, with continued improvements thereafter. In the near future, the magnetic elevator is expected to remove yet another barrier to vertical growth.

It is therefore reasonable to expect a secular downward trend in the cost of height. Indirect

evidence from correlations of land prices and building heights substantiates this hypothesis (Ahlfeldt and McMillen, 2018; Ahlfeldt and Barr, 2022). We use our construction cost data set to directly test the hypothesis that the height elasticity of construction cost has decreased over time. Since different parts of the world have adopted the skyscraper technology at different points in time, we focus on the US—the only country for which we can estimate the cost of height throughout the 20$^{\text{th}}$ century—to avoid changes in our estimates of the cost of height over time being driven by the international composition of the sample. In Table A18, we report the results from instrumental variable regressions of a log cost measure against the log of height and an interaction with a time trend. We normalize this trend to have a value of zero in 1975, the beginning of our observation period in the main stages of our analyses. Hence, the coefficient on the non-interacted log height variable gives the height elasticity of cost in 1975 while the coefficient on the interaction reveals how this elasticity changes over time. All estimates control for city fixed effects, decade fixed effects and a time trend. Columns (1) presents OLS estimates. Column (2) presents IV estimates, where the log distance from the city center (the median coordinate of buildings exceeding 100 m or the tallest building if shorter) and its interaction with a time trend serve as instrumental variables. Both models confirm the hypothesis that the cost of height has decreased over time. The OLS estimates point to a reduction in the height elasticity of costs by slightly less than one percentage point per year. The 2SLS estimates are significantly larger, pointing to a reduction of 2.2 percentage points per year.

To allow for greater flexibility in the time trend, we use a LWR-IV specification similar to the one described by Eqs (31), (32) and, (33). The only difference is that we use the year instead of bedrock as a covariate in the univariate kernel and employ a constant bandwidth of $\kappa = 30$, since we have no priors regarding when we should expect greater changes in the cost of height. Figure A4 confirms that the height elasticity of cost has declined since the beginning of the 20$^{\text{th}}$ century. Hence, the evidence supports the notion of a secular downward trend in the cost of height that should act as supply-side driver of vertical growth.

B Empirical Analysis

B.1 Analysis Using Monotonic Bedrock Depth Instruments

The engineering literature suggests a non-monotonic relationship between bedrock depth and construction cost for tall buildings. To accommodate this non-monotonic relationship, our baseline specification employs a second-order polynomial in bedrock depth as a construction cost shifter. Here, we present results using the alternative more flexible approach in which our bedrock quality measure is instead specified as a linear spline in bedrock depth. This specification allows bedrock quality to increase linearly in bedrock depth until a first kink. Beyond the first kink, there is a negative relationship between bedrock quality and bedrock depth until a second kink. Beyond the second kink, bedrock depth has no effect on bedrock quality since it is too deep to matter for the construction of tall buildings. With this approach, we obtain two bedrock quality measures–one covering depths from zero to the first kink, and one covering depths from

the first to the second kink–each of which we expect to be monotonically positively related to heights. Using these quality measures as instruments for height, we can evaluate both the monotonicity properties of our baseline IV specification and the extent to which our height elasticity estimates are identified from cities where bedrock is too close to the surface or too deep.

The quality measure for bedrock near the surface is defined as follows:

$$BRQ_a^{surf} = MBD_a \times \mathbb{1}\left(MBD_a < \mathcal{K}^1\right),$$

where MBD_a is mean bedrock depth in city a and $\mathcal{K}^1$ is the first kink of the spline function where deeper bedrock transitions from reducing to increasing construction costs for tall buildings. BRQ_a^{surf} is zero when bedrock is at the surface ($MBD_a = 0$) and increases proportionately in bedrock depth until a depth of just under $\mathcal{K}^1$. From depths of $\mathcal{K}^1$ onward, BRQ_a^{surf} is set to zero.

The quality measure for deep bedrock is defined as follows:

$$BRQ_a^{deep} = \mathcal{K}^1 \times \left(1 - \frac{1}{\mathcal{K}^2 - \mathcal{K}^1}\right) \times \left(MBD_a - \mathcal{K}^1\right) \times \mathbb{1}\left(\mathcal{K}^1 \leq MBD_a \leq \mathcal{K}^2\right),$$

where $\mathcal{K}^2$ defines the second kink of the spline function beyond which bedrock depth does not influence construction costs. BRQ_a^{deep} takes a zero value below depth $\mathcal{K}^1$, begins at its maximum value at $\mathcal{K}^1$, and declines linearly until it reaches zero at bedrock depth $\mathcal{K}^2$, beyond which it stays at zero.

With these bedrock quality measures in hand, we estimate the following second-stage regression:

$$y_{ac} = \beta\Delta \ln\left(Heights_{ac} + 1\right) + \alpha_1 BRQ_{ac}^{surf}(\mathcal{K}^1, \mathcal{K}^2) + \alpha_2 BRQ_{ac}^{deep}(\mathcal{K}^1, \mathcal{K}^2) + \alpha_3 \ln Pop_{ac75} + \kappa_c + \varepsilon_{ac},$$

where, compared to Eq. (7), the mean bedrock variables $\{MBD_{ac}, MBD_{ac}^2\}$ are replaced with the bedrock quality variables. In perfect analogy to Eq. (7), the excluded instruments in the first stage are the interaction terms between bedrock quality and 1975 log population ($BRQ_{ac}^{surf}(\mathcal{K}^1, \mathcal{K}^2) \times \ln Pop_{ac75}$, $BRQ_{ac}^{deep}(\mathcal{K}^1, \mathcal{K}^2) \times \ln Pop_{ac75}$). To find $\{\mathcal{K}^1, \mathcal{K}^2\}$, we estimate the specification for all combinations of $\mathcal{K}^1 = \{10, 11, ..., 40\}$ and $\mathcal{K}^2 = \{50, 11, ..., 158\}$, where the upper bound $\mathcal{K}^2 = 158$ is the largest bedrock depth value observed in our data, and choose the values that maximize the first-stage F-statistic.

With this approach, we obtain the bedrock quality spline function illustrated in Figure A16. In keeping with the engineering narrative, bedrock quality increases until a bedrock depth of 22 meters as the cost of removing bedrock to free space for building foundations decreases. Beyond that depth, bedrock quality decreases as the cost of anchoring tall buildings to bedrock increases. Bedrock quality decreases until the greatest depth observed in our data, suggesting that bedrock depth still matters at relatively large depths, though the slope of the downward-sloping section of the spline function is obviously driven by smaller depths as only few cities have depths beyond

80 meters. Figure A16 also illustrates how our two bedrock quality measures BRQ^{surf} (solid black line) and BRQ^{deep} (dashed red line) separately capture bedrock quality where deeper bedrock is a construction amenity (BRQ^{surf}) or a construction disamenity (BRQ^{deep}).

We illustrate the distribution first-stage F-statistics across runs with different values of $\{\mathcal{K}^1, \mathcal{K}^2\}$ in Figure A17. The left panel shows that the first-stage F-statistic is generally relatively high within a range of $\mathcal{K}^1 \in (20, 30)$. This is about the range where heights are particularly responsive to growing floor space demand as illustrated in Figure 5. The right panel confirms that irrespective of the value of the first kink ($\mathcal{K}^1$) the F-statistic is generally maximized for the second kink at $\mathcal{K}^2 = 158$ meters, the largest depth in our data. It is worth noting that the F-stat remains high even if we lower the value for the second kink by about 50% to $\mathcal{K}^2 = 80$. The first-stage and second-stage results discussed below hardly change as we alter $\mathcal{K}^2$ within this range.

We report first-stage and second-stage estimates using our bedrock quality instruments in Table A8. The estimated height elasticity of population, at 0.128, is almost identical to our baseline estimate from Table 2. The estimated height elasticity of built area is, in absolute terms, somewhat larger than in the baseline whereas the height elasticity of urban area is somewhat smaller and estimated imprecisely. The first-stage effects of the bedrock quality-population interaction terms also show the expected positive signs and are estimated precisely. The important implication is that bedrock quality matters both where bedrock is near the surface and where bedrock is deep.

Given these encouraging first-stage results, one naturally wonders whether it is possible to identify our height elasticities from variation in bedrock depth on either side of the first kink. To this end, we use one of the two bedrock quality-population interaction term as a second-stage control in Table A9, so that the other quality-population interaction term is the sole excluded instrument driving identification. In Columns (1), (3), (5), the identifying variation stems from cities with bedrock near the surface whereas it stems from cities with deep bedrock in the remaining columns. Indeed, we find that using variation in bedrock depth from either side of the first kink, we obtain height elasticity estimates that are within the range of estimates we obtain when using the quadratic bedrock depth instruments, although the height effects on urban area are, again, estimated imprecisely.

Overall, the results using the bedrock quality instruments not only substantiate our baseline height elasticity estimates, they also reveal that our findings are driven by cities where bedrock is to near the surface as well as a cities where bedrock is too deep.

B.2 Construction of Locally-Weighted Regression Estimates

In Section 3.2, we present height elasticity estimates for various outcomes by 1975 city population. To obtain these city-specific parameter estimates $\beta^{\tilde{a}}$, we implement a locally weighted regressions (LWR) variant of our baseline instrumental variable regressions. Concretely, for each city $\tilde{a}$, we estimate the following second-stage regression, which matches that in (7) except that parameters are indexed by city and observations closer in log population to city

$\tilde{a}$ are assigned more weight. For notational convenience, we globally index all cities by a and denote country as $c(a)$.

$$y_a = \beta^{\tilde{a}} \Delta \ln (Heights_a + 1) + \alpha_1^{\tilde{a}} MBD_a + \alpha_2^{\tilde{a}} MBD_a^2 + \alpha_3^{\tilde{a}} \ln Pop_{a75} + \kappa_{c(a)}^{\tilde{a}} + \varepsilon_a^{\tilde{a}}$$

In each LWR-IV regression, a second-order polynomial of city-level mean bedrock depth interacted with 1975 log city population instruments for $\Delta \ln (Heights_a + 1)$. Except for the superscript $\tilde{a}$, denoting city-specific estimates, and the re-indexing of cities and countries, all variables are defined as in Section 3 in the main paper.

In each LWR we weight observations by the Gaussian kernel weight

$$w_a^{\tilde{a}} = \frac{1}{\iota^{\tilde{a}} \sqrt{\pi}} \exp \left[-\frac{1}{2} \left(\frac{\ln Pop_a - \ln Pop^{\tilde{a}}}{\iota^{\tilde{a}}} \right)^2 \right].$$

$\iota^{\tilde{a}}$ governs the bandwidth and $\ln Pop_a - \ln Pop^{\tilde{a}}$ gives the difference between the log populations of each city a and the target city $\tilde{a}$ for which a local value of β is being estimated. Intuitively, a city a will receive a higher weight in a LWR $\tilde{a} \in J$, the more similar its population is to that of city $\tilde{a}$.

We employ the LWR-specific bandwidth $\iota^{\tilde{a}}$ because we wish to allow for a more flexible fit via a smaller bandwidth in the more populated part of the population distribution, whereas we wish to reduce standard errors in the right tail of the population distribution that is more sparsely populated by expanding the bandwidth in this region. To this end, we use a variant of Scott's rule of thumb for bandwidth selection and define

$$\iota^{\tilde{a}} = \mathcal{M} \frac{3.49 \hat{\sigma}_{\ln Pop}^{\tilde{a}}}{(N^{\tilde{a}})^{\frac{1}{3}}},$$

where the standard deviation $\hat{\sigma}_{\ln Pop}^{\tilde{a}}$ and the number of observations $N^{\tilde{a}}$ are computed for rolling sub-samples that satisfy $|\ln Pop_a - \ln Pop^{\tilde{a}}| \leq \mathcal{B} = 5$. We scale the rule-of-thumb bandwidth by a factor of $\mathcal{M} = 20$ since the non-parametric estimation of derivatives generally requires larger bandwidths than the estimation of levels (Henderson and Parmeter, 2015, Section 5.9). Importantly, these choices ensure that we can distinguish our point estimates from zero with nearly 95% confidence throughout the population distribution.

Our LWR estimates of height elasticities for population, built-up area, and urban area are in Figures A9, A8, and A10. (Figure 7 displays separate estimated population elasticity functions for two regions in the developing world.) We observe that the height elasticity of population is U-shaped with respect to initial city size. This pattern is suggestive of a sizable extensive-margin effect (introducing tall buildings) coupled with an intensive-margin effect (vertical growth conditional on having tall buildings) that increases in city size. It is noteworthy that the turning point is reached at a population of about $\exp(13.8) = 1M$, which has been found to be near the threshold at which cities typically adopt the skyscraper (buildings taller than 150 m) technology (Ahlfeldt and Barr, 2022).

The convex intensive-margin effect is plausible as a vertical expansion is likely to have a greater impact on a city's capacity to accommodate residential and commercial uses when a city has exhausted its potential for horizontal expansion. Consistent with this hypothesis, we find that a large city's (built-up and urban) areas are relatively insensitive to a technology-induced increase in height (due to favorable bedrock). The implication is that less vertical growth cannot easily be compensated by greater horizontal growth. In contrast, land area is much more responsive to technology-induced vertical growth in small cities. This is intuitive since small cities can more easily grow horizontally if they cannot grow vertically (due to unfavorable bedrock conditions).

B.3 Details of Height Gap Calculations

We adopt the regression specification to predict city heights used in Barr and Jedwab (2023, eq. (6)). The analysis uses 12,755 GHS-UCDB cities, a, in 163 countries, c, in the years $t = \{1995, 2000, 2005, 2010, 2015, 2020\}$ (N = 76,530). In each year, these cities are classified into 10 categories, indexed by p, as determined by population at time t: 0-100K, 100-250K, 250-500K, 500-750K, 750-1,000K, 1,000-2,500K, 2,500-5,000K, 5,000-7,500K, 7,500-10,000K, 10,000K+. Since city population is only available in 1990, 2000, and 2015 in the GHS-UCDB database, population categories are defined using year 2015 population data for 2010-2020 and 2000 population data for 1995-2005.

The estimation equation is

$$\begin{aligned} \text{LHEIGHTS}_{act} = \rho_1 \text{LDMSP}_{act(d)} + \rho_2 \text{LVIIRS}_{act(v)} \\ + \Sigma_{p=1}^{10} \gamma_{p,t} \mathbb{1}(\text{CAT}_{act} = p) + \Sigma_{p=1}^{10} \mathbb{1}(\text{CAT}_{act} = p) X_{ct} \beta_{p,t} \\ + \Sigma_{p=1}^{10} \mathbb{1}(\text{CAT}_{act} = p) X_{ac} \delta_{p,t} + \nu_{act}. \end{aligned} \tag{34}$$

The parameters ρ_1, ρ_2, and $\gamma_{p,t}$ are scalars. $\beta_{p,t}$ and $\delta_{p,t}$ are vectors to reflect that X_{ct} and X_{ac} are matrices that include the variables described below. LHEIGHTS_{act} is the log of (total sum of tall building heights + 1) in city a, country c, and year t. The ten population size dummies (CAT_{act}) are included fully interacted with year fixed effects to control for differing levels and trends in real estate demand and construction costs across cities of different sizes. Remaining controls for economic development and other demand and supply factors include the country-level controls (X_{ct}) and time invariant city-level controls (X_{ac}), which are fully interacted with the 10 population size dummies and year fixed effects, allowing their impacts to vary by city size over time. The objective is to estimate residuals (ν_{ac2015}), which proxy for land-use regulations and height restrictions in city ac in 2015.

The first two variables in the regression denote city total night lights and proxy for city income in different years. The log of (total sum of DMSP lights + 1) can be calculated for years $t(d)$ 1995, 2000, 2005 and 2010.[34] The log of (total sum of VIIRS lights + 1) can be calculated

[34]Night lights data corresponding to the DMSP satellites are provided by NGDC (2015). The radiance calibrated version of this data, which is available for select years between 1996 and 2011, is used to avoid top-coding complications. The data are available at a 30 arc second (≈ 1km at the equator) spatial resolution. For

for years $t(v)$ 2010, 2015 and 2020.[35] Other demand side factors (X_{ct}) are accounted for with city population and year interacted with quadratics in national per-capita GDP,[36] national population, and national land area.[37] More populated countries tend to have larger large cities. For example, the largest city of China or India is far larger than the largest city of El Salvador or Rwanda. Since the largest cities of China and India are larger, they will naturally have more demand for heights and tall buildings. Likewise, countries with more available land tend to have less vertical cities. If land is "cheap," cities can expand more horizontally (Brueckner, 1987).

Time-invariant city-level controls (X_{ac}) (interacted with city size dummies and year fixed effects) account for various demand and supply factors. On the supply (cost) side are city mean bedrock depth, earthquake risk,[38] and quadratics in the mean and standard deviation of city elevation.[39] Elevation range also controls for some demand side factors, as cities surrounded by more mountainous land may have less scope for horizontal expansion, thereby increasing the demand for heights near city centers.

Overall, regression estimates yield an adjusted R-squared of 0.64, suggesting that fundamental demand and supply factors may account for almost two thirds of the international variation in city heights. Assuming the other 0.36 can be attributed to land-use regulation, the estimated residuals ν_{act} captures the extent to which a city ac has more or less heights than other cities that are similar on observable characteristics.

Using estimated parameters in (34), we predict each city's 2015 stock of heights were it to have among the most heights for cities with similar observables. We view this prediction as the amount of heights the city would have were it unconstrained by regulation. Comparisons of actual heights to this prediction of unconstrained heights will deliver each city's height gap.

To build up to the determination of each city's counterfactual unconstrained heights, we begin by predicting the log sum of heights in 2015 for each city using parameter estimates in (34). We then select the 25 cities with the most similar predicted heights above and below each city's prediction.[40] For each city's group of 51, we obtain the 95th percentile ("p95"), or 3rd ranked city-level residual. High p95 values indicate that the city's group includes cities that are well above the world's conditional average. On the contrary, low p95 values indicate that the city's group mostly includes cities close to the world's conditional average. We use p95 instead

the years 1995, 2000, 2005, and 2010, DMSP years 1996, 2000, 2005, and 2010 are used.

[35] Night lights data from VIIRS satellites are provided by Elvidge et al. (2021). The data is not top-coded and are available at a 15 arc second (≈ 500m at the equator) spatial resolution. For the years 2010, 2015 and 2020 VIIRS years 2010, 2015, and 2019 (due to COVID-19) are used.

[36] Annual per-capita GDP is obtained for 1950 to 2018 (PPP and constant international 2011 $) from Maddison (2008) and Bolt and van Zanden (2020) To avoid short-term fluctuations in income, data for each year t reflects a 7 year moving-average.

[37] The main sources for land area and total population are United Nations (2018) and World Bank (2022).

[38] For the whole world, Giardini et al. (1999) reports peak ground acceleration (PGA; m per s^2) at the 0.0833*0.0833 degree level (≈ 9 x 9 km). PGA takes into account the probability of strong earthquakes in each pixel as well as the probability of diffusion over space. Since land-use regulations related to earthquake risk tend to be adopted based on fuzzily defined local conditions, Barr and Jedwab (2023) consider buffers of 0.05 degree (5.55 km) around each city. They then obtain the mean PGA for each city/buffer.

[39] The elevation data comes from GMTED (2010) (resolution: 15 arc-seconds, or 500 meters close to the equator).

[40] The 24 cities at the bottom and top of the world ranking are still combined with 50 cities, with some necessary imbalance between the number of over and under predictions in the group.

of the max or p99 to allow for the possibility that 2 cities in each group may have a lot of heights due to idiosyncratic city-specific factors rather than laissez-faire planning regulations. For example, they may have a large government sector or developers with interests in marquee skyscrapers that are not justified by city fundamentals.

Figure A11 plots the local polynomial relationship (bandwidth = 1) between p95 and predicted 2015 log heights.[41] We denote this function describing inferred unconstrained heights as $h^{95}(\cdot)$. By construction, cities that are predicted to have little heights (on the left of the graph) belong to groups where the least constrained cities do not have measurably more heights than the world's conditional average. Cities that are predicted to have a lot of heights (on the right of the graph) belong to relatively homogeneous groups in terms of heights. Cities with the largest height fundamentals all have similar height stocks, *ceteris paribus*, meaning that their height gaps are relatively low. Much larger differences can be observed for cities with intermediate height predictions. Such cities disproportionately belong to developing economies, where more varied patterns of vertical development can be observed within a group of otherwise similar cities. We verify that similar relationships are obtained when excluding Chinese and Middle Eastern cities (unreported). The high p95 values suggest that regulatory differences account for the observed within-group differences.

We calculate the height gap (%) for city ac in the year 2015 using both the actual heights (unlogged) and the counterfactual log heights:

$$Gap_{ac} = \max\left(1 - \frac{Heights_{ac2015}}{H^{95}(\widehat{LHEIGHTS}_{ac2015})}, 0\right),$$

where $\widehat{H^{95}}(\cdot) = \exp\left[\widehat{h^{95}}(\cdot)\right]$ and $\widehat{LHEIGHTS}_{ac2015}$ is predicted log heights for city ac in 2015. A gap of 20% means that the city has built 80% of what the p95 city in the city's group has built despite sharing similar economic conditions. Cities with residual values above the p95 value have their gaps set to 0%. The median height gap is 0%, reflecting the many small cities in our data whose fundamentals do not justify tall buildings. However, the distribution has a thick right tail driven by larger cities. Equally weighted, the mean and standard deviation are 24% and 41%, respectively. Weighting by city population, the median is 66%, the mean is 50%, and the standard deviation is 45%.

Among the 100 largest cities in the world, we obtain gaps of 0% for cities including Chicago, Kuala Lumpur, Sao Paulo, Seoul, and Shanghai (these are cities at, or above, the 95p value). We obtain small gaps of 11% for Guangzhou, 26% for New York, 37% for Ho Chi Minh City, and 45% for Miami. We obtain larger gaps of 66% for Bangkok, Paris, London, and Mexico City. We obtain larger gaps of 73% for Beijing, 80% for Buenos Aires, 91% for Karachi, and 93% for Cairo. Sensible differences are obtained within the US. Lower-gap large cities include Chicago (0%), New York (26%) and Miami (45%). Higher-gap large cities include Boston (70%), Los Angeles (82%), Washington DC (86%) and San Francisco (94%). Lastly, to compute global or regional gaps, we use 2015 city populations as weights. We find a global gap of 50%. Thus, the

[41] We drop cities in groups with no heights above 55 meters. By construction, these cities have no height gaps.

world could accommodate twice as many tall buildings per-capita.

C Model

This appendix goes with Section 4 in the main paper.

C.1 Equilibrium solver

Values of endogenous objects $\{y, \bar{U}\}$, parameters $\{\alpha^U, \beta, \omega^U, \theta^U, \tau^U, \underline{x}^U, \bar{a}^U, \tilde{c}^U, \bar{S}^U, r^a, \zeta, \ell, \tilde{U}\}$, and the endowment $\bar{N}$ deliver a unique mapping to all other endogenous objects. Hence, the equilibrium can be referenced by $\{y, \bar{U}\}$. To solve for these equilibrium values, we implement an algorithm described by the pseudo-code in Algorithm 1.

Algorithm 1: Equilibrium solver

Data: Given values for primitives $\{\alpha^U, \beta, \omega^U, \theta^U, \tau^U, \underline{x}^U, \bar{a}^U, \tilde{c}^U, \bar{S}^U, r^a, \zeta, \ell, \bar{N}, \tilde{U}\}$
Guesses of equilibrium values of $\{\bar{U}, y\}$

while $\bar{U} \neq \widehat{\bar{U}}$ *or* $y \neq \hat{y}$ **do**
- Compute N using Eq. (13)
- Compute $\bar{p}^U(x)$ using Eqs. (16) & (20)
- Compute $\tilde{S}^U(x)$ using Eq. (22)
- Compute $r^U(x)$ using Eq. (23)
- Allocate land to use with the highest land rent
- Compute market-clearing wage $\hat{y}$ using Eqs. (21) and (24)
- Compute endogenous city-utility $\widehat{\bar{U}}$ using Eq. (27)
- Update guesses to weighted combination of old guesses and $\{U, \hat{y}\}$

Equilibrium values of $\{\bar{U}, y\}$

C.2 Quantification

This section provides further details on how we determine parameter values, adding to Section 4.2 in the main paper.

C.2.1 Amenity decay (τ^U)

In the absence of binding height limits, we can use equations (3) and (15) or (19) to obtain the structural equation for building height by use at each location $x > \underline{x}^U$:

$$\ln S^U(x) = \frac{1}{(1-\alpha^U)(\theta^U - \omega^U)} k^U - \frac{1}{\theta^U - \omega^U} \ln\left[c^U(1+\theta^U)\right] - \frac{\tau^U}{(1-\alpha^U)(\theta^U - \omega^U)} x,$$

where $k^R = \ln \frac{\alpha^{\bar{R}} y}{\bar{U}}$ and $k^C = \ln \frac{\bar{\alpha}^C N^\beta}{y^{\alpha^C}}$. This equation motivates the following reduced form building type-specific log-linear regression specification that has been used to estimate various

price and density gradients (Ahlfeldt and Barr, 2022):

$$\ln S_{ib}^{U} = \mathcal{G}_{0}^{U} + \mathcal{G}_{1}^{U} DIST_{ib} + \mathcal{E}_{ib}^{U}$$

$DIST_{ib}$ is the distance from building i in distance ring b to the city center and $\mathcal{E}_{ib}^{U}$ is a residual term that captures deviations in observed height from a smooth gradient. It is straightforward to recover the amenity decay from an estimate of the reduced-form parameters $\mathcal{G}^{U}$:

$$\tau^{U} = -\mathcal{G}^{U}(1-\alpha^{U})(\theta^{U} - \omega^{U})$$

To estimate $\mathcal{G}^{U}$, we use the number of stories for all commercial or residential buildings within 10km of the Chicago city center, excluding industrial and government buildings. We define the city center as the average location of the tallest 5 commercial buildings in the city. We use the CoreLogic property assessment data set from 2021/2022. The main advantage of CoreLogic over the Emporis data, which has previously been used to estimate height gradients, is that it contains the near universe of buildings, including those with heights of less than 55 meters. We weight by the inverse of the number of observations in each 250 meter wide distance ring bin b, giving each bin equal weight in the regressions. We choose Chicago as our case in point because it is arguably the stereotype of an unconstrained, monocentric city that conforms to our land-use model. Estimated height gradients are reported in Table A14. From those estimates, we infer the values of our structural parameters $\tau^{C} = 0.014$ and $\tau^{R} = 0.016$.

We are, of course, interested in the degree to which the height gradients estimated for Chicago generalize to other cities. Therefore, we also examine urban structure in a broader set of height unconstrained global cities. As comprehensive building-level data akin to CoreLogic does not exist globally, we make use of a global 80X80 meter raster data set of remote-sensed building volumes (Esch et al., 2023). We include cities with height gaps below 50% (see Section 3.4 for calculation of height gaps), some height in the Emporis data, and with populations of at least 1 million in 2015. This gives us 39 cities in developing economies and 11 cities in developed economies, including Chicago.

One limitation of the volume data is that it does not distinguish between commercial and residential uses. As such, we exploit our model's prediction of a change in the slope of the height gradient at the border between the commercial and the residential zones. Therefore, for each of the 50 cities with building volume data mentioned above, we estimate the following piece-wise linear spline specification with one endogenous knot:

$$\ln FAR_{b} = \mathcal{B}_{0} + \mathcal{B}_{1} DIST_{b} + (\mathcal{B}_{2} - \mathcal{B}_{1})(DIST_{b} - \mathcal{K}_{1})\mathbb{1}(DIST_{b} \geq \mathcal{K}_{1}) + \mathcal{E}_{b}$$

FAR_{b} is the total building volume divided by land area across all 80X80 meter pixels in city center distance ring b out to 10 km. Each distance $DIST_{b}$ is 250 meters wide. Therefore, the outcome measure is close to a floor area ratio (FAR) measure of building density, though the denominator includes area of land in all uses (including roads and parks), not just land parcels on which building construction can take place. For each of the 50 cities, we identify the city

center location using information on lights at night and the tallest buildings in each city. $\mathcal{K}_1$ gives the distance from the endogenous knot to the city center, $\mathcal{B}_1$ is the height gradient for $DIST_b < \mathcal{K}_1$ and $\mathcal{B}_2$ is the gradient when $DIST_b \geq \mathcal{K}_1$. We use non-linear least squares to estimate $\{\mathcal{B}_0, \mathcal{B}_1, \mathcal{B}_2, \mathcal{K}_1\}$ for each city. Figure A18 summarizes the results, with estimates for Chicago indicated with vertical dashed lines. Chicago's internal structure is not an outlier. Within the building volume data, Chicago's overall gradient, knot location and location-specific gradients are close to the mean and the mode across these 50 cities.

C.2.2 Rural utility

We treat rural utility, $\tilde{U}$, as a fundamental that we can invert for given values of other primitives and an observed or user-specified urban population share, μ, using a procedure described in Algorithm 2.

Algorithm 2: $\tilde{U}$ inverter

Data: Given values of primitives $\{\alpha^U, \beta, \omega^U, \theta^U, \tau^U, \underline{x}^U, \bar{a}^U, \tilde{c}^U, \bar{S}^U, r^a, \zeta, \ell, \bar{N}\}$
Guess of $\tilde{U}$
User-chosen μ

while $\tilde{U} \neq \widehat{\tilde{U}}$ **do**
- Compute $\bar{U}$ using Algorithm 1
- Compute rural utility, $\widehat{\tilde{U}}$, using Eq. (13)
- Update guess of $\tilde{U}$ to weighted combination of old guess and $\widehat{\tilde{U}}$

Result: $\tilde{U}$ that rationalizes given μ

C.2.3 Preference heterogeneity

We seek to find the value of ζ under which the model generates our key empirical moments. These are our estimates of the height elasticity of population, $\hat{\beta}^N$, and the height elasticity of area, $\hat{\beta}^{\mathcal{L}}$. In our empirical identification strategy, we exploit subsoil geography to ensure that we identify these parameters from variation in the cost of height, holding housing demand factors constant. Since we have full control over the data-generating process, it is straightforward to mimic this source of variation in the model.

To this end, we solve the model multiple times for values of $\theta \in \Theta$, where $\theta^C = \theta$ and $\theta^R = \theta + 0.05$ to maintain the same difference between the commercial and residential height elasticity as in the baseline specification in Table 6. Holding all other parameters constant, we obtain differences in equilibrium outcomes that are solely driven by variations in the cost of height. To operationalize our SMM approach, we nest this loop over $\theta \in \Theta$ within a search over a parameter space defined by $\zeta \in \mathcal{Z}$ and $\mathcal{T} \in \mathcal{R}$. We invert $\tilde{U}$ each time we adjust ζ, setting $\mu = \bar{\mu}$ and all parameters to the values in Table 6 to keep the city population constant. For each

combination of $\{\theta, \zeta, \mathcal{T}\}$, we solve the model and compute (the endogenous outcomes) city area

$$\mathcal{L}_\theta^{\zeta,\mathcal{T}} = \int_0^{(x_1)^{\theta,\zeta,\mathcal{T}}} \mathcal{L}(x)dx,$$

city population

$$N_\theta^{\zeta,\mathcal{T}} = \int_{(x_0)^{\theta,\zeta,\mathcal{T}}}^{(x_1)^{\theta,\zeta,\mathcal{T}}} (n(x))^{\theta,\zeta}dx,$$

and city tall building height

$$H_\theta^{\zeta,\mathcal{T}} = \int_0^{(x_1)^{\theta,\zeta,\mathcal{T}}} \mathcal{L}(x)\left((S^C(x))^{\theta,\zeta} - \mathcal{T}\right)dx + \int_{(x_0)^{\theta,\zeta,\mathcal{T}}}^{(x_1)^{\theta,\zeta,\mathcal{T}}} \mathcal{L}(x)\left((S^R(x))^{\theta,\zeta} - \mathcal{T}\right)dx. \tag{35}$$

For each combination of $\{\zeta, \mathcal{T}\}$, we run the following regressions on the model-based outcomes to recover our moments in the model $\{\tilde{\beta}^N, \tilde{\beta}^{\mathcal{L}}\}$:

$$\ln \mathcal{L}_\theta^{\zeta,\mathcal{T}} = c^{\mathcal{L},\zeta,\mathcal{T}} + \tilde{\beta}^{\mathcal{L}}_{\zeta,\mathcal{T}} \ln H_\theta^{\zeta,\mathcal{T}} + \tilde{\epsilon}_\theta^{\mathcal{L},\zeta,\mathcal{T}}$$
$$\ln N_\theta^{\zeta,\mathcal{T}} = c^{N,\zeta,\mathcal{T}} + \tilde{\beta}^{N}_{\zeta,\mathcal{T}} \ln H_\theta^{\zeta,\mathcal{T}} + \tilde{\epsilon}_\theta^{N,\zeta,\mathcal{T}}$$

We find our preferred combination of $\{\zeta, \mathcal{T}\}$ by minimizing the value of the residual sum of squares of the moments in model and data:

$$\zeta, \mathcal{T} = \arg \min_{\zeta \in \mathcal{Z}, \mathcal{T} \in \mathcal{R}} \sum_{o \in N, \mathcal{L}} \left(\hat{\beta}^o - \tilde{\beta}^o\right)^2 \tag{36}$$

We provide a compact summary of the procedure using pseudo code Algorithm 3.

Algorithm 3: Calibrating $\{\zeta, \mathcal{T}\}$

Data: Given values of primitives $\{\alpha^U, \beta, \omega^U, \theta^U, \tau^U, \underline{x}^U, \bar{a}^U, \tilde{c}^U, \bar{S}^U, r^a, \zeta, \ell, \bar{N}\}$
Moments in data $\{\widehat{\beta}^N, \widehat{\beta}^{\mathcal{L}}\}$
User-chosen μ

foreach $\zeta \in \mathcal{Z}$ **do**
  Use Algorithm 2 to invert $\tilde{U}$ so to match $\mu = 0.3(\Rightarrow)N = \mu\bar{N} = 3M)$ under baseline values of $\{\theta^C = 0.5, \theta^R = 0.55\}$
  foreach $\mathcal{T} \in \mathcal{R}$ **do**
    foreach $\theta \in \Theta$ **do**
      Use Algorithm 1 to solve for equilibrium outcomes of $\{\mathcal{L}_\theta^{\zeta,\mathcal{T}}, N_\theta^{\zeta,\mathcal{T}}, H_\theta^{\zeta,\mathcal{T}}\}$
    foreach $o \in N, \mathcal{L}$ **do**
      Regress $\ln o_\theta^{\zeta,\mathcal{T}}$ against $\ln H_\theta^{\zeta,\mathcal{T}}$ to obtain model moment $\tilde{\beta}^o$
Use moments in data $\{\widehat{\beta}^N, \widehat{\beta}^{\mathcal{L}}\}$ and model $\{\tilde{\beta}^N, \tilde{\beta}^{\mathcal{T}}\}$ in Eq. (36) to find $\{\zeta, \mathcal{T}\}$

Result: $\{\zeta, \mathcal{L}\}$ values that match moments in model and data

Guided by Figure A5, we define a grid of height costs $\Theta = \{0.2, 0.3, ..., 1\}$ and set $\bar{\mu} = 0.3$. For the moments in the data, we use $\hat{\beta}^N = 0.21$ and $\hat{\beta}^{\mathcal{L}} = -0.38$ estimated from a subset of cities that are relatively unconstrained by height regulation (third column in Table reftab:IVbyregion). Under $\zeta = 2.3$ and $\mathcal{T} = 3$, we almost exactly match the moments. Figure A12 plots the value of the objective function against the two dimensions of the parameter space. There is a clearly defined minimum in the objective function at our identified value of ζ. In contrast, the choice of $\mathcal{T}$ is less consequential. As long as $\mathcal{T} \geq 3$, the model generates height elasticities that are close to those estimated from data. Figure A13 shows that as long as $\mathcal{T} \geq 3$, we also find values for ζ that hover around 2.3.

It is plausible that we obtain the best fit under a value of $\mathcal{T} = 3$ (corresponds to about 15 m) that is smaller than the bottom-coding in the data (55 m). To see this, consider that the model generates an average height of 14 floors, which corresponds to 55 m. Setting $\mathcal{T} = 15$, we would generate a tall building height measure in the model of $H = 0$. In reality, we would most likely observe a positive value for H because the mean height of 55 m would be generated by a mix of taller and shorter buildings.

Figure 8 provides some intuition into how matching moments in model and data pins down ζ. At $\zeta = 0$, workers are immobile. Therefore, the population does not respond to bedrock depth-induced changes in floor space supply. Consequently, a vertical expansion leads to a relatively large contraction of the city area. Given a fixed population, the added supply of floor space results in lower rents. This implies lower costs to firms, leading to an expansion of floor space input, production, labor demand, and, eventually, higher wages. At higher values of ζ, we observe a larger population response to the supply-driven reduction in rent. The larger the population response, the smaller the response in the other outcomes. Since the relationships between height elasticities and ζ are monotonic, we obtain the well-behaved objective function displayed in the top panel of Figure A12.

C.3 Counterfactuals

This section complements Section 4.3 in the main paper.

C.3.1 Illustrative examples

Figure 9 in the main paper illustrates gradients in selected model outcomes under the baseline parameterization (first row) and two counterfactuals in which we increase the cost of height by 20% (second row) and add a binding height limit (third row). The first two columns in Table A15 report relative changes in various model outcomes from the baseline parameterization to these counterfactuals.

In keeping with intuition, both counterfactuals, which correspond to different negative floor space supply shocks, deliver a lower urban indirect utility, and consequentially, a lower urban population and expected utility, overall. As the city contracts vertically, it expands horizontally, resulting in a larger total urban area. As seen in Figure 9, the CBD expands horizontally, pushing the residential zone outwards. As a result, commuting costs $e^{\tau^R x}$ increase. This is one

of the main mechanisms through which the height constraints indirectly affects residents, even if a height limit primarily affects commercial developments. The other channel is the wage. For one thing, limits to vertical development displace firms to less productive locations. For another, the cost of commercial floor space increases. Both act as negative shocks to labor demand, lowering the equilibrium wage. Since greater commuting costs and lower wages imply lower housing demand, residential rents do not necessarily increase by much, even if residential floor space supply falls. Indeed, residential rents even decrease by about 15% in the counterfactual where we impose a height ban. Given the expenditure share on housing of one-third, the ceteris paribus effect on indirect utility amounts to about 5%. This effect compensates for commuting cost and wage effects, each of which amounts to about 7-8%, resulting in a negative net effect on indirect urban utility ($\bar{U}$) of about 10%. Since, in this example, we have an urban population share, μ, of slightly below one-third, the negative effect on expected utility in the total population is to about 3%.

C.3.2 Heterogeneity in welfare effects

Algorithm 4 uses pseudo code to describe the numerical procedure we use to compute welfare effects for cities of a given cost of height, population, and height gap, which we use in Sections 4.3.2 and 4.4.

Algorithm 4: Welfare effects

Data: Given values of primitives $\{\alpha^U, \beta, \omega^U, \tau^U, \underline{x}^U, \bar{a}^U, \tilde{c}^U, \bar{S}^U, r^a, \zeta, \ell, \bar{N}, \mathcal{T}\}$
City population, Pop_a, observed in data
Height gap, HG_a, observed in data
Bedrock depth, MBD_a, observed in data

Use MBA_a and non-linear mapping in Figure A5 to obtain cost of height, θ_a^C
Set $\theta_A^R = \theta_a^C + 0.05$
Set height limit in model to $\bar{S}^U = \mathcal{T}$
while *Height gap in model,* $\tilde{HG} < HG_a$ **do**
    Use Algorithm 2 to invert rural utility, $\tilde{U}$, that satisfies $\mu\bar{N} = Pop_a$
    Use Eq. (35) to compute constrained tall building height H
    Use Algorithm 1 to solve for counterfactual under no height limit, $\bar{S} = \infty$
    Use Eq. (35) to compute unconstrained tall building height H^*
    Compute $\tilde{HG} = \frac{H}{H^*} - 1$
    Marginally increase height limit in model, $\bar{S}$
Use Algorithm 1 to solve for $\mathcal{W}^{actual}$, where $\mathcal{W} \in \{\mathcal{V}, \mathcal{R}\}$, under calibrated height limit $\bar{S}$
Use Algorithm 1 to solve for welfare $\mathcal{W}^{ban}$ under counterfactual height limit $\bar{S} = \mathcal{T}$
Use Algorithm 1 to solve for welfare $\mathcal{W}^{market}$ under counterfactual height limit $\bar{S} = \infty$
Compute welfare effect of existing tall buildings $\hat{\mathcal{W}}^{actual} = \frac{\mathcal{W}^{actual}}{\mathcal{W}^{ban}} - 1$
Compute welfare potential of tall buildings $\hat{\mathcal{W}}^{potential} = \frac{\mathcal{V}^{market}}{\mathcal{W}^{ban}} - 1$
Compute welfare effect of existing height regulation $\hat{\mathcal{W}}^{regulation} = \frac{\mathcal{V}^{actual}}{\mathcal{W}^{market}} - 1$

Result: Effects of existing tall buildings, all potential tall buildings, and height limits on expected utility $\{\hat{\mathcal{V}}_a^{actual}, \hat{\mathcal{V}}_a^{potential}, \hat{\mathcal{V}}_a^{regulation}\}$ and land rent $\{\hat{\mathcal{R}}_a^{actual}, \hat{\mathcal{R}}_a^{potential}, \hat{\mathcal{R}}_a^{regulation}\}$ for city a

C.3.3 The contribution of tall buildings to welfare

Table A16 complements Table 7 in the main paper by summarizing the effects of height constraints on the equilibrium wage, the average residential rent, and commuting cost. Since these endogenous variables feed into expected utility, the reported effects offer insights into the mechanisms through which the welfare effect operates. Notice that the effects on wages, rents, and commuting costs jointly determine the effect on the indirect urban utility, $\bar{U}$, not the expected utility, $\mathcal{V}$, reported in Table 7. In keeping with he discussion of mechanisms in Section C.3.1, Table A16 reveals that the worker welfare cost of height constraints originates from greater commuting costs and lower wages due to lower productivity.

Table A17 replicates Table 7 with the only difference being that we lower the cost of height, θ, by 20%. As a result, all welfare effects increase by about 50%.

Appendix References

Ahlfeldt, Gabriel M. and Daniel P. McMillen, "Tall buildings and land values: Height and construction cost elasticities in Chicago, 1870-2010," *Review of Economics and Statistics*, 2018, *100* (5), 861–875.

_ and Jason Barr, "The economics of skyscrapers: A synthesis," *Journal of Urban Economics*, 5 2022, *129*, 103419.

Barr, Jason and Remi Jedwab, "Exciting, boring, and nonexistent skylines: Vertical building gaps in global perspective," *Real Estate Economics*, 2023.

Bolt, Jutta and Jan Luiten van Zanden, *Maddison style estimates of the evolution of the world economy. A new 2020 update* 2020.

Brueckner, Jan K., "The structure of urban equilibria: A unified treatment of the muth-mills model," *Handbook of Regional and Urban Economics*, 1987, *2*, 821–845.

Cleveland, William S and Susan J Devlin, "Locally Weighted Regression: An Approach to Regression Analysis by Local Fitting," *Journal of the American Statistical Association*, 1988, *83* (403), 596–610.

Elvidge, Christopher D., Mikhail Zhizhin, Tilottama Ghosh, Feng-Chi Hsu, and Jay Taneja, "Annual Time Series of Global VIIRS Nighttime Lights Derived from Monthly Averages: 2012 to 2019," *Remote Sensing*, 2021, *13* (5).

Esch, Thomas, Klaus Deininger, Remi Jedwab, and Daniela Palacios-Lopez, "Outward and Upward Construction: A 3D Analysis of the Global Building Stock," Working Papers 2023-09, The George Washington University, Institute for International Economic Policy September 2023.

Giardini, D, G Grunthal, KM Shedlock, and Zhang P, "The GSHAP Global Seismic Hazard Map," *Ann. Geophys.*, 1999, *42* (6).

GMTED, *GMTED2010 Global Grids* 2010.

Henderson, Daniel J. and Christopher F. Parmeter, *Applied Nonparametric Re- gression* 2015.

Maddison, Angus, *Statistics on World Population, GDP and Per Capita GDP, 1-2008 AD* 2008.

McMillen, Daniel P., "One Hundred Fifty Years of Land Values in Chicago: A Nonparametric Approach," *Journal of Urban Economics*, 7 1996, *40* (1), 100–124.

NGDC, *Global Radiance Calibrated Nighttime Lights* 2015.

United Nations, *World Urbanization Prospects: The 2018 Revision* 2018.

World Bank, *World Development Indicators* 2022.

Figure A1: Trends in Construction Costs by Height: Developing Economies

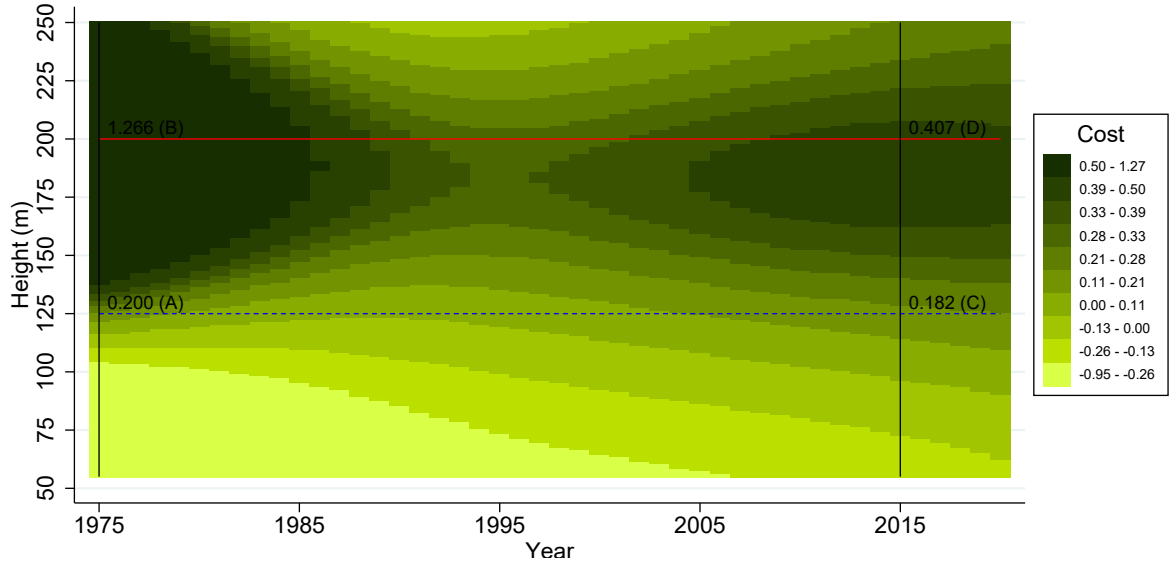

Notes: Cost is the log cost per floor area, residualized for city and country-by-decade of construction fixed effects. The sample consists of 136 buildings in 24 developing countries. We use locally weighted regressions with a bivariate Gaussian kernel to estimate local means of the residualized cost measure within the height-bedrock plane with a bandwidth parameter for both covariates of $\kappa = 50$. Appendix Section A.1 has details and provides results from locally weighted regressions with univariate kernels that deliver confidence bands for height categories that roughly correspond to the dotted blue and solid red lines.

Figure A2: Distribution of Building Heights (m) in Emporis circa 2022

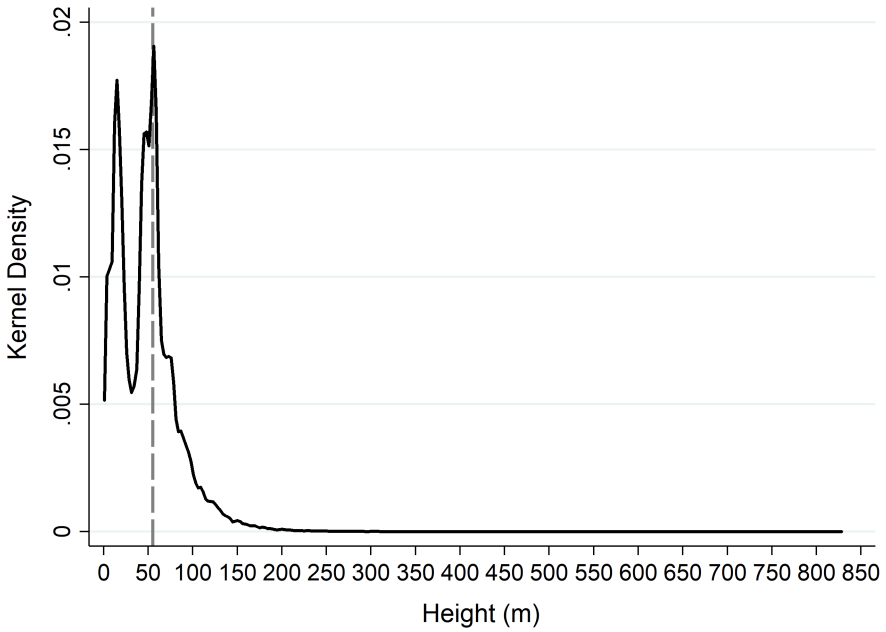

Notes: This figure shows the kernel density of heights (meters) for all 693,855 "existing [completed]" buildings in Emporis (accessed 02-07-2022). We only include "building with towers", "high-rise building", "low-rise building", "multi-story building", and "skyscraper" property types.

Figure A3: Schematic Diagram of Bedrock Depth and Tall Building Foundations

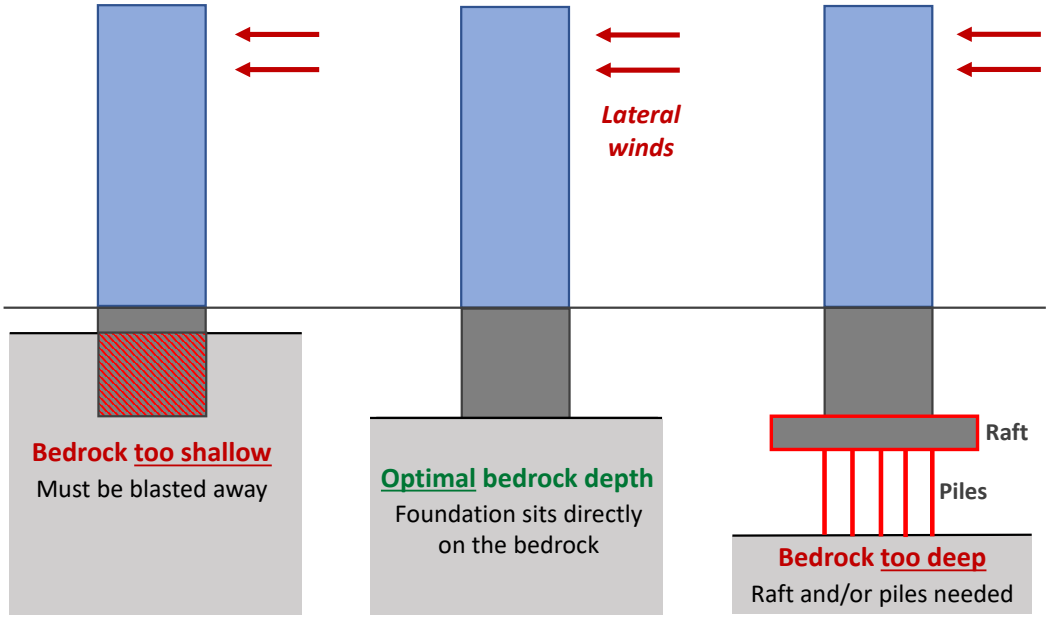

Notes: This figure shows why building foundation costs are minimized at intermediate bedrock depths.

Figure A4: Construction cost as function of height and bedrock depths

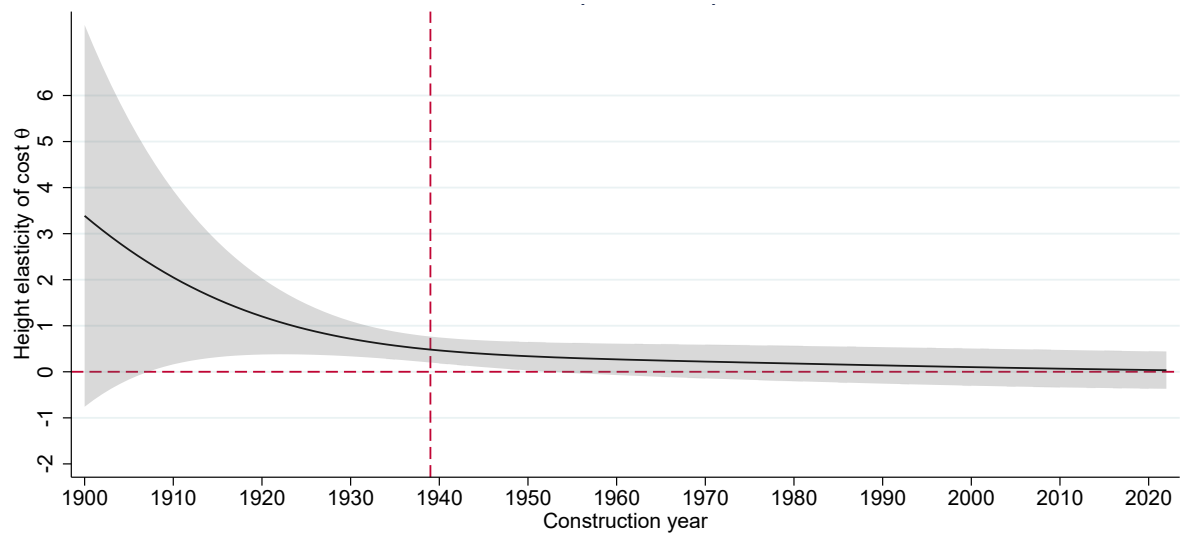

Notes: We show non-parametric estimates of the cost of height from an LWR-IV approach. In each LWR, we estimate the height elasticity from a regression of the log of construction cost per floor area against building height, controlling for city fixed effects and decade of construction effects. We use distance from the city center as an instrumental variable for height. The city center is defined as the median coordinate of buildings exceeding 100 m height and or the tallest building where building exceeds 100 m. We use locally weighted regressions with a univariate Gaussian kernel and a bandwidth of four to estimate local means of the cost measure for varying bedrock depths. Confidence bands are at the 95% level. The sample consists of 591 constructions in US cities (see Panel A in Table A1).

Figure A5: Cost of height as function of bedrock depths

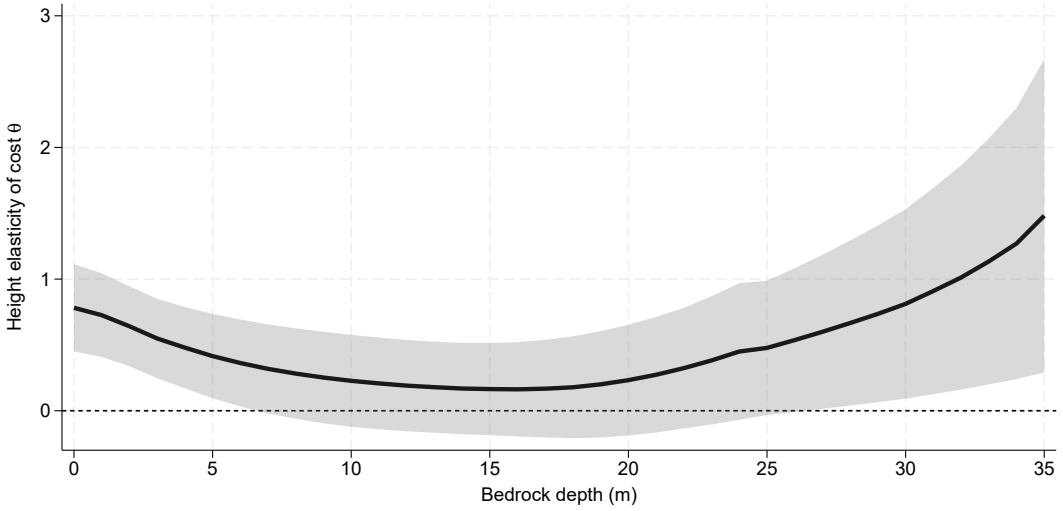

Notes: The plot shows non-parametric estimates of the cost of height using the LWR-IV approach explained in Section A.2. In each LWR, we estimate the height elasticity from a regression of the log of construction cost per floor area on building height, controlling for city fixed effects and country by decade of construction effects. The sample consists of 785 buildings in 118 cities and 6 countries. We drop countries with fewer than 25 observations to obtain more precise estimates. We use distance from the city center as an instrumental variable for height to remove the effects of unobserved factors that affect construction cost (such as ruggedness) that could be correlated with bedrock depth. The city center is defined as the median coordinate of buildings exceeding 100 meters, or the location of the tallest building if no building exceeds 100 meters. The median first-stage F-statistic is 10.4. We use a Gaussian kernel with a locally varying bandwidth that is inversely related to the density of observations. Confidence bands are at the 95% level.

Figure A6: Relationships Between Tall Buildings and ln 1975 Population by Bedrock Depth in 1975 and 2015

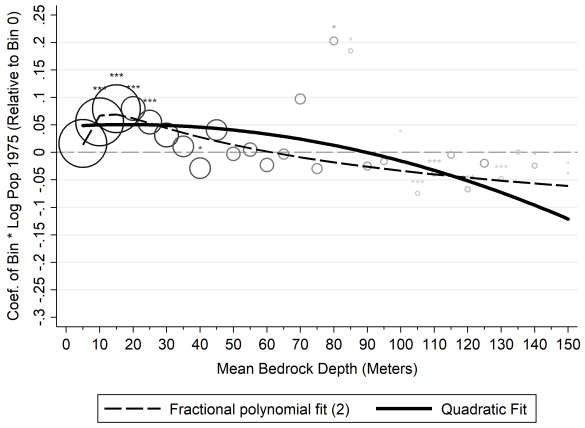

(a) Tall Building Indicator, 1975

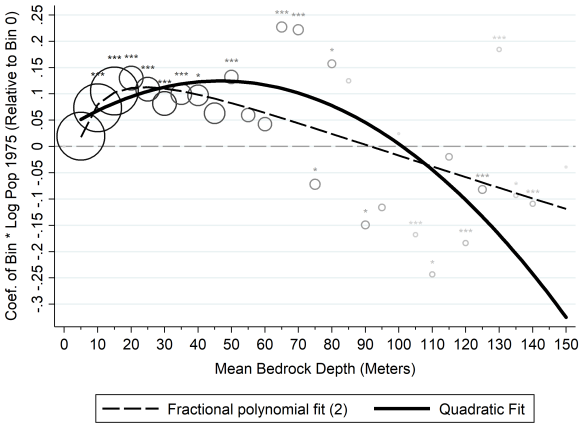

(b) Tall Building Indicator, 2015

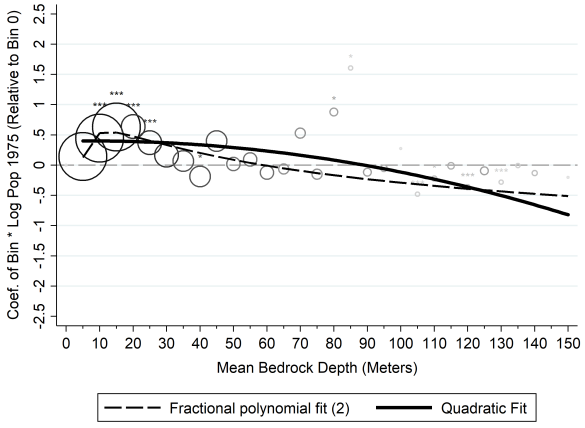

(c) ln Sum of Heights, 1975

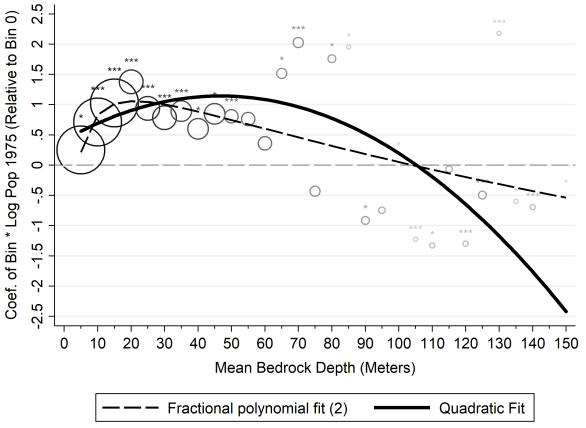

(d) ln Sum of Heights, 2015

Notes: The top panels graph coefficients on ln 1975 city population for each 5 meter bin of bedrock depth in which the dependent variable is an indicator for whether the city had any height growth. The bottom panels graph analogous coefficients in which the dependent variable is the ln sum of heights constructed. 1975 is on the left and 2015 is on the right.

Figure A7: The Skyscraper Revolution in Developed Economies, 1880-1975

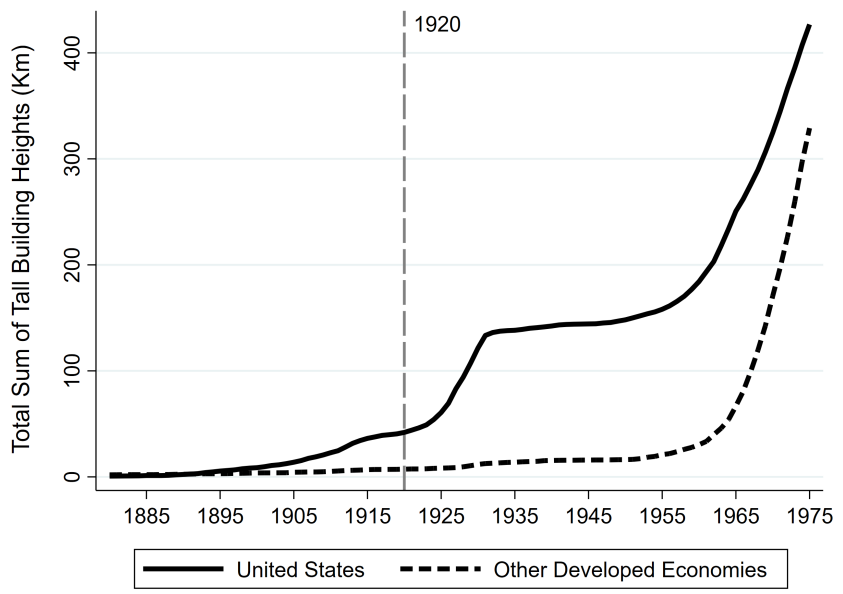

Notes: This figure shows the evolution of the total stock of tall (55m+) building heights (km) separately for the United States and other developed economies.

Figure A8: LWR estimates of height elasticity of built-up area

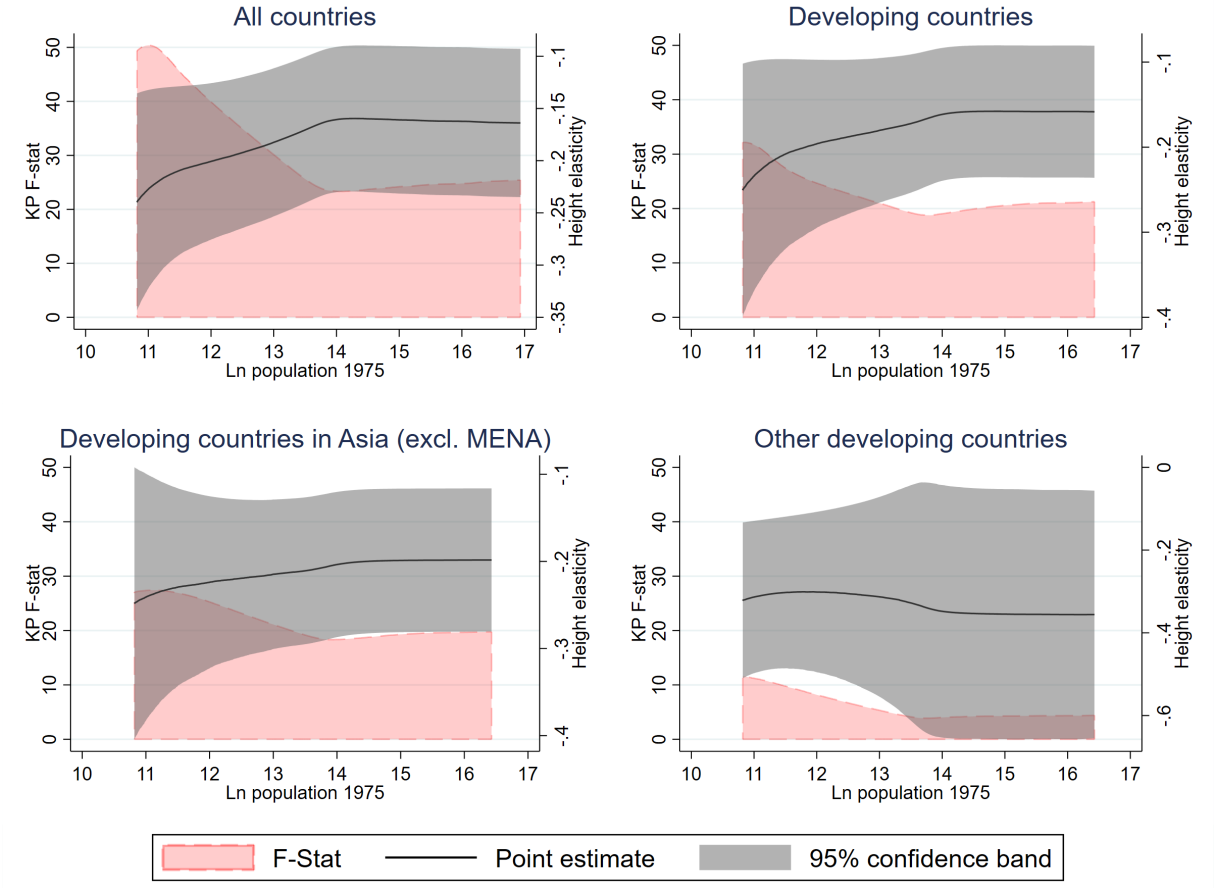

Note: We show non-parametric estimates of the height elasticity from an LWR-IV approach. In each LWR, we estimate the height elasticity from a regression of the 1975-2015 long-difference in the log outcome against the long-difference in log building height using a second-order polynomial of bedrock depth interacted with initial 1975 log population as instrumental variables. Controls are a second-order polynomial of bedrock depth, initial log population, and country fixed effects. We use a Gaussian kernel with a locally varying bandwidth that is inversely related to the density of observations. Confidence bands are at the 95% level.

Figure A9: LWR estimates of height elasticity of population

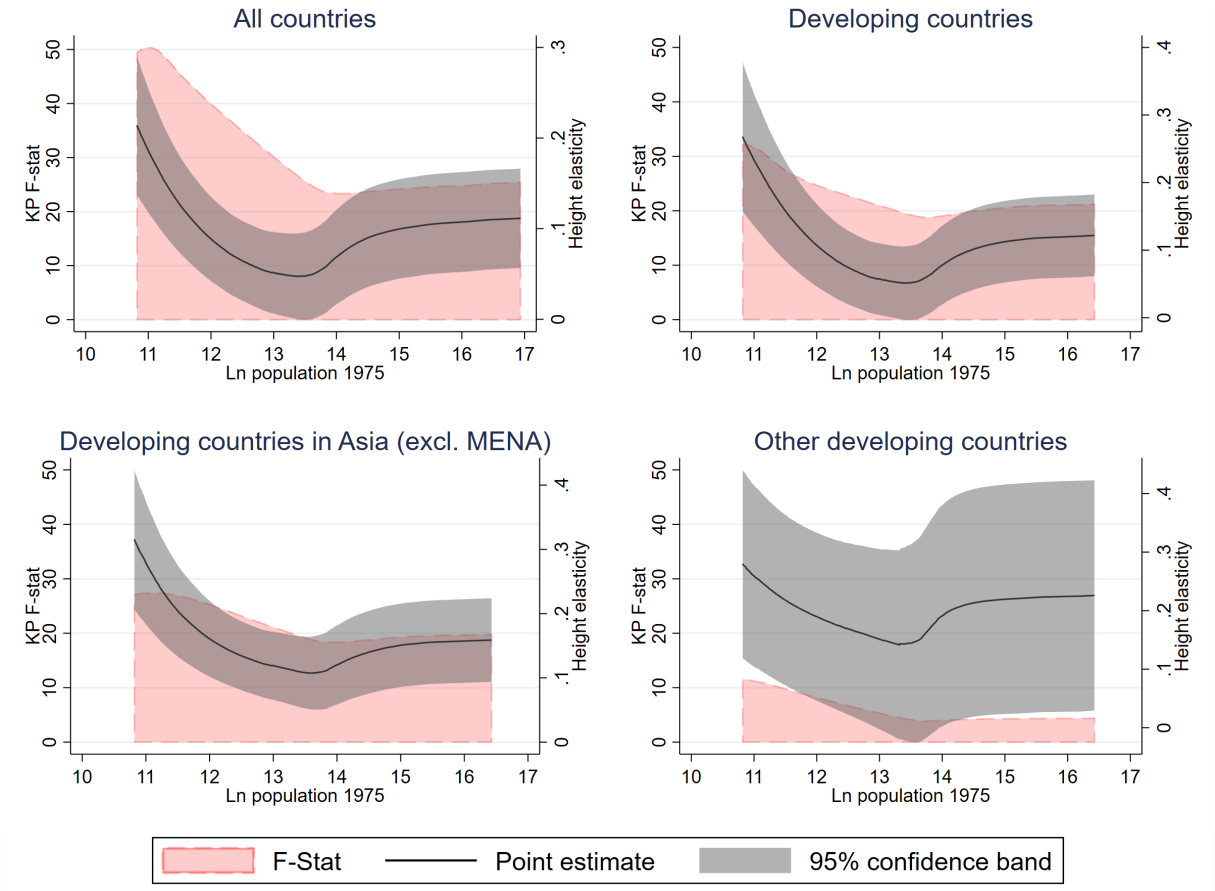

Note: We show non-parametric estimates of the height elasticity from an LWR-IV approach. In each LWR, we estimate the height elasticity from a regression of the 1975-2015 long-difference in the log outcome against the long-difference in log building height using a second-order polynomial of bedrock depth interacted with initial 1975 log population as instrumental variables. Controls are a second-order polynomial of bedrock depth, initial log population, and country fixed effects. We use a Gaussian kernel with a locally varying bandwidth that is inversely related to the density of observations. Confidence bands are at the 95% level.

Figure A10: LWR estimates of height elasticity of urban area

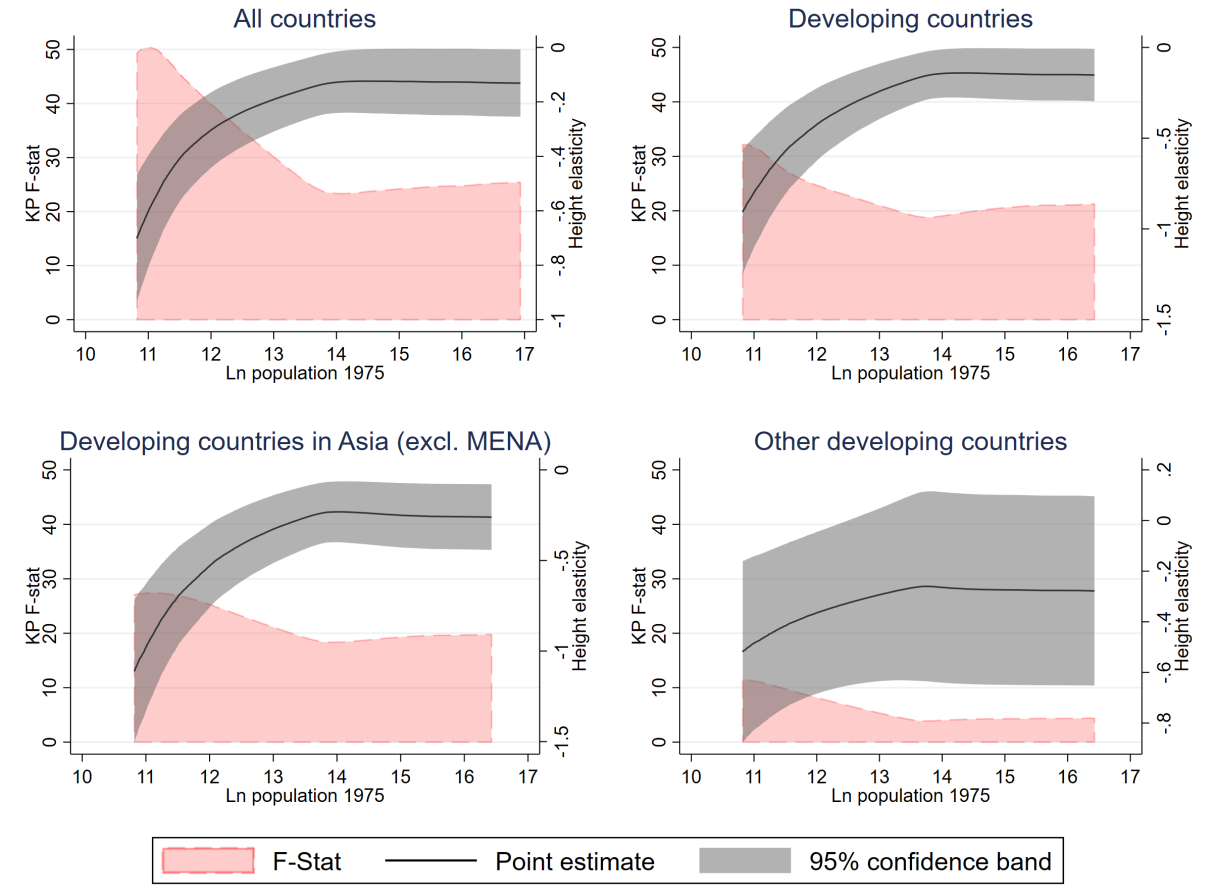

Note: We show non-parametric estimates of the height elasticity from an LWR-IV approach. In each LWR, we estimate the height elasticity from a regression of the 1975-2015 long-difference in the log outcome against the long-difference in log building height using a second-order polynomial of bedrock depth interacted with initial 1975 log population as instrumental variables. Controls are a second-order polynomial of bedrock depth, initial log population, and country fixed effects. We use a Gaussian kernel with a locally varying bandwidth that is inversely related to the density of observations. Confidence bands are at the 95% level.

Figure A11: 95th Percentile Residuals and Predicted Log Heights, 2015.

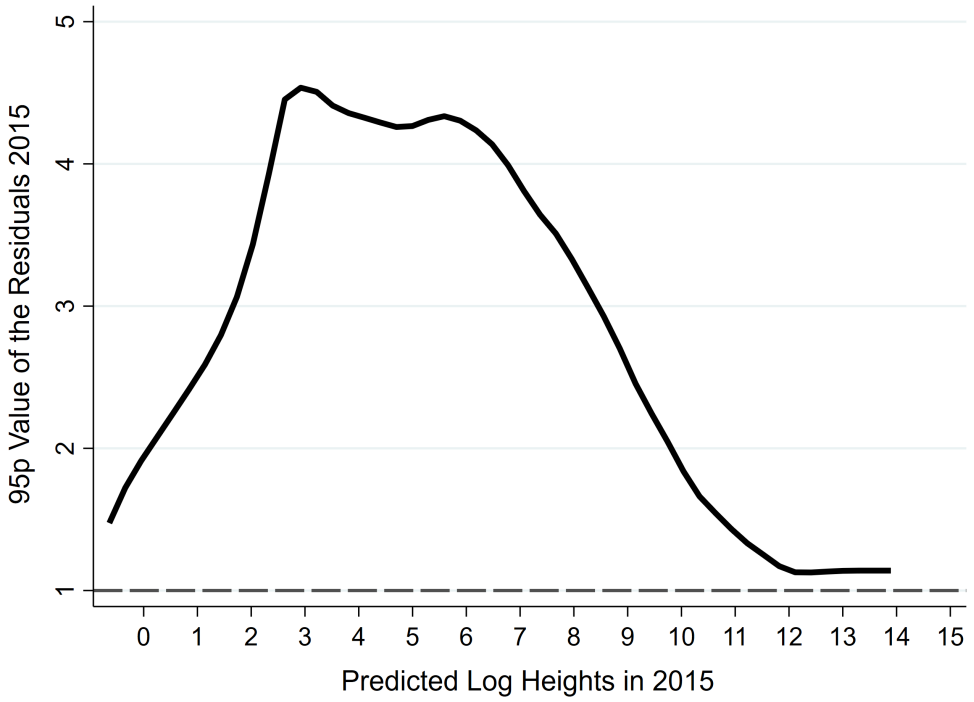

Notes: This figure shows for the 12,755 cities the local polynomial relationship (bandwidth = 1) between the 95th percentile value in the residuals of their respective group of 51 cities and their predicted 2015 log heights.

Figure A12: Value of objective function by $\zeta, \mathcal{T}$

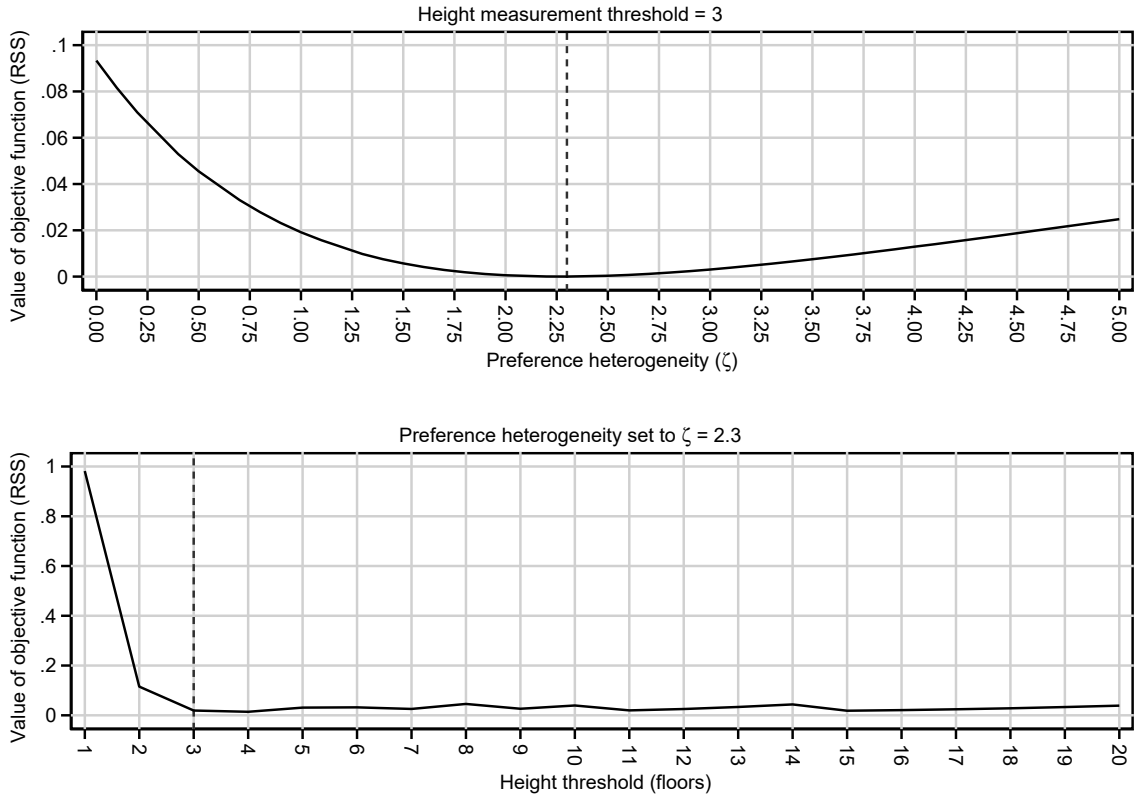

Note: Value of objective function is the residual sum of squares of moments in model and data (height elasticity of built area and height elasticity of population).

Figure A13: Preference heterogeneity (ζ) for given height thresholds

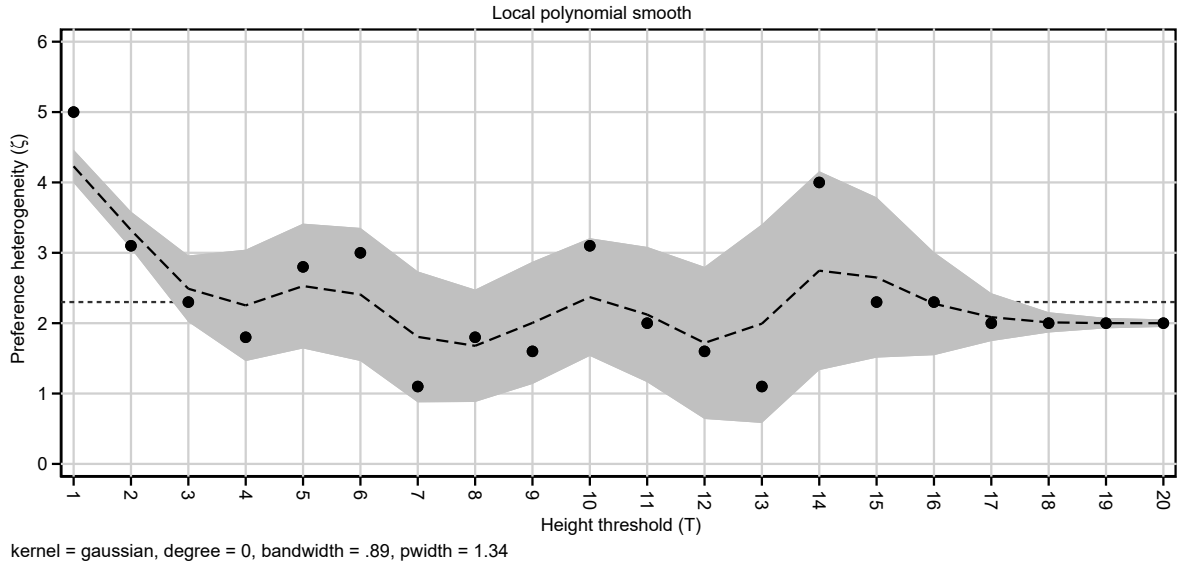

Note: Figure shows the value of ζ that minimizes the objective function conditional on a given $\mathcal{T}$. We use a local polynomial fit of degree zero with a Gaussian kernel.

Figure A14: Construction cost as function of height and construction year

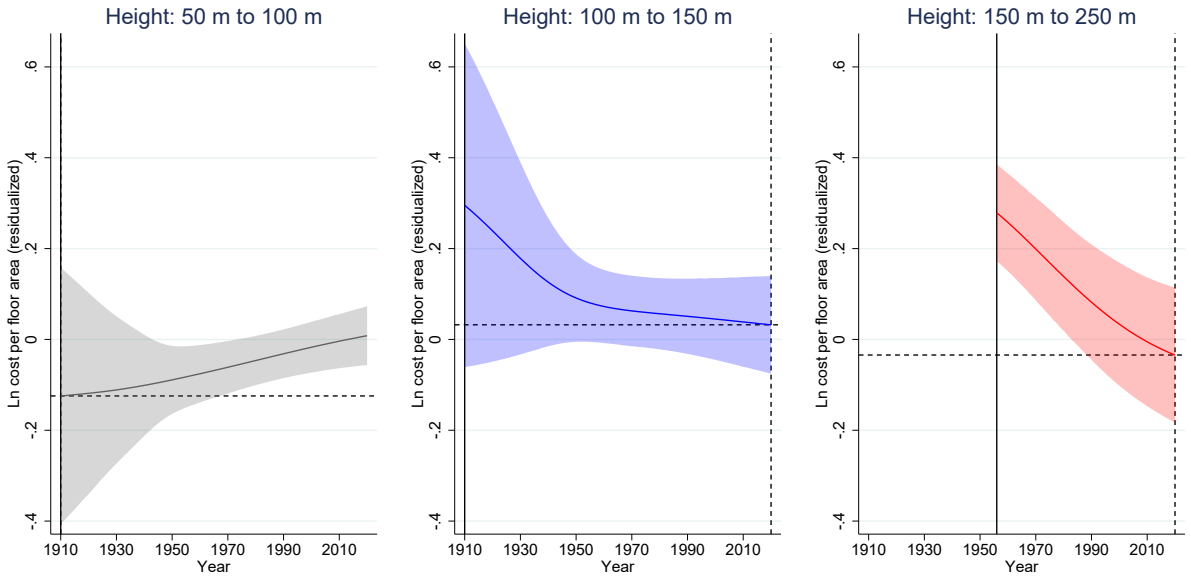

Notea: The sample consists of 591 constructions in US cities (see Panel A in Table A1). Ln cost per floor area is residualized to control for city fixed effects and country-by-decade of construction effects. We use locally weighted regressions with a univariate Gaussian kernel and a bandwidth of $\kappa = 25$ to estimate local means of the cost measure for varying bedrock depths. Confidence bands are at the 95% level.

Figure A15: Construction cost as function of height and bedrock depths

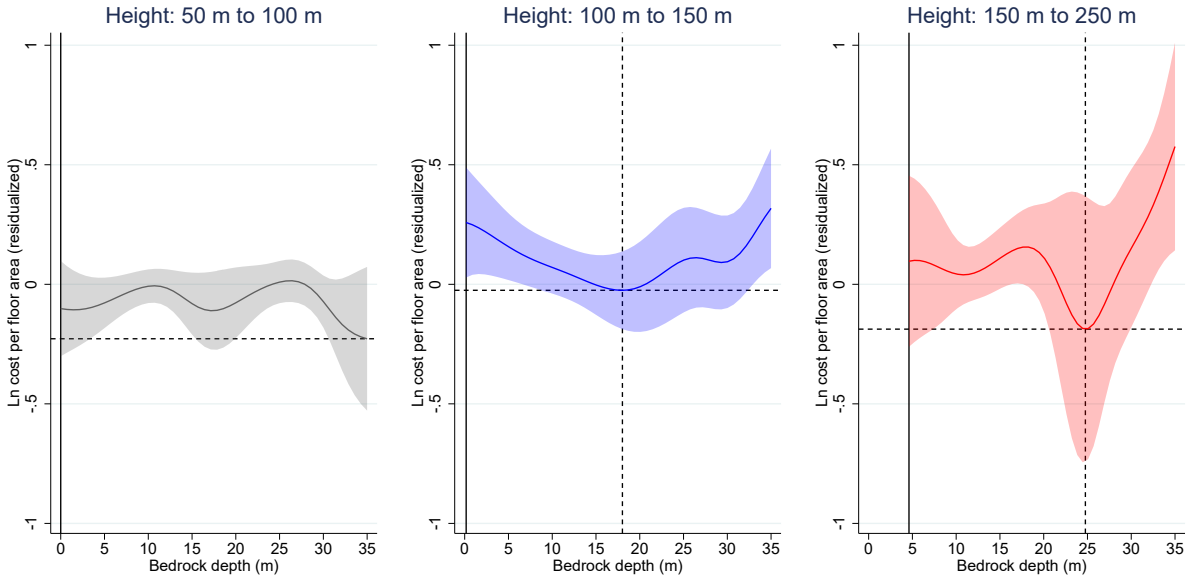

Note: The sample consists of 1,033 constructions in 206 cities in 55 countries (see Panel A in Table A1). Ln cost per floor area is residualized to control for city fixed effects and country-by-decade of construction effects. We use locally weighted regressions with a univariate Gaussian kernel and a bandwidth of $\kappa = 4$ to estimate local means of the cost measure for varying bedrock depths. Confidence bands are at the 95% level.

Figure A16: Bedrock quality

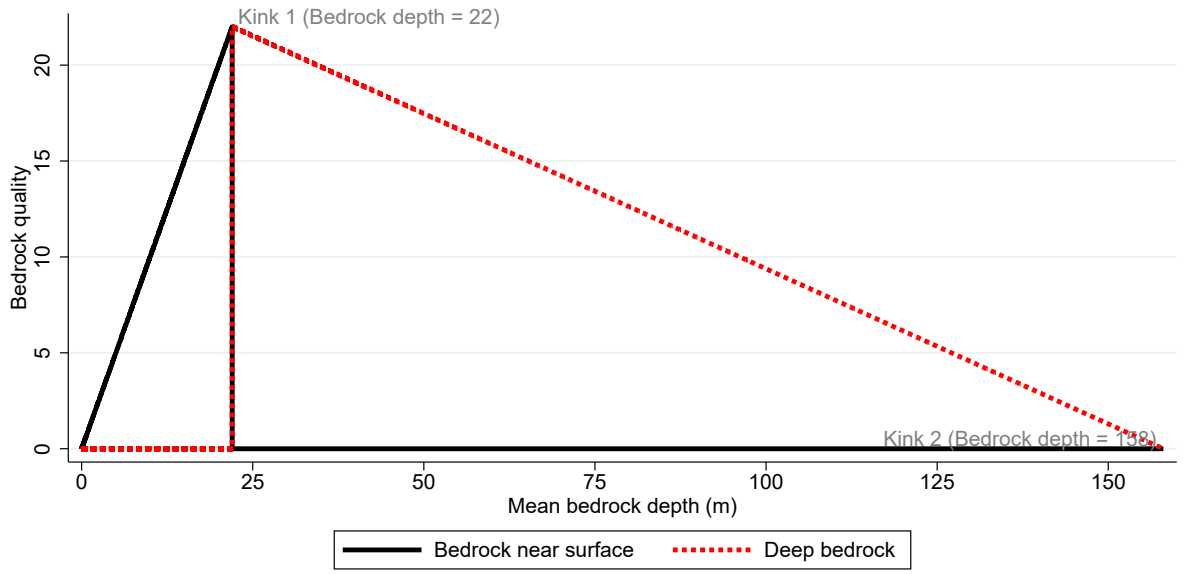

Note: To identify Kink 1 ($\mathcal{K}^1$) and Kink 2 ($\mathcal{K}^2$), we estimate our specification for all combinations of $\mathcal{K}^1 = \{10, 11, ..., 40\}$ and $\mathcal{K}^2 = \{50, 11, ..., 158\}$, where the upper bound $\mathcal{K}^2 = 158$ is the largest bedrock depth value observed in our data, and choose the variable that maximize the first-stage F-statistic.

Figure A17: Bedrock quality

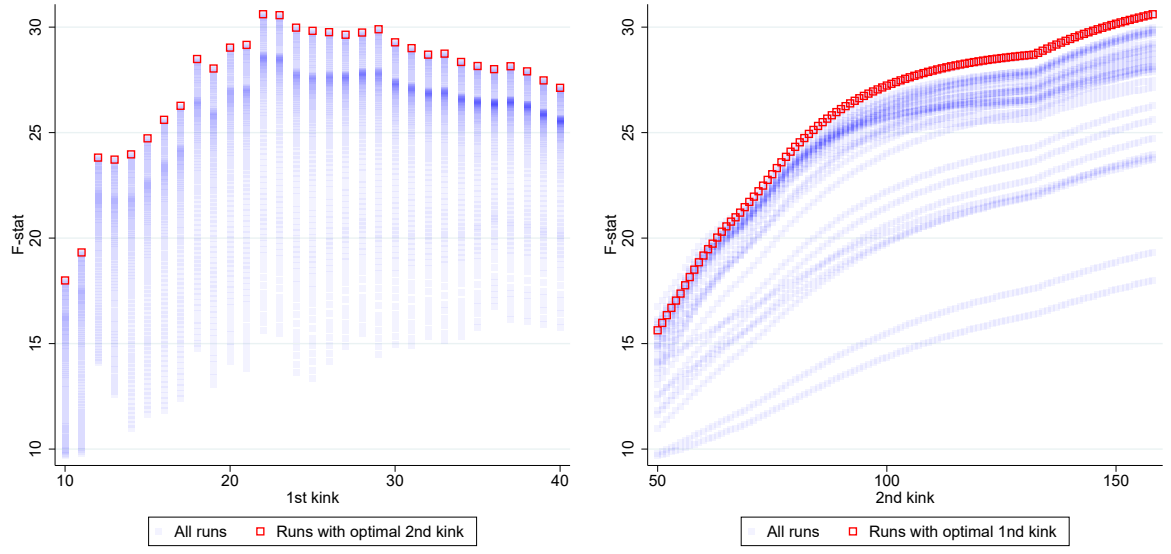

Note: To identify Kink 1 ($\mathcal{K}^1$) and Kink 2 ($\mathcal{K}^2$), we estimate our specification for all combinations of $\mathcal{K}^1 = \{10, 11, ..., 40\}$ and $\mathcal{K}^2 = \{50, 11, ..., 158\}$, where the upper bound $\mathcal{K}^2 = 158$ is the largest bedrock depth value observed in our data, and choose the variable that maximize the first-stage F-statistic.

Figure A18: Urban spatial structure recovered from building volumes

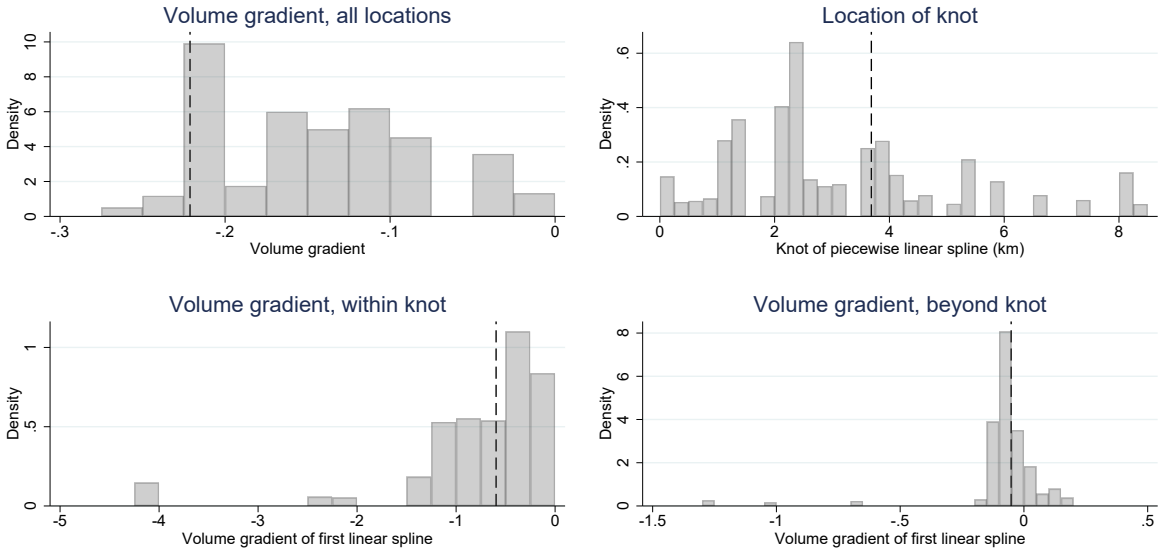

Note: the upper left panel shows esimates of log-linear building volume gradients (with repsect to distance from the center) for 24 cities in the developing world and 11 cities in the developed world. The other panels illustrate estimates of piecewise linear spline functions with one endogenous knot that approximate the relationship between log volume and distance from the devd world. Dotted vertical lines represent Chicago.

Table A1: Summary Statistics of Emporis Construction Cost Data

	Mean	SD	Min	Max
	Panel A: 591 (55m+) Buildings in 93 U.S. Cities			
Construction year	1988.23	23.95	1902.00	2021.00
Height (m)	102.15	55.72	55.03	541.33
Bedrock depth (m)	19.66	14.72	2.50	113.01
Ln construction cost	7.05	1.20	3.18	10.98
Ln cost (residulized)	-0.00	0.53	-1.61	2.65
	Panel B: 1,033 (55m+) Buildings in 206 Cities in 55 Countries			
Construction year	1994.98	21.00	1902.00	2021.00
Height (m)	113.42	71.52	55.00	828.00
Bedrock depth (m)	20.08	13.05	0.00	117.53
Gross floor area (m^2)	53972.87	61268.07	934.00	9.8e+05
Ln construction cost	7.12	1.58	-5.25	10.98
Ln cost (residulized)	-0.00	0.85	-7.60	5.14

Table A2: Summary Statistics: Full Sample

		City Population in 1975			
		< 100k	100k-500k	> 500k	
		(1)	(2)	(3)	(3) - (2)
Avg Sum of Heights >55 m in 1975		3	36	1,441	1,404
Frac of Cities with Tall Bldgs in 1975		0.01	0.09	0.41	0.32
MBD	Mean 1975-2015 Δ ...				
<10m	ln Pop	0.55	0.45	0.55	0.10
	ln Built Area	0.46	0.76	0.75	-0.01
	ln (Heights + 1)	0.05	0.37	2.05	1.68
	Heights (m)	9	72	5,206	5,134
	Any Tall Bldgs	0.01	0.06	0.21	0.15
	Observations	3,876	788	113	
10m - 30m	ln Pop	0.46	0.29	0.42	0.13
	ln Built Area	0.50	0.60	0.55	-0.05
	ln (Heights + 1)	0.21	1.20	3.40	2.20
	Heights (m)	63	694	26,540	25,846
	Any Tall Bldgs	0.03	0.18	0.32	0.14
	Observations	4,561	1,547	313	
> 30m	ln Pop	0.47	0.27	0.44	0.17
	ln Built Area	0.73	0.94	0.78	-0.16
	ln (Heights + 1)	0.10	0.69	4.09	3.40
	Heights (m)	26	220	11,780	11,560
	Any Tall Bldgs	0.02	0.11	0.46	0.35
	Observations	1,151	436	89	

Notes: The sample includes 12,874 cities. Each city in the main estimation sample is one observation. Entries in columns (1), (2) and (3) are conditional means as a function of 1975 city population and city mean bedrock depth in meters (MBD). All differences in the final column are statistically significant at the 5 percent level except growth in population for cities with bedrock depths between 0 and 10 meters and built area for cities with bedrock depths between 0 and 10 meters or 10 and 30 meters.

Table A3: First-Stage Estimates: Remaining Coefficients

	Tall Building Indicator			ln (Heights + 1)		
	1975	2015	Δ 1975-2015	1975	2015	Δ 1975-2015
	Panel A: All Countries (N = 12,849)					
ln Pop 1975	0.0773***	0.1286***	0.0512***	0.5272***	1.0025***	0.4753***
	[0.0076]	[0.0093]	[0.0093]	[0.0498]	[0.0769]	[0.0653]
Bedrock Depth	-0.0208***	-0.0538***	-0.0330***	-0.1473***	-0.4721***	-0.3248***
	[0.0054]	[0.0079]	[0.0079]	[0.0362]	[0.0698]	[0.0612]
(Bedrock Depth)^2	0.0002***	0.0005***	0.0002**	0.0018***	0.0039***	0.0021**
	[0.0001]	[0.0001]	[0.0001]	[0.0004]	[0.0011]	[0.0009]
	Panel B: Developing Economies (N = 11,257)					
ln Pop 1975	0.0517***	0.1140***	0.0623***	0.2998***	0.8206***	0.5208***
	[0.0079]	[0.0098]	[0.0098]	[0.0477]	[0.0804]	[0.0674]
Bedrock Depth	-0.0048	-0.0420***	-0.0372***	-0.0353	-0.3417***	-0.3064***
	[0.0055]	[0.0078]	[0.0084]	[0.0323]	[0.0687]	[0.0638]
(Bedrock Depth)^2	0.0001	0.0003***	0.0003**	0.0005*	0.0025**	0.0020**
	[0.0000]	[0.0001]	[0.0001]	[0.0003]	[0.0010]	[0.0009]

Notes: This table reports additional coefficient estimates from regressions in Table 1.

Table A4: Main IV Results: Remaining Coefficients

Period *s*-*t*:	Δ ln Pop 1975-2015	Δ ln Built Area 1975-2015	Δ ln Urban. Area 1975-2015	Δ ln Pop Dens. 1975-2015	Δ ln Lights 1990-2015
ln Initial Pop *s*	-0.12***	0.24***	-0.68***	0.56***	-0.15***
	[0.03]	[0.03]	[0.06]	[0.04]	[0.04]
Bedrock Depth	0.00***	0.00***	0.02***	-0.02***	0.00**
	[0.00]	[0.00]	[0.00]	[0.00]	[0.00]
(Bedrock Depth)^2	-0.00	-0.00**	-0.00***	0.00***	-0.00
	[0.00]	[0.00]	[0.00]	[0.00]	[0.00]

Notes: This table shows coefficients on control variables for our main IV regressions in Table 2 Panel A.

Table A5: Alternative Standard Error Calculations

	(1)-(4): Δ ln Population				(5)-(8) Δ ln Built Area			
Standard Errors:		200 km	400 km	Admin 1		200 km	400 km	Admin 1
	Panel A: Developed Economies (Observations = 12,873)							
Δ ln(Heights+1)	0.12***	0.12***	0.12***	0.12***	-0.17***	-0.17***	-0.17**	-0.17**
	[0.03]	[0.04]	[0.04]	[0.04]	[0.04]	[0.06]	[0.07]	[0.08]
F-statistic	28.42	20.06	15.35	21.38	28.42	20.06	15.35	21.38
	Panel B: Developing Economies (Observations = 11,257)							
Δ ln(Heights+1)	0.13***	0.13***	0.13***	0.13***	-0.16***	-0.16**	-0.16*	-0.16*
	[0.03]	[0.04]	[0.05]	[0.05]	[0.04]	[0.06]	[0.08]	[0.09]
F-statistic	22.84	15.34	11.46	17.00	22.84	15.34	11.46	17.00

Notes: (1) Baseline results. (2)-(3): Standard errors corrected for spatial autocorrelation out to 200 km or 400 km using a Bartlett (triangular) kernel. (4) SEs are clustered at the first administrative level (e.g., "provinces" for China and "states" for India and the United States).

Table A6: Robustness of Results in Table 2 with Various Controls

	(1)	(2)	(3)	(4)	(5)	(6)	(7)	(8)
Panel A:	Dependent Variable = Δ ln Population; All Countries							
Δ ln Height	0.12***	0.12***	0.09***	0.10**	0.13***	0.11***	0.12***	0.13***
	[0.03]	[0.03]	[0.03]	[0.04]	[0.04]	[0.03]	[0.03]	[0.03]
Panel B:	Dependent Variable = Δ ln Built Area; All Countries							
Δ ln Height	-0.17***	-0.17***	-0.19***	-0.14***	-0.08**	-0.12***	-0.15***	-0.18***
	[0.04]	[0.03]	[0.04]	[0.05]	[0.04]	[0.03]	[0.04]	[0.04]
Observations	12,849	12,849	12,647	6,097	9,698	12,628	12,628	12,849
F-statistic	28.42	29.38	25.08	10.47	15.25	20.35	16.79	23.66
Panel C:	Dependent Variable = Δ ln Population; Developing Countries							
Δ ln Height	0.13***	0.14***	0.10***	0.10**	0.17***	0.09**	0.11**	0.13***
	[0.03]	[0.03]	[0.04]	[0.04]	[0.06]	[0.04]	[0.04]	[0.03]
Panel D:	Dependent Variable = Δ ln Built Area; Developing Countries							
Δ ln Height	-0.16***	-0.18***	-0.18***	-0.11**	-0.10*	-0.13**	-0.15***	-0.16***
	[0.04]	[0.04]	[0.05]	[0.05]	[0.05]	[0.05]	[0.05]	[0.04]
Observations	11,257	11,257	11,169	5,272	8,141	11,050	11,050	11,257
F-statistic	22.84	23.56	16.22	7.480	9.167	8.665	9.903	20.76
Country FE	Yes	Yes	Yes	Yes	Yes	Yes	Yes	Yes
Infrastructure Controls	No	Yes	No	No	No	No	Yes	No
Drop Subway Cities	No	No	Yes	No	No	No	No	No
Drop Mining & Oil Cities	No	No	No	Yes	No	No	No	No
Drop Bedrock 0-6 m	No	No	No	No	Yes	No	No	No
Geographic Controls	No	No	No	No	No	Yes	Yes	No
Δ ln 100m+ Height	No	No	No	No	No	No	No	Yes

Notes: Each column presents separate estimates from a variant of the baseline model in Table 2 for the full sample of cities (Panels A-B) and the sample of developing country cities (Panels C-D). (2) Infrastructure controls are second-order polynomials of log number of subway stations in 1975 and log market access in 1975. Market access for city i is the total sum of the 1975 population of other cities j in the same country weighted by the inverse of Euclidean distance between cities i and j. (3) Subway cities are cities with a subway as of 2015. (4) Mining & oil cities are cities located within 50 km from a mine c. 2010 or an offshore or onshore oil or gas field c. 2000. (6) Geographic controls are second-order polynomials in log Euclidean distance from the coast, log Euclidean distance from a major lake, log mean altitude, the log of the standard deviation in altitude, log agricultural suitability, mean annual temperature (1961-1990), log Euclidean distance from a mine c. 2010, and log Euclidean distance from an offshore or onshore oil or gas field c. 2000, which we interact with log population in 1975.

Table A7: Robustness Checks on Functional Form

	Δ ln Population (Pop)			ln Pop	Δ ln Built Area (BA)			ln BA
Period:	1975-2015	1975-2015	1990-2015	2015	1975-2015	1975-2015	1990-2015	2015
Test:	Bedrock Vars in IV	Built Area Ctrl 1975	Pop 1975 in IV	Cross Section	Bedrock Vars in IV	Built Area Ctrl 1975	Pop 1975 in IV	Cross Section
	Panel A: Developed Economies (Observations = 12,849)							
Δ ln(Heights+1)	0.12***	0.07***	0.09***		-0.18***	-0.12***	-0.23***	
	[0.03]	[0.02]	[0.03]		[0.04]	[0.03]	[0.05]	
ln(Heights+1) 2015				0.09***				-0.11***
				[0.02]				[0.01]
F-statistic	23.96	23.92	15.14	41.97	23.96	23.92	15.14	35.5
	Panel B: Developing Economies (Observations = 11,257)							
Δ ln(Heights+1)	0.13***	0.07***	0.09***		-0.16***	-0.11***	-0.23***	
	[0.03]	[0.03]	[0.03]		[0.04]	[0.04]	[0.05]	
ln(Heights+1) 2015				0.13***				-0.12***
				[0.03]				[0.04]
F-statistic	18.53	18.92	14.57	19.91	18.53	18.92	14.57	16.31

Notes: Specifications match those in Table 2 except as indicated. (1) and (5) "Bedrock Vars in IV": Mean bedrock depths and its square enter as instruments instead of as controls. (2) and (6) "Built Area Ctrl 1975": Additional control for log city built area in 1975. (3) and (7) "Pop 1975 in IV": 1990 is the base year though instruments are constructed using log city population in 1975. (4) and (8) "Cross Section ": Dependent variables and heights are for 2015 only. Instruments are constructed using log city population size in 1975. Column (8) includes an additional control for log city built area in 1975. Robust standard errors in brackets.

Table A8: Bedrock Quality Instruments: Kinked Functional Form

First Stage: Dependent Variable:	Δ log height 1975-2015	
BRQ^{deep} × ln pop 1975	0.039***	(0.005)
BRQ^{surf} × ln pop 1975	0.030***	(0.006)
F-stat	30.6	
Second stage: Dependent Variable:	Δ log pop 1975-2015	Δ log built area 1975-2015
Log change height 1975-2015	0.128*** (0.026)	-0.222*** (0.039)
Country FE, Controls	Yes	Yes

Notes: Specifications are analogous to those in Table 2, except that the quadratic in mean bedrock depth is replaced by a linear spline in mean bedrock depth. See Section B.1 for details. There are 12,849 observations. Robust standard errors in parenthesis.

Table A9: Bedrock Quality Instruments: Local Identification

	Δ log pop 1975-2015		Δ log built area 1975-2015	
Log change height 1975-2015	0.200***	0.132***	-0.362***	-0.229***
	(0.047)	(0.027)	(0.084)	(0.040)
BRQ^{deep} × ln pop 1975	-0.003**		0.005**	
	(0.001)		(0.002)	
BRQ^{surf} × ln pop 1975		0.002***		-0.004***
		(0.001)		(0.001)
F-stat	23.0	61.1	23.0	61.1
Country FE, Controls	Yes	Yes	Yes	Yes

Notes: Specifications are analogous to those in Table A8, except that instruments enter one at a time, with the other as a control. Regressions in Columns 1 and 3 use variation within shallow bedrock (up to 22 meters) and those in Columns 2 and 4 use variation within deep bedrock (beyond 22 meters) only for identification. See Section B.1 for details. There are 12,849 observations. Robust standard errors in parenthesis.

Table A10: Robustness Checks on Bedrock Depth Measures

	(1)-(4): Δ ln Population				(5)-(8) Δ ln Built Area			
Bedrock Depth in the IVs:	In 2.5 km	Out 2.5 km	In 5 km	Out 5 km	In 2.5 km	Out 2.5 km	In 5 km	Out 5 km
				Panel A: Developed Economies				
Δ ln(Heights+1)	0.11***	0.08**	0.12***	0.05	-0.16***	-0.12***	-0.16***	-0.10**
	[0.03]	[0.03]	[0.03]	[0.04]	[0.03]	[0.04]	[0.03]	[0.05]
Observations	12,844	11,070	12,845	6,341	12,844	11,070	12,845	6,341
F-statistic	33.03	22.35	32.34	11.82	33.03	22.35	32.34	11.82
				Panel B: Developing Economies				
Δ ln(Heights+1)	0.12***	0.09**	0.12***	0.06	-0.16***	-0.11***	-0.15***	-0.11*
	[0.03]	[0.04]	[0.03]	[0.05]	[0.03]	[0.04]	[0.03]	[0.06]
Observations	11,252	9,482	11,253	4,995	11,252	9,482	11,253	4,995
F-statistic	28.86	17.34	28.31	7.939	28.86	17.34	28.31	7.939

Notes: In 2.5 km (5km): The main bedrock variable is calculated as mean bedrock depth (MBD) within 2.5 km (5 km) from the central business district (CBD) of each city. Out 2.5 km (5km): We use MBD beyond 2.5 km (5 km) from the CBD of each city. These samples exclude cities for which the maximum distance from the CBD is below that cut-off. Robust standard errors in brackets. *** Significant at 1%, ** 5%, * 10%, † 15%.

Table A11: Estimates as a Function of Within Country Inequality in Bedrock

Countries:	All (Baseline)		> 5 Cities		All (Baseline)		> 5 Cities	
Bedrock Depth:			Gini > 0.75p				Gini > 0.75p	
	All Economies				Developing Economies			
Estimator	(1) OLS	(2) IV	(3) OLS	(4) IV	(5) OLS	(6) IV	(7) OLS	(8) IV
				Panel A: Δ ln Pop				
Δ ln(Heights+1)	0.06***	0.12***	0.09***	0.13***	0.08***	0.13***	0.09***	0.12***
	[0.00]	[0.03]	[0.01]	[0.02]	[0.00]	[0.03]	[0.01]	[0.02]
				Panel B: Δ ln Built Area				
Δ ln(Heights+1)	-0.01***	-0.17***	-0.03***	-0.13***	-0.02***	-0.16***	-0.03***	-0.12***
	[0.00]	[0.04]	[0.01]	[0.04]	[0.01]	[0.04]	[0.01]	[0.04]
Observations	12,849	12,849	7,473	7,473	11,257	11,257	7,402	7,402
F-statistic		28.42		23.54		22.84		22.38

Notes: IV regressions use the same specification as those in Table 2. OLS regressions do not instrument for change in heights. Differences across columns are in the indicated sample restrictions and estimator used. Gini > 0.75p indicates that the Gini coefficient of the distribution of bedrock depth across cities within a country exceeds the 75th percentile value in the same Gini coefficient across all countries in our sample (here, 32%). Robust standard errors in brackets.

Table A12: Displacement Effects: Robustness to Different Fixed Effects and Samples

	(1)-(4) All Economies				(5)-(9) Developing Economies				
Panel A: Δ ln Population									
Δ ln Height	0.12***	0.10***	0.15***	0.14***	0.13***	0.10***	0.16***	0.14***	0.13***
	[0.03]	[0.03]	[0.02]	[0.02]	[0.03]	[0.03]	[0.03]	[0.02]	[0.04]
Panel B: Δ ln Built Area									
Δ ln Height	-0.17***	-0.22***	-0.23***	-0.21***	-0.16***	-0.21***	-0.25***	-0.22***	-0.08
	[0.04]	[0.04]	[0.04]	[0.03]	[0.04]	[0.05]	[0.04]	[0.03]	[0.05]
Level of FE	Baseline	Subregion	Admin 1	Admin 2	Baseline	Subregion	Admin 1	Admin 2	Baseline
Sample	Full	Full	Full	Full	Full	Full	Full	Full	<20% Urb
Observations	12,849	12,873	11,967	7,848	11,257	11,269	10,606	7,439	4,594
IV F-stat	28.42	26.74	35.51	35.52	22.84	20.02	28.96	35.23	9.77

Notes: Columns (1)-(8) present variants of the baseline empirical specification in Table 2 with the following alternative fixed effects (FE). Subregion: 2018 United Nations Geoscheme, grouping countries into 20 world regions (e.g., South America, Central America, and North America). We do not include country FE. Admin 1: First-level administrative divisions that subdivide countries into large sub-national units (e.g., provinces for China) (2,081 divisions in Panel A, 1,584 divisions in Panel B). Admin 2: Second-level administrative divisions that subdivide countries into smaller sub-national units (6,408 divisions in Panel A, 5,176 divisions in Panel B). The final column (9) only uses cities in the sample of developing economies that were less than 20% urbanized in 1975 (source: World Urbanization Prospects database of the United Nations).

Table A13: Displacement Effects: Controls for Heights-Based Changes in Market Potential

	(1)-(5) Δ ln Population					(6)-(10) Δ ln Built Area				
Panel A: Full Sample (N = 12,849) - IV for Δ ln(Hgt+1), OLS for Δ ln(MP^H)										
Δ ln(Hgt+1)	0.12***	0.12***	0.12***	0.12***	0.13***	-0.17***	-0.17***	-0.17***	-0.16***	-0.16***
	[0.03]	[0.03]	[0.03]	[0.03]	[0.03]	[0.04]	[0.04]	[0.04]	[0.04]	[0.04]
Δ ln(MP^H)	-0.01*	-0.01*	-0.01**	0.00	0.04***	-0.01**	-0.01*	0.00	0.03***	0.07***
	[0.00]	[0.00]	[0.00]	[0.00]	[0.00]	[0.00]	[0.00]	[0.00]	[0.01]	[0.01]
1st Stage F	27.34	27.42	27.59	27.93	28.73	27.34	27.42	27.59	27.93	28.73
Panel B: Full Sample (N = 12,849) - IV for Δ ln(Hgt+1), IV for Δ ln(MP^H)										
Δ ln(Hgt+1)			0.09***	0.08***	0.18***			-0.12**	-0.12***	-0.14***
			[0.03]	[0.03]	[0.04]			[0.05]	[0.04]	[0.04]
Δ ln(MP^H)			0.22***	0.05**	0.11*			0.39***	0.17***	0.21**
			[0.05]	[0.02]	[0.06]			[0.08]	[0.03]	[0.08]
1st Stage F			15.34	13.76	10.55			15.34	13.76	10.55
Panel C: Developing Economies (N = 11,257) - IV for Δ ln(Hgt+1), OLS for Δ ln(MP^H)										
Δ ln(Hgt+1)	0.13***	0.13***	0.13***	0.13***	0.14***	-0.16***	-0.16***	-0.16***	-0.15***	-0.16***
	[0.03]	[0.03]	[0.03]	[0.03]	[0.03]	[0.04]	[0.04]	[0.04]	[0.04]	[0.04]
Δ ln(MP^H)	-0.01*	-0.01*	-0.01**	-0.00	0.04***	-0.01	-0.00	0.00	0.04***	0.08***
	[0.00]	[0.00]	[0.00]	[0.00]	[0.00]	[0.00]	[0.00]	[0.00]	[0.00]	[0.01]
1st Stage F	21.88	21.96	22.18	22.59	23.12	21.88	21.96	22.18	22.59	23.12
Panel D: Developing Economies (N = 11,257) - IV for Δ ln(Hgt+1),IV for Δ ln(MP^H)										
Δ ln(Hgt+1)			0.10***	0.09**	0.18***			-0.13**	-0.09**	-0.14***
			[0.03]	[0.04]	[0.04]			[0.05]	[0.04]	[0.04]
Δ ln(MP^H)			0.14***	0.02	0.08			0.35***	0.17***	0.19***
			[0.04]	[0.02]	[0.06]			[0.07]	[0.03]	[0.07]
1st Stage F			16.83	11.12	13.60			16.83	11.12	13.60
Decay Param	0.33	0.5	1	2	3	0.33	0.5	1	2	3
Country FE	Yes	Yes	Yes	Yes	Yes	Yes	Yes	Yes	Yes	Yes

Notes: Regressions have the same specification as in Table 2, except that we also include the log change in heights-based market potential 1975-2015 (Δ ln(MP^H)). We instrument Δ ln(MP^H) using similarly constructed instruments as for Δ ln(Hgt+1). See the text for details of MP calculation and included controls. Robust standard errors in brackets.

Table A14: Height Gradients

	(1) Ln floors, Commercial	(2) Ln floors, Residential
Distance (km)	–0.203***	–0.100***
	(0.004)	(0.001)
Observations	4,709	129,496

Notes: Each 0.25 km distance bin to the Chicago city center, as defined by the average location of the tallest 5 commercial buildings in the city, receives equal weight. Each building (observation) in each regression is weighted by the inverse of the number of buildings in its city center distance bin.

Table A15: Counterfactuals: Illustrative Examples

	20% higher cost of height	Binding height limit	Binding height limit under 20% higher cost of height
Total population	–8.2%	–16.5%	–11.5%
Total area	16.1%	18.5%	9.3%
Average commuting cost	2.6%	8.2%	5.3%
Average residential rent	–0.2%	–14.2%	–10.6%
Average commercial rent	7.8%	2.5%	–1.8%
Average productivity	–0.9%	–5.1%	–4.1%
Wage	–2.5%	–6.8%	–4.8%
Total land value	–0.2%	12.6%	8.8%
Urban utility (U})	–5.3%	–10.5%	–6.9%
Expected utility ({V})	–1.6%	–3.0%	–1.8%

Notes: The first two scenarios directly correspond to the counterfactuals in the second and third rows of Figure 9. Averages are weighted by the number of workers.

Table A16: Wefare effects of tall buildings by world regions: Mechanisms

		Wage (y)		Rent (p^R)		Commuting cost ($e^{\tau^R \times x}$)	
World region	Urban pop. (BN)	No tall building	Actual height limit	No tall building	Actual height limit	No tall building	Actual height limit
Africa, G	0.55	–6.5%	–5.5%	–8.3%	–6.9%	8.4%	7.4%
Asia, G	1.95	–5.8%	–3.4%	–8.6%	–5.3%	7.3%	4.3%
Europe, G	0.04	–3.7%	–2.1%	–6.9%	–4.0%	4.3%	2.4%
LAC, G	0.33	–8.3%	–5.7%	–11.8%	–9.3%	10.6%	7.0%
Mean, G	2.87	–6.2%	–4.0%	–8.9%	–6.1%	7.8%	5.2%
Asia, D	0.19	–12.2%	–7.9%	–15.5%	–11.1%	16.3%	10.5%
Europe, D	0.25	–8.9%	–7.7%	–11.7%	–11.4%	11.3%	9.5%
LAC, D	0.02	–2.6%	–1.9%	–6.4%	–5.1%	3.0%	2.3%
North America, D	0.17	–10.5%	–8.0%	–13.8%	–12.1%	13.9%	10.2%
Oceania, D	0.01	–10.2%	–9.6%	–14.9%	–14.5%	13.3%	12.5%
Mean, D	0.64	–10.2%	–7.7%	–13.3%	–11.4%	13.3%	9.9%
Mean, all	3.51	–6.9%	–4.7%	–9.7%	–7.0%	8.8%	6.0%

Notes: We report population-weighted average percentage changes in outcomes across cities within a region. City-specific effects are from counterfactual analyses within the model, in each case using a parameterization that matches a real-world city in terms of population, cost of height and height gap, an empirical estimate of how much of the potential height has not been realized taken from Barr & Jedwab, 2023. Height ban means no tall building exceeding four floors.

Table A17: Wefare effects of tall buildings by world regions: 20% lower cost of height

World region	City characteristics: Urban pop. (BN)	Share large cities	Cost of height θ	Est. height gap	Expected utility ($\mathcal{V}$): No tall building	Actual height limit	Agg. land rent ($\mathcal{R}$): No tall building	Actual height limit
Africa, G	0.53	35.2%	0.35	69.4%	–6.0%	–5.5%	8.3%	8.6%
Asia, G	1.94	44.5%	0.47	63.6%	–4.8%	–3.5%	6.3%	5.7%
Europe, G	0.04	29.6%	0.39	63.6%	–1.4%	–0.9%	2.2%	1.8%
LAC, G	0.33	52.9%	0.32	69.9%	–6.6%	–4.3%	8.5%	7.6%
Mean, G	2.85	43.5%	0.43	65.4%	–5.2%	–3.9%	6.8%	6.4%
Asia, D	0.19	77.2%	0.32	62.4%	–12.4%	–9.1%	15.8%	14.0%
Europe, D	0.25	41.5%	0.25	79.6%	–7.1%	–6.1%	9.5%	10.6%
LAC, D	0.02	49.6%	0.81	61.6%	–0.9%	–0.6%	1.4%	1.1%
North America, D	0.17	67.4%	0.34	76.4%	–10.3%	–8.1%	12.8%	13.8%
Oceania, D	0.01	64.9%	0.27	87.6%	–8.8%	–8.6%	10.5%	10.7%
Mean, D	0.64	59.7%	0.31	73.4%	–9.4%	–7.4%	12.1%	12.2%
Mean, all	3.49	46.5%	0.41	66.9%	–5.9%	–4.6%	7.8%	7.5%

Notes: We report population-weighted average percentage changes in welfare across cities within a region. City-specific welfare effects are from counterfactual analysis within the model, in each case using a parameterization that matches a real-world city in terms of population, cost of height and height gap, an empirical estimate of how much of the potential height has not been realized taken from Barr & Jedwab, 2023. Height ban means no tall building exceeding four floors. Large city population share is the share of urban population in cities with a population of at least 1M. Compared to the actual cost of height used in Table 7, we have reduced the cost of height, θ, by 20%.

Table A18: Cost of Height Over Time

	Ln cost per space		Ln cost per space	
Ln height	0.255***	(0.08)	0.578**	(0.26)
Year - 1975	0.086***	(0.01)	0.146***	(0.04)
Ln height × Year - 1975	-0.008***	(0.00)	-0.022**	(0.01)
IV, KPF	-		Yes, 3.13	
City FE, Decade FE	Yes		Yes	
Observations, R^2	554, 0.82		554, -	

Notes: Each unit of observation is a U.S. building. All buildings with height $\leq$ 55m are excluded. In column (2), IV variables are the log Euclidean distance from the city center and its interaction with a yearly time trend. The city center is defined as the median coordinate of buildings exceeding 100 m of height or the tallest building where building exceeds 100 m. Robust SE's clustered at the city level.